LIGAND EXCHANGE ON THE ZINC(II) AND BERYLLIUM(II) IONS.

Michael Nicholas Tkaczuk

B.Sc. (Hons.)

This thesis is presented for the degree of Doctor of Philosophy.

Department of Physical and Inorganic Chemistry

University of Adelaide

December, 1981.

CONTENTS

CHAPTER 3 (Continued) Page

SUMMARY

The study of ligand exchange processes on metal ions in solution is of fundamental importance as such elementary reactions form the basis of a large range of complex processes in solution.

This thesis deals with the study of the ligand exchange kinetics of a number of ligands on the metal ions zinc(II) and beryllium(II).

A range of unidentate oxygen donor ligands were used to prepare complexes with beryllium(II) and zinc(II) (unidentate sulphur donors were also used for zinc(II)). Solutions of these complexes with free ligand in the non-coordinating diluents CD_2Cl_2, CD_3CN and CD_3NO_2 were prepared. Variable temperature nmr spectroscopy of these solutions was employed to obtain exchange modified spectra which were simulated using a complete lineshape analysis program to obtain kinetic data for the exchange process. The rate law for the ligand exchange process was established by changing the concentration of free ligand and observing the variation in the rate of ligand exchange. Ligand exchange mechanisms were assigned on the basis of the observed rate law.

For the zinc(II) systems examined two rate laws were observed; for the $[Zn(tmtu)_4]^{2+}/tmtu/CD_2Cl_2$ system the exchange rate = $4k_1[Zn(tmtu)_4{}^{2+}]$ where typically $k_1(200\ K) = 16.0 \pm 0.5\ s^{-1}$, $\Delta H^{\neq} = 63.4 \pm 0.6\ kJ\ mol^{-1}$ and $\Delta S^{\neq} = 98 \pm 3\ J\ K^{-1}\ mol^{-1}$ for a solution where $[Zn(tmtu)_4{}^{2+}]$, $[tmtu]_{free}$ and $[CD_2Cl_2]$ are 0.0427, 0.143 and 14.98 mol dm^{-3} respectively and a dissociative ligand exchange mechanism was assigned. For the $[Zn(hmpa)_4]^{2+}/hmpa/CD_2Cl_2$ system the exchange rate = $4k_2[Zn(hmpa)_4{}^{2+}][hmpa]_{free}$ where $k_2(240\ K) = 304 \pm 17\ dm^3\ mol^{-1}\ s^{-1}$, $\Delta H^{\neq} = 22.7 \pm 0.9\ kJ\ mol^{-1}$ and $\Delta S^{\neq} = -101 \pm 4\ J\ K^{-1}\ mol^{-1}$ and on the basis of the observed rate law an associative ligand exchange mechanism was assigned.

For the beryllium(II) systems examined three forms of rate law were observed. In several cases the rate of ligand exchange was

independent of $[ligand]_{free}$. Typically for the $[Be(tmu)_4]^{2+}/tmu/CD_3NO_2$ system the ligand exchange rate = $4k_1[Be(tmu)_4^{2+}]$ where $k_1(298.2\ K)$ = $1.46 \pm 0.04\ s^{-1}$, $\Delta H^{\neq} = 80.0 \pm 0.6\ kJ\ mol^{-1}$ and $\Delta S^{\neq} = 26.5 \pm 1.7\ J\ K^{-1}\ mol^{-1}$ for a solution where $[Be(tmu)_4^{2+}]$, $[tmu]_{free}$ and $[CD_3NO_2]$ are 0.328, 1.475 and 12.39 mol dm^{-3} respectively and on the basis of the observed rate law a dissociative ligand exchange mechanism was assigned. For the $[Be(dmso)_4]^{2+}/dmso/CD_3NO_2$ and $[Be(mmpp)_4]^{2+}/mmpp/CD_3NO_2$ systems the rate of ligand exchange was found to be linearly dependent on $[ligand]_{free}$ with the ligand exchange rate = $4k_2[BeL_4^{2+}][L]_{free}$ where typically $k_2(298.2\ K) = 0.220 \pm 0.1\ dm^3\ mol^{-1}\ s^{-1}$, $\Delta H^{\neq} = 68.7 \pm 0.9\ kJ\ mol^{-1}$ and $\Delta S^{\neq} = -26.1 \pm 2.7\ J\ K^{-1}\ mol^{-1}$ and the k_2 rate constant was interpreted in terms of an associative ligand exchange mechanism. However for the $[Be(dmmp)_4]^{2+}/dmmp/CD_3CN$ system and all the amide systems examined (dmf, nma, dma and dea) two term ligand exchange rate laws were observed where the exchange rate = $4(k_1 + k_2[L]_{free})[BeL_4^{2+}]$. Typical of these results is the $[Be(dma)_4]^{2+}/dma/CD_3NO_2$ system where $k_1(340\ K) = 7.3 \pm 0.7\ s^{-1}$, $\Delta H_1^{\neq} = 56.9 \pm 1.5\ kJ\ mol^{-1}$, $\Delta S_1^{\neq} = -62.1 \pm 4.6\ J\ K^{-1}\ mol^{-1}$, $k_2(340\ K) = 10.5 \pm 1.0\ dm^3\ mol^{-1}\ s^{-1}$, $\Delta H_2^{\neq} = 66.7 \pm 2.7\ kJ\ mol^{-1}$ and $\Delta S_2^{\neq} = -30.1 \pm 7.4\ J\ K^{-1}\ mol^{-1}$. The k_1 and k_2 rate constants were interpreted in terms of dissociative and associative ligand exchange mechanisms respectively. The kinetics and mechanisms of ligand exchange on the various $[BeL_4]^{2+}$ species are discussed in terms of the steric and electron donating characteristics of the ligands concerned and the effect of the diluent.

For the beryllium(II) systems an isokinetic correlation between activation enthalpy and activation entropy is observed. It is demonstrated that this correlation has chemical significance and is not a statistical artefact and the results obtained from this correlation are discussed with reference to results obtained for other metal centres.

STATEMENT

This thesis contains no material previously submitted for a degree or diploma in any University and to the best of my knowledge and belief, contains no material previously published or written by another person, except where due reference is made in the text of the thesis.

M.N. Tkaczuk

ACKNOWLEDGEMENTS

I wish to thank my supervisor, Dr. S.F. Lincoln for his encouragement and guidance throughout the course of this project. I wish to express my gratitude to Prof. D.O. Jordan and Prof. M.I. Bruce for making available the facilities of this department, Dr. T.M. Spotswood and Dr. E.H. Williams for their assistance with the operation of the Bruker HX-90E NMR spectrometer and computing and my fellow research students for their help and friendship.

Finally I wish to thank my sister for her help and understanding, Mrs. A. Hounslow for proof reading and the typist for typing this manuscript.

ABBREVIATIONS

The following abbreviations have been used in the text of this thesis:-

dea	N,N-diethylacetamide
def	N,N-diethylformamide
dma	N,N-dimethylacetamide
dmadmp	N,N-dimethylamido-O,O-dimethylphosphate
dmf	N,N-dimethylformamide
dmmp	dimethylmethylphosphonate
dmso	dimethylsulphoxide
hmpa	hexamethylphosphoramide
mmpp	methylmethylphenylphosphinate
nipa	nonamethylimidodiphosphoramide
nma	N-methylacetamide
nmf	N-methylforamide
nmtu	N-methylthiourea
nmu	N-methylurea
npa	N-phenylacetamide
teof	triethyl orthoformate
tmdamp	bis(N,N-dimethylamido)-O-methylphosphate
tmp	trimethylphosphate
tmtu	1,1,3,3-tetramethylthiourea
tmu	1,1,3,3-tetramethylurea
tpp	triphenylphosphate
tppo	triphenylphosphine oxide
tu	thiourea
$[L]_{free}$	concentration of free ligand L in solution
c.f.	compared with
C.W.	Continuous Wave

CD_3NO_2	The D is used to represent ^2H
Hz	Hertz
nmr	nuclear magnetic resonance
ppm	parts per million
$\hat{T}$	isokinetic temperature

ADDENDUM

Listed hereunder are corrections to "Ligand Exchange on the Zinc(II) and Beryllium(II) Ions" by Michael Nicholas Tkaczuk, B.Sc (Hons.).

Page 6 Line 27	"doning" should be "donating"
Page 12 Para. 2	"determination .... have" should be "determination .... has"
Page 39 Ref. 4	H. Ohlaki should be H. Ohtaki
Page 45 Line 26	".... respectively.)"
Page 48 Line 27	"this data" should be "the data"
Page 49 Line 3	"larger" should be "largest"
Page 54 Para. 3	".... assigned; whereas ...."
Page 67 Para. 4	"analysis .... allow" should be "analyses .... allow", and "data was" should be "data were"
Page 82 Line 18	".... each system.]"
Page 85 Line 7	".... respectively,"
Page 88 Line 30	"data does" should be "data do"
Page 89 Line 1	"data .... is" should be "data .... are"
Page 94 Para. 3	"data .... provides" should be "data .... provide"
Page 95 Line 4	".... does reflect" should be "do reflect"
Page 96 Line 20	"data is" should be "data are"
Page 96 Line 21	"data lies" should be "data lie"
Page 99 Line 5	"is controlled" should be "are controlled"
Fig. 5.1 Line 31	"elipsoid" should be "ellipsoid"
Page 102 Line 19	".... precipitated, after which"

for the more labile metal ions, eg. Cs^+, K^+ and Ca^{2+} as the solvent residence time will be short for these cases.

1.3 Mechanisms of solvent and ligand exchange

The study of ligand exchange processes where no nett chemical reaction occurs

$$[MS_n]^{m+} + S^* \rightleftharpoons [MS^*S_{n-1}]^{m+} + S$$

(where * represents a typographical distinction only)

represents the simplest type of exchange process and is regarded as a special case of ligand substitution. The range of first order rate constants observed for solvent exchange at (298 K) on metal ions in aqueous solution range from 10^{10} s^{-1} for Cr^{2+} to 10^{-7} s^{-1} for Rh^{3+}.

Eigen and coworkers[6-9] and others[10-12] have used relaxation techniques to study ligand substitution processes for $MgSO_4$, $MnSO_4$ and $BeSO_4$ in aqueous solution and have concluded that a three step mechanism for complex formation operates. This has been called the Eigen mechanism and involves

(i) the reacting ions coming together to form a solvent separated ion pair - this process is diffusion controlled,

(ii) elimination of a solvent molecule from between the ions leading to the formation of an outer sphere complex,

and

(iii) removal of a solvent molecule from the first coordination sphere of the metal ion and replacement by the ligand.

$$M^{m+}_{SOLV} + {SO_4}^{2-}{}_{SOLV} \rightleftharpoons [M^{m+}\ldots\ldots SS\ldots\ldots {SO_4}^{2-}]$$

solvent separated ion pair

$$\Big\downarrow\uparrow$$

$$[MSO_4]^{m+-2} \rightleftharpoons [M^{m+}\ldots\ldots S\ldots\ldots {SO_4}^{2-}]$$

outer sphere complex

Strehlow[13], using a simple electrostatic model, calculated the activation energy for the formation of the $BeSO_4$ complex and obtained values with the correct orders of magnitude for the activation process. A comparison of the activation energies required for the substitution reaction at Be^{2+} showed that the Eigen mechanism is favoured compared with the pure SN1 mechanism[14]. Langford and Gray[15] have proposed that the ligand exchange and substitution processes can proceed via one of four mechanistic pathways to allow for better characterisation of the ligand exchange process.

(1) Dissociative (D) mechanism

For this mechanism the rate determining step involves the loss of one ligand to form a transition state or reactive intermediate of reduced coordination number

$$[MS_n]^{m+} \underset{\longleftarrow}{\xrightarrow{k_1 \text{ slow}}} [MS_{n-1}]^{m+} + S$$

$$\text{fast} \downarrow S^*$$

$$[MS_{n-1}S^*]^{m+}$$

If the concentration of free ligand is then varied over a large range, the rate of exchange should be independent of the concentration of free ligand and a first order rate law observed, hence

$$\text{Rate} = nk_{ex}[MS_n^{m+}]$$

where $k_{ex} = k_1$ and n = coordination number of the metal ion M^{m+}.

(2) Associative (A) mechanism

The rate determining step involves the formation of a reactive intermediate of increased coordination number

$$[MS_n]^{m+} + S^* \underset{\longleftarrow}{\xrightarrow{k_2 \text{ slow}}} [MS_nS^*]^{m+} \xrightarrow{\text{fast}} [MS_{n-1}S^*]^{m+} + S$$

If the concentration of the free ligand is varied the rate of exchange should be directly dependent on the concentration of free ligand and a

second order rate law observed:

$$\text{Rate} = nk_{ex}[MS_n^{m+}] \text{ where } k_{ex} = k_2[S]$$

and [S] is the concentration of free ligand.

(3) The Interchange (I_D and I_A) mechanisms

The Dissociative Interchange (I_D) and Associative Interchange (I_A) mechanisms involve the formation of an associated outer sphere complex before exchange occurs and the associated ligand then interchanges synchronously with a coordinated ligand and vice versa,

$$[MS_n]^{m+} + S^* \overset{K_{ass}}{\rightleftharpoons} [S^*....MS_n]^{m+} \xrightarrow{k_i} [MS^*S_{n-1}]^{m+} + S$$

where K_{ass} is the rapid equilibrium constant. (This mechanistic scheme is very similar to the Eigen mechanism.)

A gradation of these interchange mechanisms from the extremes of dissociative to associative mechanisms is possible depending on the nature of the ligand where

$$\text{Rate} = nk_{ex}[MS_n^{m+}]$$

$$= \frac{nk_iK_{ass}[MS_n^{m+}][S]}{1 + K_{ass}[S]}$$

and also on the value of K_{ass}, estimates of which can be made from equations derived by Fuoss[16] and Eigen[17]. If $K_{ass}[S] >> 1$ then the Rate = $nk_i[MS_n^{m+}]$ which is indistinguishable from a D mechanism. If $K_{ass}[S] << 1$ then the Rate = $nk_{ex}[MS_n^{m+}][S]$ (where $k_{ex} = k_iK_{ass}$) which is the form of the rate equation for an A mechanism.

Another type of ligand exchange mechanism has been proposed[18] which is analogous to that suggested for the square planar platinum(II) species[19] where the rate law is of the form Rate = $n(k_1 + k_2[S])[MS_n^{m+}]$. The k_1 term characterises the rate of formation of $[MS_{n-1}D]^{m+}$ and the k_2 term characterises direct exchange via an A mechanism

$$[MS_n]^{m+} + D \overset{k_1}{\rightleftharpoons} [MS_nD]^{m+} \rightleftharpoons [MS_{n-1}D]^{m+} + S$$

$$[MS_n]^{m+} + S^* \overset{k_2}{\rightleftharpoons} [MS_nS^*] \rightleftharpoons [MS_{n-1}S^*]^{m+} + S$$

1.4 Experimental Methods for obtaining ligand exchange parameters

Two experimental methods allow the rate of ligand exchange and the coordination numbers of metal ions in solution to be directly determined. The first of these methods, isotopic dilution[21-24], usually uses ^{18}O labelled water in either the bulk solvent or in the first coordination sphere of the hydrated metal ion. This method is limited in use in that the rate of exchange between the first coordination sphere and the bulk solvent has to be slow enough to allow for the sampling and separation of the metal ion from the bulk solvent, and is only applicable to reasonably inert metal ions.

The second method is nuclear magnetic resonance spectroscopy of which a number of techniques can be used to obtain kinetic data, these include the paramagnetic shift method[2,25], $T_{1\rho}$ measurements[26,27], spin saturation transfer methods[28,29] and the nmr lineshape analysis method[27,29] utilising either time or frequency domain spectra.

Several problems arise if the solvent or ligand exchange process is studied in pure solvent, firstly it is impossible to vary the concentration of solvent so that the order of reaction can be established and secondly if the solvent is water then protolysis will affect the solvent exchange process occurring at the metal centre. Both these problems can be eliminated[20] if the ligand or solvent exchange process is studied in a non-aqueous inert diluent which allows the concentration of free ligand to be varied and the order of reaction with respect to the free ligand to be established.

The nmr lineshape analysis method allows the kinetics of ligand exchange for a wide range of labile metal ions to be determined, if the

frequency of ligand exchange is comparable with the reciprocal of the difference in frequency between the coalescing nmr signals over the accessible temperature range then significant modifications to the absorption mode (v) lineshape will occur as the temperature is varied. Activation parameters for the exchange process are readily obtained by observing the variation of exchange rate with temperature. (Theoretical and practical considerations of this method are dealt with in Chapter 2 of this thesis.)

1.5 Previous Ligand Exchange Studies

The following section surveys previous ligand exchange studies for a variety of spherical closed shell metal complexes in solutions of an inert diluent. Before proceeding it will be beneficial to define the term "system", which is often used, as being a specific combination of metal complex species and free ligand in an inert diluent.

From an examination of the results for the systems (Table 1.1) which have been previously studied it becomes evident that no single factor determines the kinetics and mechanisms for the ligand exchange process on any particular species. A subtle interplay of several factors including the surface charge density of the metal ion, the electron donating ability of the ligand, the steric characteristics of the ligand and the nature of the diluent determine the lability and mechanism of the ligand exchange process.

For the beryllium(II) ion the rate of ligand exchange covers almost seven orders of magnitude[45-52] and demonstrates that the nature of the ligand plays an important role in determining the lability toward ligand exchange.

Correlations between the observed ligand exchange parameters and several parameters[53-58] for the relative doning properties of the ligands have been attempted but with little or no success. The Gutmann

Table 1.1

Metal ion/Complex	Diluent	k_{ex}(298.2 K) s^{-1} or $dm^3\ mol^{-1}\ s^{-1}$	$\Delta H^{\neq}$ kJ mol^{-1}	$\Delta S^{\neq}$ J K^{-1} mol^{-1}	Assigned Mechanism	Ref.
Aluminium(III)						
$[Al(H_2O)_6]^{3+}$[b]	?	16	65.3	0	D?	30
$[Al(dmso)_6]^{3+}$	CD_3NO_2	0.3	83	22	D	31
$[Al(tmp)_6]^{3+}$	CH_3NO_2	0.38	98	76	D	32
$[Al(tmp)_6]^{3+}$	CD_3NO_2	0.78	85	38	D	31
$[Al(tmp)_6]^{3+}$	CD_3NO_2	0.36	87	35	D	33
$[Al(dmmp)_6]^{3+}$	CH_3NO_2	5.1	84	48	D	32
$[Al(dmmp)_6]^{3+}$	CH_3NO_2	5.0	75	18	D	32
$[Al(dmmp)_6]^{3+}$	CD_3NO_2	4.8	83	46	D	34
$[Al(dmf)_6]^{3+}$	CD_3NO_2	0.05	93	43	D	31
$[Al(hmpa)_4]^{3+}$	CH_3NO_2	4800[a]	32	-43	A	32
Gallium(III)						
$[Ga(H_2O)_6]^{3+}$	?	760	69	42	?	30
$[Ga(dmso)_6]^{3+}$	CD_3NO_2	1.9	73	4	D	31
$[Ga(tmp)_6]^{3+}$	CD_3NO_2	6.4	74	19	D	31
$[Ga(tmp)_6]^{3+}$	CD_3NO_2	5.0	88	63	D	35
$[Ga(dmf)_6]^{3+}$	CD_3NO_2	1.7	86	46	D	31

Table 1.1 (Continued)

Metal ion/Complex	Diluent	k_{ex}(298.2 K) s^{-1} or $dm^3\ mol^{-1}\ s^{-1}$	$\Delta H^{\neq}$ kJ mol^{-1}	$\Delta S^{\neq}$ J K^{-1} mol^{-1}	Assigned Mechanism	Ref.
Indium(III)						
$[In(H_2O)_6]^{3+}$	?	4.0×10^3[a]	19	-96	A	30
$[In(tmp)_6]^{3+}$	CD_3NO_2	34[a]	29	-117	A	31
$[In(tmp)_6]^{3+}$	CD_3NO_2	7.2[a]	36	-109	A	35
$[In(dmmp)_6]^{3+}$	CD_3NO_2	2.3	18.8	-175	D[c]	34
$[In(dmmp)_6]^{3+}$	CD_3NO_2	3.8[a]	34.5	-118	A[c]	34
Scandium(III)						
$[Sc(tmp)_6]^{3+}$	CD_3CN	29.9	32.7	-107	D	36
$[Sc(tmp)_6]^{3+}$	$C_2H_2Cl_4$	38.8	41.3	-76	D	36
$[Sc(tmp)_6]^{3+}$	CD_3NO_2	45.5	26.0	-126	A	36
$[Sc(dmmp)_6]^{3+}$	CD_3CN	2.9	42.8	-92.4	D[c]	37
$[Sc(dmmp)_6]^{3+}$	CD_3CN	12.5[a]	29.5	-125	A[c]	37
$[Sc(dmmp)_6]^{3+}$	CD_3NO_2	13.6[a]	26.0	-136	A	37

Table 1.1 (Continued)

Metal ion/Complex	Diluent	k_{ex}(298.2 K) s^{-1} or $dm^3\ mol^{-1}\ s^{-1}$	$\Delta H^{\neq}$ kJ mol^{-1}	$\Delta S^{\neq}$ J $K^{-1}\ mol^{-1}$	Assigned Mechanism	Ref.
$[Sc(tmu)_6]^{3+}$	CD_3CN	0.79	70.7	-9.8	D	18
$[Sc(tmu)_6]^{3+}$	CD_3NO_2	0.06	101	70.7	D	18
$[Sc(nma)_6]^{3+}$	CD_3CN	79.4	27.3	-117	D^c	38
$[Sc(nma)_6]^{3+}$	CD_3CN	380[a]	26.1	-108	A^c	38
$[Sc(dma)_6]^{3+}$	CD_3CN	12.4	32.2	-116	D^c	18
$[Sc(dma)_6]^{3+}$	CD_3CN	151[a]	27.2	-112	A^c	18
$[Sc(dma)_6]^{3+}$	CD_3NO_2	3.6	30.8	-131	D^c	18
$[Sc(dma)_6]^{3+}$	CD_3NO_2	105[a]	26.0	-119	A^c	18
$[Sc(dea)_6]^{3+}$	CD_3CN	10.7	43.9	-78	D^c	38
$[Sc(dea)_6]^{3+}$	CD_3CN	18.2[a]	23.5	-142	A^c	38
$[Sc(dea)_6]^{3+}$	CD_3NO_2	0.1	81.6	9.9	D^c	38
$[Sc(dea)_6]^{3+}$	CD_3NO_2	13.5[a]	28.1	-129	A^c	38
Yttrium(III)						
$[Y(tmu)_6]^{3+}$	CD_3CN	245	26.3	-111	D	39
$[Y(mmpp)_6]^{3+}$	CD_2Cl_2	5.4×10^4	31.4	-49	D^c	40
$[Y(mmpp)_6]^{3+}$	CD_2Cl_2	1.6×10^5[a]	35.3	-27	A^c	40

Table 1.1 (Continued)

Metal ion/Complex	Diluent	k_{ex}(298.2 K) s^{-1} or $dm^3\ mol^{-1}\ s^{-1}$	$\Delta H^{\neq}$ kJ mol^{-1}	$\Delta S^{\neq}$ J K^{-1} mol^{-1}	Assigned Mechanism	Ref.
Magnesium(II)						
$[Mg(H_2O)_6]^{2+}$		5×10^5	42.7	8.4	?	41
$[Mg(tmp)_6]^{2+}$	CD_2Cl_2	6.8×10^5	50.8	37.2	D	42
$[Mg(tmp)_6]^{2+}$	$(CD_3)_2CO$	6.5×10^5	51.2	38.1	D	42
$[Mg(dmf)_6]^{2+}$	CD_2Cl_2	5.5×10^{12}	23.5	77.8	D	43
$[Mg(dmf)_6]^{2+}$	$(CD_3)_2CO$	6.5×10^4	61.7	54.2	D	43
$[Mg(tppo)_5]^{2+}$	CD_2Cl_2	1.5×10^6	69.6	107	D	44
Beryllium(II)						
$[Be(H_2O)_4]^{2+}$	H_2O	1800	42	-44	I_A?	45
$[Be(dmf)_4]^{2+}$	$OC(H)N(CH_3)_2$	310	61	11	D?	46
$[Be(tmp)_4]^{2+}$	CH_2Cl_2	3.6	57	-44	D	47
$[Be(tmp)_4]^{2+}$	CH_3NO_2	1.5[a]	56	-54	A	48
$[Be(dmmp)_4]^{2+}$	CH_3NO_2	0.81[a]	60	-44	A	48
$[Be(dmadmp)_4]^{2+}$	CH_3NO_2	7.3×10^{-3}	89	13	D	48
$[Be(dmadmp)_4]^{2+}$	pc[e]	9×10^{-2}	77	-5	D	48
$[Be(tmdamp)_4]^{2+}$	pc[e]	6.9×10^{-3}	89	13	D	48
$[Be(hmpa)_4]^{2+}$	pc[e]	2.7×10^{-4}	117	78	D	48

[a] Second order rate constant. [b] 0.55 M Mn^{2+} present. [c] From a two term rate law where A and D mechanisms operate in parallel. [d] 0.06 M Mn^{2+} present. [e] propylene carbonate, 4-methyl-1,3-dioxolan-2-one.

Donor Number[56-58] (DN) is perhaps the most frequently quoted and is equal to $-\Delta H_f$ in kcal mol^{-1} for the formation of the $SbCl_5.D$ complex species in dilute dichloroethane solution (D is the ligand) with only one ligand molecule binding to the antimony (V) species. That no direct correlation exists between the DN and the kinetic parameters for the ligand exchange process may be due to the soft acid nature of Sb^{5+} and the important role steric contributions make in determining the ligand exchange process. On the hard/soft, acid/base classification scheme[59] Sb^{5+} is considered a relatively soft acid compared with the metal ions examined in Table 1.1. Ligands that bind well with Sb^{5+} may not do so with metal ions such as those in Table 1.1 which are considered as hard acids.

The importance of steric factors in determining the ligand exchange process is seen for the Al^{3+} ion where the ground state stoichiometry is $[AlS_6]^{3+}$ for tmp and dmf, (whose DN's are 23.0 and 26.6 respectively) however hmpa forms the $[Al(hmpa)_4]^{2+}$ species even though the DN for hmpa is 38.8. Steric crowding in the latter case restricts the number of hmpa molecules in the first coordination sphere of aluminium(III) to four.

Studies of tmp exchange on Al^{3+}[32], Ga^{3+}[35], In^{3+}[35] and Sc^{3+}[36] in CH_3NO_2 and CD_3NO_2 have been interpreted in terms of D and A mechanisms for the first two and second two ions respectively. This change in mechanism can be explained in terms of steric crowding of the first coordination sphere for Al^{3+} and Ga^{3+} which have small ionic radii[60] (0.053 nm and 0.062 nm respectively) allowing only a transition state of reduced coordination number, compared with In^{3+} and Sc^{3+} which have larger ionic radii[60] (0.08 nm and 0.074 nm respectively) and can thus accommodate transition states of increased coordination number.

1.6 Aim of this Research

The intention of the research work reported herein is to determine the rates and mechanisms of ligand exchange for the tetrahedral divalent metal ions zinc and beryllium, utilising variable temperature nmr/lineshape analysis techniques.

The direct determination of coordination numbers and kinetic data for ligand exchange on zinc(II)-unidentate ligand complexes in non-aqueous inert diluents have not been reported previously, whereas for the beryllium(II) ion several studies have already given insights into the dynamics of the processes occurring at the metal centre.

Different mechanistic results have been reported for tmp exchange on $[Be(tmp)_4]^{2+}$ in CH_3NO_2 [48] and CH_2Cl_2 [47]. These results prompted the systematic investigation of the effects of the nature of the ligand and diluent on the ligand exchange processes occurring at the beryllium(II) and zinc(II) metal centres. This investigation forms the topic of this thesis.

REFERENCES: CHAPTER 1

1. R.E. Connick and D. Fiat, *J. Chem. Phys.*, 39, 1349 (1963).
2. M. Alei and J.A. Jackson, *J. Chem. Phys.*, 41, 3402 (1964).
3. A. Fratiello, R.E. Lee, V.M. Nishida and R.E. Schuster, *J. Chem. Phys.*, 48, 3705 (1968).
4. H.S. Frank and W.Y. Wen, *Discuss. Far. Soc.*, 24, 133 (1957).
5. S.F. Lincoln, *Coord. Chem. Rev.*, 6, 309 (1971).
6. M. Eigen, *Pure Appl. Chem.*, 6, 97 (1963).
7. M. Eigen and K. Tamm, *Z. Elektrochem.*, 66, 107 (1962).
8. M. Eigen, *Ber. Bunsenges. Phys. Chem.*, 67, 753 (1963).
9. H. Diebler and M. Eigen, *Z. Physik. Chem. N.F.*, 20, 299 (1959).
10. G. Atkinson and S. Kor, *J. Phys. Chem.*, 69, 128 (1965).
11. G. Atkinson and S. Petrucci, *J. Phys. Chem.*, 70, 3122 (1966).
12. G. Atkinson and S.K. Kor, *J. Phys. Chem.*, 71, 673 (1967).
13. H. Strehlow and W. Knoche, *Ber. Bunsenges. Phys. Chem.*, 73, 427 (1969).
14. C.K. Ingold in "*Structure and Mechanism in Organic Chemistry*", Cornell University Press, Ithaca, N.Y. 1953, Chapter 5.
15. C.H. Langford and H.B. Gray in "*Ligand Substitution Processes*", W.A. Benjamin, New York, N.Y. 1966.
16. R.M. Fuoss, *J. Amer. Chem. Soc.*, 80, 5059 (1958).
17. M. Eigen, *Z. Physik. Chem. N.F.*, 1, 176 (1954).
18. D.L. Pisaniello and S.F. Lincoln, *J. Chem. Soc. (Dalton)*, 699 (1980).
19. R.G. Wilkins in "*The Study of Kinetics and Mechanism of Reactions of Transition Metal Complexes*", Allyn and Bacon, Boston, 1974.
20. S.F. Lincoln, *Pure Appl. Chem.*, 51, 2059 (1979).
21. J.P. Hunt and H. Taube, *J. Chem. Phys.*, 18, 757 (1950).
22. J.P. Hunt, H. Taube and H.L. Friedman, *J. Chem. Phys.*, 18, 759 (1950).
23. D.R. Stranks in "*Modern Coordination Chemistry*", ed. J. Lewis and R.G. Wilkins, Interscience N.Y., 1960, Page 78.

24. T.E. Rogers, J.H. Swinehart and H. Taube, *J. Phys. Chem.*, 69, 134 (1965).

25. D. Fiat and R.E. Connick, *J. Amer. Chem. Soc.*, 88, 4754 (1966).

26. T.C. Farrar and E.D. Becker in "*Pulsed and Fourier Transform NMR*", Academic Press N.Y. 1971.

27. S.F. Lincoln, *Prog. React. Kinetics*, 9, 1 (1977).

28. H.M. McConnell and D.D. Thompson, *J. Chem. Phys.*, 31, 85 (1959).

29. R.A. Hoffman and S. Forsén, *Prog. NMR Spectros.*, 1, 15 (1966).

30. J.W. Neely, *Ph.D. Dissertation*, University of Berkeley, 1971.

31. A.E. Merbach, P. Moore, O.W. Howarth and C.H. McAteer, *Inorg. Chim. Acta*, 39, 129 (1980).

32. J.-J. Delpuech, M.R. Khadder, A.A. Péguy and P.R. Rubini, *J. Amer. Chem. Soc.*, 97, 3373 (1975).

33. L.S. Frankel and E.R. Danielson, *Inorg. Chem.*, 11, 1964 (1972).

34. A. Nelson, *Honours Report*, University of Adelaide, 1980.

35. L. Rodehüser, P.R. Rubini and J.-J. Delpuech, *Inorg. Chem.*, 16, 2837 (1977).

36. D.L. Pisaniello and S.F. Lincoln, *J. Chem. Soc. (Dalton)*, 1473 (1979).

37. D.L. Pisaniello and S.F. Lincoln, *Inorg. Chim. Acta*, 36, 85 (1979).

38. S.F. Lincoln and D.L. Pisaniello, *Inorg. Chem.*, (in press).

39. D.L. Pisaniello, S.F. Lincoln, E.H. Williams and A.J. Jones, *Aust. J. Chem.*, 34, 495 (1981).

40. D.L. Pisaniello and S.F. Lincoln, *Aust. J. Chem.*, 34, 1195 (1981).

41. J. Neely and R. Connick, *J. Amer. Chem. Soc.*, 92, 3476 (1970).

42. D.L. Pisaniello, S.F. Lincoln and E.H. Williams, *Inorg. Chim. Acta*, 31, 237 (1978).

43. D.L. Pisaniello and S.F. Lincoln, *Aust. J. Chem.*, 32, 715 (1979).

44. D.L. Pisaniello, T.M. Spotswood, S.F. Lincoln and M.N. Tkaczuk, *Aust. J. Chem.*, 34, 283 (1981).

45. J. Frahm and H.-H. Füldner, *Ber. Bunsenges. Phys. Chem.*, 84, 173 (1980).

46. N.A. Matwiyoff and W.G. Movius, *J. Amer. Chem. Soc.*, 89, 6077 (1967).

47. J. Crea and S.F. Lincoln, *J. Chem. Soc. (Dalton)*, 2075 (1973).

48. J.-J. Delpuech, A. Peguy, P.R. Rubini and J. Steinmetz, *Nouv. J. Chim.*, 1, 133 (1977).

49. H.-H. Fuldner, D.H. Devia and H. Strehlow, *Ber. Bunsenges. Phys. Chem.*, 82, 499 (1978).

50. D.H. Devia and H. Strehlow, *Ber. Bunsenges. Phys. Chem.*, 83, 627 (1979).

51. J. Frahm, *Ber. Bunsenges. Phys. Chem.*, 84, 754 (1980).

52. H. Strehlow, D.H. Devia, S. Dagnall and G. Busse, *Ber. Bunsenges. Phys. Chem.*, 85, 281 (1981).

53. R.H. Erlich, E. Roach and A.I. Popov, *J. Amer. Chem. Soc.*, 92, 4989 (1970).

54. R.H. Erlich and A.I. Popov, *J. Amer. Chem. Soc.*, 93, 5620 (1971).

55. R.S. Drago and B.B. Wayland, *J. Amer. Chem. Soc.*, 87, 3571 (1965).

56. V. Gutmann, "*Coordination Chemistry in Non-aqueous Solutions*", Springer-Verlag, Wein 1968.

57. V. Gutmann and E. Wychera, *Inorg. Nucl. Chem. Lett.*, 2, 257 (1966).

58. V. Gutmann, *Fortschr. Chem. Forsch.*, 27, 59 (1972).

59. R.G. Pearson, *J. Amer. Chem. Soc.*, 85, 3533 (1963).

60. R.D. Shannon and C.T. Prewitt, *Acta Cryst.*, B25, 925 (1969), B26, 946 (1970).

CHAPTER 2

2.1 Kinetic Applications of NMR

The derivation of kinetic parameters from nmr lineshapes modified by chemical exchange processes may be readily achieved through the exchange modified Bloch[1] equations. The steady state solution of the Bloch equations for the absorption mode (v) lineshape of an nmr signal is given by

$$v = \frac{-\gamma B_1 M_{z(eq)} T_2}{1 + T_2^2(\omega_o-\omega)^2 + \gamma^2 B_1^2 T_1 T_2} \qquad (2.1)$$

where γ = the magnetogyric ratio of the observed nucleus

B_1 = magnitude of the small oscillating magnetic field associated with ω

T_2 = transverse relaxation time

T_1 = spin lattice relaxation time

ω = frequency of r.f. field B_1

ω_o = Larmor (resonant) frequency of the nucleus under study

and $M_{z(eq)}$ = Z component of magnetisation along $\vec{B}_o$ at thermal equilibrium.

If as usual (slow passage experiment) B_1 is so small that $\gamma^2 B_1^2 T_1 T_2 << 1$ then the absorption mode (v) lineshape becomes Lorentzian;

$$v = \frac{-M_{z(eq)}\gamma B_1 T_2}{1 + T_2^2(\omega_o-\omega)^2} \qquad (2.2)$$

Several authors[3-9] have demonstrated that the classical Bloch[1] equation can be modified to give a quantitative relationship between the nmr lineshape and the rate of a chemical exchange reaction.

$$\frac{dM_x}{dt} = -\frac{M_x}{T_2} + \gamma(M_y B_o + M_z B_1 \sin\omega t) \qquad (2.3)$$

$$\frac{dM_y}{dt} = -\frac{M_y}{T_2} + \gamma(M_z B_1 \cos\omega t - M_x B_o) \qquad (2.4)$$

$$\frac{dM_z}{dt} = -\frac{1}{T_1}(M_{z(eq)} - M_z) - \gamma(M_x B_1 \sin\omega t + M_y B_1 \cos\omega t) \qquad (2.5)$$

The effects of chemical exchange on the classical nmr lineshape equations can be introduced through the mean site lifetimes of the exchanging species in each of the chemical sites between which it exchanges.

If one considers a nucleus X, exchanging between uncoupled magnetic sites A and B (equivalent to coordinated and free sites) at a rate $k_A[A] = \tau_A^{-1}[A] = k_B[B] = \tau_B^{-1}[B]$ where [A], [B] are the relative populations of the sites and τ_A, τ_B are the mean site lifetimes of X at sites A and B respectively.

If the time required for the nucleus to exchange between sites A and B is so small that no dephasing of the sites occurs between exchange, the nucleus will arrive at site B (from site A) with its phase memory of site A intact and vice-versa. This causes dephasing to occur at site B and results in an increase in M_{xy_B} (the transverse component of magnetization) at a rate $\tau_A^{-1}M_{xy_A}$ while also causing a corresponding decrease in M_{xy_A}. Similarly the movement of nucleus X from site B to site A causes dephasing at site A with an increase in M_{xy_A} at a rate $\tau_B^{-1}M_{xy_B}$ and a corresponding reduction in M_{xy_B}: i.e.

$$\frac{dM_{xy_A}}{dt} = \frac{M_{xy_B}}{\tau_B} - \frac{M_{xy_A}}{\tau_A} \qquad (2.6)$$

$$\frac{dM_{xy_B}}{dt} = \frac{M_{xy_A}}{\tau_A} - \frac{M_{xy_B}}{\tau_B}$$

which will result in the following modifications to the Bloch equations:

$$\frac{dM_{xy_A}}{dt} = -\alpha_A M_{xy_A} - i\gamma B_1 M_{z(eq)_A} + \frac{M_{xy_B}}{\tau_B} - \frac{M_{xy_A}}{\tau_A}$$

$$\frac{dM_{xy_B}}{dt} = -\alpha_B M_{xy_B} - i\gamma B_1 M_{z(eq)_B} + \frac{M_{xy_A}}{\tau_A} - \frac{M_{xy_B}}{\tau_B}$$

where
$$\alpha_B = \frac{1}{T_{2A}} - i(\omega_{o_A} - \omega) \tag{2.7}$$

$$\alpha_B = \frac{1}{T_{2B}} - i(\omega_{o_B} - \omega)$$

Under continuous wave slow passage experimental conditions where $M_{z(eq)_A} = P_A M_{z(eq)}$, $M_{z(eq)_B} = P_B M_{z(eq)}$ and $\frac{dM_{xyA}}{dt} = \frac{dM_{xyB}}{dt} = 0$, the total transverse magnetization $M_{xy} = M_{xy_A} + M_{xy_B}$ which can be given as the steady state solution to equation (2.7).

$$M_{xy} = \frac{i\gamma B_1 M_{z(eq)}(\tau_A + \tau_B + \tau_A\tau_B(\alpha_A P_B + \alpha_B P_A))}{(1 + \alpha_A\tau_A)(1 + \alpha_B\tau_B) - 1} \tag{2.8}$$

where P_A and P_B are the relative populations of sites A and B respectively. The absorption mode lineshape (v) is proportional to the imaginary part of M_{xy}:

$$v = \frac{-\gamma B_1 M_{z(eq)}[Y(1 + \tau(P_B/T_{2A} + P_A/T_{2B})) + QR]}{Y^2 + R^2} \tag{2.9}$$

where $\tau = \tau_A P_B = \tau_B P_A$

$$Y = \tau\left[\frac{1}{T_{2A}T_{2B}} - \delta\omega^2 + \frac{\Delta\omega^2}{4}\right] + \frac{P_B}{T_{2B}} + \frac{P_A}{T_{2A}}$$

$$Q = \tau(\delta\omega - \frac{\Delta\omega}{2}(P_A - P_B))$$

$$R = \delta\omega\left[1 + \tau(\frac{1}{T_{2A}} + \frac{1}{T_{2B}})\right] + \frac{\Delta\omega}{2}\tau(\frac{1}{T_{2B}} - \frac{1}{T_{2A}})$$

$$\Delta\omega = \omega_{o_A} - \omega_{o_B}$$

$$\delta\omega = \tfrac{1}{2}|\omega_{o_A} - \omega_{o_B}| - \omega$$

This general lineshape expression can be simplified if one considers a series of limiting conditions.

(1) Very Slow Exchange

If $$\tau_A^{-1},\ \tau_B^{-1} << |\omega_{o_A} - \omega_{o_B}|,\ T_A^{-1}T_B^{-1}$$

then equation (2.9) approximates to:

$$v = \frac{-\gamma B_1 P_A M_{z(eq)_A}\ T_{2A}}{T_{2A}^{-2} + (\omega_{o_A} - \omega)^2} - \frac{-\gamma B_1 P_B M_{z(eq)_B}\ T_{2B}}{T_{2B}^{-2} + (\omega_{o_B} - \omega)^2} \qquad (2.10)$$

which represents two Lorentzian lineshapes centred at ω_{o_A} and ω_{o_B}, but containing no kinetic information.

(2) Slow Exchange

If $$\tau_A^{-1}\tau_B^{-1} << |\omega_{o_A} - \omega_{o_B}| \text{ with } \tau_A^{-1} = T_{2A}^{-1}$$

and $\tau_B^{-1} = T_{2B}^{-1}$ equation (2.9) simplifies to:

$$V = \frac{-\gamma B_1 P_A M_{z(eq)_A}(T_{2A}^{-1} + \tau_A^{-1})}{(T_{2A}^{-1} + \tau_A^{-1}) + (\omega_{o_A} - \omega)^2} \quad \frac{\gamma B_1 P_B M_{z(eq)_B}(T_{2B}^{-1} + \tau_B^{-1})}{(T_{2B}^{-1} + \tau_B^{-1})^2 + (\omega_{o_B} - \omega)^2}$$

which corresponds to two Lorentzian lineshapes, centred at ω_{o_A} and ω_{o_B}. However $1/T_{2Aobs} = \frac{1}{T_{2A}} + \frac{1}{\tau_A}$ and $\frac{1}{T_{2Bobs}} = \frac{1}{T_{2B}} + \frac{1}{\tau_B}$ which compared to T_{2A}^{-1} and T_{2B}^{-1} respectively are "exchange broadened" and contain kinetic information.

(3) Fast Exchange

If $$\tau_A^{-1}\tau_B^{-1} > |\omega_{o_A} - \omega_{o_B}|$$

a single broad Lorentzian lineshape centred at $(\omega_{o_A}P_A + \omega_{o_B}P_B)$ is observed, where

$$T_{2obs}^{-1} = \frac{P_A}{T_{2A}} + \frac{P_B}{T_{2B}} + P_A^2P_B^2(|\omega_{o_A} - \omega_{o_B}|)^2(\tau_A + \tau_B)$$

(4) Very Fast Exchange

If $$\tau_A^{-1},\ \tau_B^{-1} >> |\omega_{o_A} - \omega_{o_B}|,\ T_{2A}^{-1}\ T_{2B}^{-1}$$

equation (2.9) simplifies to:

$$v = \frac{-\gamma B_1 M_{z(eq)}(P_A T_{2A}^{-1} + P_B T_{2B}^{-1})}{(P_A T_{2A}^{-1} + P_B T_{2B}^{-1})^2 + (P_A \omega_{o_A} + P_B \omega_{o_B} - \omega)^2}$$

which describes a single narrow Lorentzian lineshape centred at $(\omega_{o_A} P_A + \omega_{o_B} P_B)$, containing no kinetic information where

$$T_{2obs}^{-1} = (P_A T_{2A}^{-1} + P_B T_{2B}^{-1})$$

In Figure 3.1 the variation of nmr lineshape with increase in temperature (coalescence phenomenon) ranging from the limiting conditions of slow to fast exchange is shown.

2.2 Lineshape Analysis

The total lineshape analysis of experimental nmr spectra was achieved using an interactive program "LINSHP" which was based on the published methods of Nakagawa[10] and Sidall, Stewart and Knight[11] and adapted[12] for use on the BNC-12 mini computer of the Bruker HX-90E spectrometer. This program uses a visual comparison of the experimental and calculated lineshapes utilising a difference display to obtain accurate values for the rates of exchange for the process.

As the lineshape analysis program used in this research is based on a continuous wave treatment and most of the dynamic nmr spectra were recorded in the Fourier transform mode the question of whether Fourier transform and C.W. spectra are equivalent will arise. It has been shown that for simple uncoupled spin systems undergoing chemical exchange the lineshapes obtained from a Fourier transform experiment are equivalent to those obtained from a C.W. experiment[13,14]. If coupling occurs between exchanging nuclear spins the above methods cannot be applied. However if

coupling occurs within an exchanging group (e.g. ^{31}P-^{1}H coupling in tmp or dmmp) then equation (2.10) can be applied to each of the coalescing doublets with the summation of the two applications giving the total lineshape.

The accuracy of the kinetic information obtained from the total lineshape analysis of coalescing nmr spectra is critically dependent upon a number of input parameters[20]. The parameters of importance are the chemical shift difference, relative populations and transverse relaxation times (linewidths). In order to minimise systematic errors (from being introduced,) the variation of these parameters with temperature in the region of very slow or no exchange were obtained and subsequently extrapolated into the temperature range where the rate of exchange varied from slow to fast.

For all the "systems" examined little or no variation of the expected relative populations with temperature was observed in the region of very slow exchange. However a marked variation of chemical shift and line width with temperature was observed for certain systems (as indicated in later sections), and for these systems an iterative fitting procedure based on the extrapolated values was applied.

The use of Fourier Transform nmr and a difference display for the comparison of the experimental and calculated spectra enabled minor problems such as spectral phasing, baseline irregularities and superimposed diluent impurity signals to be eliminated.

2.3 Calculation of Activation Parameters

Transition State Theory describes the dependance of the rate constant on temperature and is expressed by the Eyring equation[15] (2.10)

$$k_{ex} = \frac{k_B T}{h} \exp\left(-\frac{\Delta G^{\neq}}{RT}\right) \qquad (2.10)$$

$$= \frac{k_B T}{h} \exp\left(\frac{-\Delta H^{\neq}}{RT}\right) \exp\left(\frac{\Delta S^{\neq}}{R}\right)$$

where k_B = Boltzmann's constant

h = Planck's constant

and T = Temperature (K)

The linear form of the Eyring equation

$$\ln(\frac{T}{k_{ex}}) = \frac{\Delta H^{\neq}}{RT} + \ln(\frac{h}{k_B} - \frac{\Delta S^{\neq}}{R}) \qquad (2.11)$$

is usually used so that a linear least squares fitting method can be employed.

For the systems where the rate law had a single term the activation enthalpies and entropies were calculated using a computer program ACTENG[17] which utilised the above method. (The mechanistic interpretation of the rate laws and the experimental $\Delta H^{\neq}$ and $\Delta S^{\neq}$ values obtained will be discussed in later chapters.) The errors quoted for the activation parameters obtained using this program are the standard deviations for the linear least squares fit.

However if the solvent exchange rate consists of two or more elementary steps (in this work rate laws of the form rate = $4k_{ex}[MS_4^{m+}] = 4[k_1 + k_2[S]][MS_4^{m+}]$ were obeyed) then a plot of $\ln k_{ex}/T$ versus T^{-1} will not necessarily be linear since the slope, $\Delta H^{\neq}/R$, consists of two terms, i.e. $\Delta H^{\neq}_1/R + \Delta H^{\neq}_2/R$.

For such systems the experimental data were fitted to a two term Eyring equation of the form:

$$k_{ex} = k_1 + k_2[S]$$

$$= \frac{k_B T}{h}\left[\exp(\frac{\Delta S_1^{\neq}}{R} - \frac{\Delta H_1^{\neq}}{RT}) + [S]\exp(\frac{\Delta S_2^{\neq}}{R} - \frac{\Delta H_2^{\neq}}{RT})\right] \qquad (2.12)$$

A non-linear least squares fitting computer program DATAFIT[21] was utilised in conjunction with equation (2.12) to obtain the four activation parameters $\Delta H_1^{\neq}$, $\Delta S_1^{\neq}$, $\Delta H_2^{\neq}$ and $\Delta S_2^{\neq}$. (Pisaniello[16] has briefly outlined the advantages of this method over those employed previously[18].) DATAFIT

minimises the residual differences in an n-dimensional sum of squares space between a calculated and an experimental surface (as defined by $[S]_{free}$, temperature and k_{ex}) by one of the methods developed by Pitha and Jones[19]. The errors quoted for these activation parameters are the standard deviations for each parameter in the sum of squares space.

An advantage of using DATAFIT is that it provides a means of simplifying difficult kinetic decisions, for example if a plot of k_{ex} vs. $[S]_{free}$ is linear but there is an uncertainty as to whether the intercept is real then DATAFIT provides a statistical means of accepting or rejecting the nature of the intercept and associated mechanism. At this point it is worth mentioning another factor which is important in determining the accuracy of the activation parameters obtained from the lineshape analysis of the variable temperature nmr spectra, that is the sample temperature itself. Even small variations in the sample temperature (1 - 2 K) can produce major changes to the activation parameters concerned. For all the work reported herein the inaccuracy of the sample temperature was limited to 0.3 K by using a copper-constantan thermocouple.

REFERENCES: CHAPTER 2

1. F. Bloch, *Phys. Rev.*, 70, 460 (1946).
2. H.S. Gutowsky, D.M. McCall and C.P. Slichter, *J. Chem. Phys.*, 28, 430 (1953).
3. E.L. Hahn and D.E. Maxwell, *Phys. Rev.*, 88, 1070 (1952).
4. H.M. McConnell, *J. Chem. Phys.*, 28, 430 (1958).
5. R. Kubo, *J. Phys. Soc. Jap.*, 9, 935 (1954).
6. R. Kubo and K. Tomita, *J. Phys. Soc. Jap.*, 9, 888 (1954).
7. R.A. Sack, *J. Mol. Phys.*, 1, 163 (1958).
8. H.S. Gutowsky and A. Saika, *J. Chem. Phys.*, 21, 1688 (1953).
9. H.S. Gutowsky and C.H. Holm, *J. Chem. Phys.*, 25, 1228 (1956).
10. T. Nakagawa, *Bull. Chem. Soc. Jap.*, 39, 1006 (1966).
11. T.E. Sidall III, W.E. Stewart and F.D. Knight, *J. Phys. Chem.*, 74, 3580 (1970).
12. E.H. Williams, *Ph.D. Dissertation*, The University of Adelaide, 1980.
13. R.K. Gupta, T.P. Pitner and R. Wasylishen, *J. Mag. Res. Comm.*, 13, 383 (1974).
14. T.C. Farrar and E.D. Becker, "*Pulsed Fourier Transform NMR*", Academic Press, N.Y. 1971.
15. (a) W.F.K. Wynne-Jones and H. Eyring, *J. Chem. Phys.*, 3, 492 (1935).
    (b) S. Glasstone, K.J. Laidler and H. Eyring in "*Theory of Rate Processes*", McGraw-Hill, N.Y. 1941.
16. D.L. Pisaniello, *Ph.D. Dissertation*, The University of Adelaide, 1980.
17. ACTENG Quantum Chemistry Program Exchange, 79.
18. G.J. Honan, S.F. Lincoln and E.H. Williams, *Inorg. Chem.*, 17, 1855 (1978).
19. J. Pitha and R.N. Jones, *Can. J. Chem.*, 44, 3031 (1966).
20. S. Szymanski, M. Witanowski and A. Gryff-Keller, in "*Annual Report on NMR Spectroscopy*", 8, 228 (1978).
21. T. Kurucsev, unpublished data.

CHAPTER 3: LIGAND EXCHANGE ON ZINC(II)

3.1 Introduction

Since zinc(II) is one of the more labile metal ions[1-3] and also lacks d-d absorption bands it is one of the metal ions less amenable to ligand exchange studies. X-ray[4] and ^1H nmr[5] studies have shown that the octahedral $[Zn(H_2O)_6]^{2+}$ species is predominant in aqueous solution in the presence of non-coordinating anions, and from ultrasonic[6] and T-Jump[7] studies the rate constant for the exchange of a single water molecule on this species is estimated to be $k_{ex}(298.2\ K) \approx 3 \times 10^7\ s^{-1}$. In methanol, nmr studies indicate that $[Zn(MeOH)_6]^{2+}$ is the predominant species in dilute solution[8,9] where $k_{ex}(298.2\ K) = 1.7 \times 10^4\ s^{-1}$. Furthermore stopped-flow spectrophotometric studies in dmso where $[Zn(dmso)_6]^{2+}$ is assumed to be the exchanging species[10] has an estimated $k_{ex}(298.2\ K) \approx 8.7 \times 10^5\ s^{-1}$.

From these ligand exchange studies[1-3,6-7,10] it appears that the Eigen[1-3] or dissociative interchange mechanism[11] is consistent with the kinetics of ligand exchange at the octahedrally coordinated zinc(II) centre. In contrast a ^1H nmr study[12] of zinc(II) thiourea complexes (where the assumed zinc(II) species in solution is $ZnCl_2tu_2$) gives $k_{ex}(298.2\ K) \approx 1.5 \times 10^4\ dm^3\ mol^{-1}\ s^{-1}$ where an associative ligand exchange mechanism has been assigned. X-ray studies[14] have shown that zinc(II) thiourea complexes have tetrahedral geometry (common for zinc(II)[31]) and are bound through the sulphur atom of the ligand. The range of the above kinetic investigations is very limited and no published reports of the simultaneous determination of the rate law for the ligand exchange process plus stoichiometry of the $[ZnL_m]^{2+}$ species have appeared.

One aim of this research project was to provide insights into the rates and mechanisms of ligand exchange on zinc(II) species in non-aqueous

solutions and this was achieved by the systematic study of ligand exchange on the zinc(II) centre which is reported in this chapter.

3.2 Ligand exchange on tetrakis(1,1,3,3-tetramethylthiourea) zinc(II)

The white air stable solid $[Zn(tmtu)_4](ClO_4)_2$, obtained from the preparative procedure outlined in section 6.2 was used in this study. Solutions containing $[Zn(tmtu)_4](ClO_4)_2$ and tmtu in CD_2Cl_2 (solution compositions given in Table 3.1) were prepared under anhydrous conditions.

A typical set of ^1H nmr spectra characterising the exchange of tmtu on $[Zn(tmtu)_4]^{2+}$ in CD_2Cl_2 solution is shown in Figure 3.1, the low and high field singlets arise from the methyl groups of the coordinated and free tmtu respectively and a comparison of the integrated areas of these signals in the slow exchange spectra in the temperature range 170 - 185 K indicate that $[Zn(tmtu)_4]^{2+}$ is the dominant zinc(II) species in solution over the 180 fold concentration range of free tmtu studied.

The observation of the singlet resonances for both the coordinated and free ligands (low temperature ^1H nmr spectra of tmtu in CD_2Cl_2 and $[Zn(tmtu)_4]$ $(ClO_4)_2$ in CD_2Cl_2 verified these results) indicate that the rate of rotation about the C-N bond is in the fast eachange limit in both environments.

A complete lineshape analysis of the temperature dependent spectra in the range 185 - 220 K yields the kinetic parameters for ligand exchange on $[Zn(tmtu)_4]^{2+}$ which are given in Table 3.1. The rate constants are quoted at 200 K which is in the middle of the spectral coalescence temperature range.

From the k_{ex} values (in Table 3.1) it is apparent that the predominant ligand exchange path is independent of free ligand concentration and that unless there is an exceptional degree of preferential occupation of the second coordination sphere of $[Zn(tmtu)_4]^{2+}$ by tmtu, the mechanism of ligand exchange is of the

Figure 3.1

^1H (90 MHz) nmr temperature dependent spectra characterising tmtu exchange on $[Zn(tmtu)_4]^{2+}$ in a solution 0.00101 and 0.00376 mol dm^{-3} in $[Zn(tmtu)_4{}^{2+}]$ and $[tmtu]_{free}$ respectively. The low and high field singlets arise from coordinated and free tmtu respectively in the experimental spectra at the left of the Figure. Experimental temperatures appear at the left of the Figure, and calculated best fit spectra and the corresponding τ_c(ms) values appear at the right.

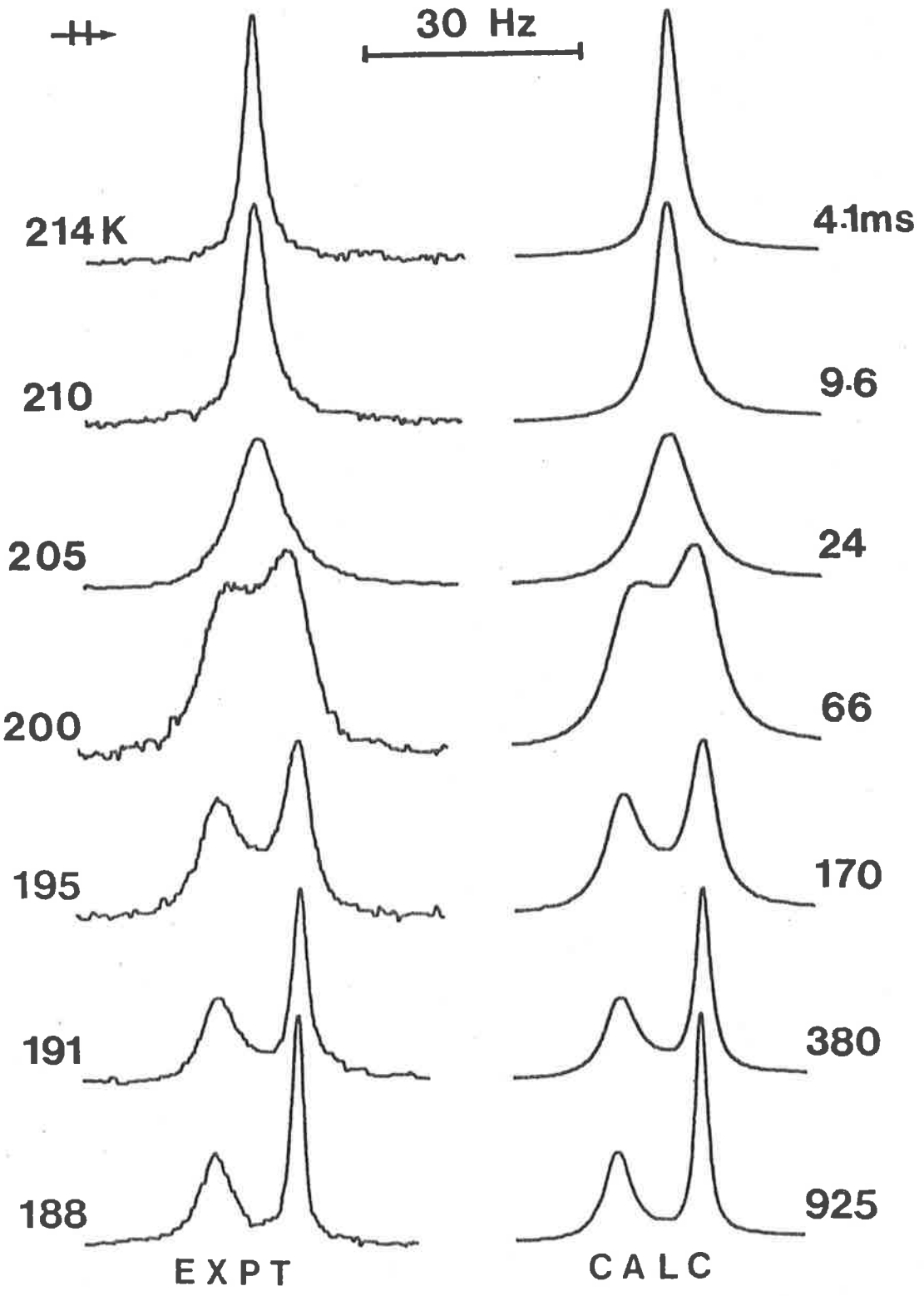
30 Hz
214 K
210
205
200
195
191
188
4.1ms
9.6
24
66
170
380
925
EXPT
CALC

Table 3.1 Solution Compositions and kinetic parameters for tmtu exchange on $[Zn(tmtu)_4]^{2+}$

Solution	$[Zn(tmtu)_4{}^{2+}]$	$[tmtu]_{free}$	$[CD_2Cl_2]$	k_{ex}(200 K)	$\Delta H^{\neq}$	$\Delta S^{\neq}$	CN
	mol dm^{-3}	mol dm^{-3}	mol dm^{-3}	s^{-1}	kJ mol^{-1}	J K^{-1} mol^{-1}	
(i)	0.00101	0.00376	15.24	16.0 ± 0.6	64.9 ± 0.8	106 ± 4	4.05 ± 0.05
(ii)	0.00245	0.00907	15.24	16.3 ± 0.5	62.9 ± 0.7	96 ± 3	4.10 ± 0.10
(iii)	0.00411	0.0138	15.23	16.4 ± 0.6	62.9 ± 0.8	96 ± 4	3.95 ± 0.05
(iv)	0.00804	0.0427	15.23	15.8 ± 0.7	64.3 ± 0.9	103 ± 5	4.05 ± 0.05
(v)	0.0427	0.143	14.98	16.0 ± 0.5	63.4 ± 0.6	98 ± 3	4.00 ± 0.05
(vi)	0.0618	0.207	14.87	16.1 ± 0.6	63.5 ± 0.8	99 ± 4	3.95 ± 0.05
(vii)	0.201	0.675	13.99	18.7 ± 0.9	62.1 ± 1.2	93 ± 6	4.00 ± 0.05

dissociative type[10] where the rate determining step is the formation of the reactive intermediate $[Zn(tmtu)_3]^{2+}$ and $k_{ex} = k_1$, the specific rate constant for the process.

The positive $\Delta S^{\neq}$ values characterising the exchange process are consistent with the formation of a dissociative transition state in which the production of virtually two species, the incipient reactive intermediate and the leaving ligand, from a single species leads to an increase in entropy. However solvent rearrangements outside the first coordination sphere[15] and changes in the rotational and vibrational states of ligands[16] occurring synchronously with the formation of the transition state may make contributions to $\Delta S^{\neq}$ which outweigh those arising from the primary ligand dissociation process thereby making mechanistic judgements on the basis of $\Delta S^{\neq}$ of dubious value.

For the $[Zn(tmtu)_4]^{2+}$ species the rate of ligand exchange $k_{ex}(298.2\ K) = 9.2 \times 10^6\ s^{-1}$ falls well within the range defined for ligand exchange on the octahedral zinc(II) centres, $[Zn(MeOH)_6]^{2+}$ and $[Zn(H_2O)_6]^{2+}$ where $k_{ex}(298.2\ K) = 1.7 \times 10^4\ s^{-1}$ and $3 \times 10^7\ s^{-1}$ respectively.

3.3 Ligand exchange on tetrakis(1,1,3,3-tetramethylurea) zinc(II), tetrakis(N-methylacetamide) zinc(II), hexakis(N,N-dimethylformamide) zinc(II) and hexakis(N,N-dimethylacetamide) zinc(II).

The white hygroscopic complexes $[Zn(tmu)_4](ClO_4)_2$, $[Zn(nma)_4](ClO_4)_2$, $[Zn(dmf)_6](ClO_4)_2$ and $[Zn(dma)_6](ClO_4)_2$ were isolated from the preparative procedures outlined in section 6.2. All the above complexes were soluble in CD_2Cl_2.

No separate ^1H nmr resonances arising from coordinated and free ligands were observed for any of the above species in the presence of four and six fold excesses of free ligand for the first two and second two zinc(II) complexes above respectively, in CD_2Cl_2 solution down to

170 K the lowest temperature accessible for these systems. This indicates that the rate of ligand exchange for the above species is in the nmr fast exchange limit and the exchange rates and solution state stoichiometries could not be obtained for these systems.

3.4 Ligand exchange on tetrakis(hexamethylphosphoramide) zinc(II)

The air stable white solid $[Zn(hmpa)_4](ClO_4)_2$ was isolated from the preparation described in section 6.2. This complex has previously been prepared by Donoghue and Drago[19], however no kinetic study had been reported.

Broad band ^1H decoupled ^{31}P nmr spectroscopy was employed in this study as the ^1H nmr chemical shift difference between the free and bound ligand signals was too small to allow accurate kinetic measurements to be made. Solutions containing $[Zn(hmpa)_4](ClO_4)_2$ and hmpa in CD_2Cl_2 were prepared (see Table 3.2 for solution compositions).

A typical set of broad band ^1H decoupled ^{31}P (36.43 MHz) nmr spectra characterising the exchange of hmpa on $[Zn(hmpa)_4]^{2+}$ in CD_2Cl_2 solution is shown in Figure 3.2. The low and high field singlets arise from coordinated and free hmpa respectively and a comparison of the integrated areas over the temperature range 175 -- 195 K indicates that $[Zn(hmpa)_4]^{2+}$ is the dominant zinc(II) species in the six solutions examined. Because the rate of ligand exchange was found to be dependent upon $[hmpa]_{free}$ the temperature at which the ^{31}P singlets coalesce increases as the $[hmpa]_{free}$ decreases in solutions (vi) - (i).

Complete lineshape analysis of the spectra for all six solutions yields the mean site lifetime of hmpa coordinated to zinc(II), τ_c, which is related to the observed first order exchange rate constant $k_{ex} = \frac{1}{\tau_c}$.

It is seen from Figure 3.3 that τ_c decreases systematically as $[hmpa]_{free}$ increases and consequently all the datum points were fitted

Figure 3.2

Broad band ^{1}H decoupled Fourier transformed ^{31}P nmr temperature dependent spectra for hmpa exchange on $[Zn(hmpa)_4]^{2+}$ in a solution 0.337 and 1.49 mol dm^{-3} in $[Zn(hmpa)_4{}^{2+}]$ and $[hmpa]_{free}$ respectively. The low and high field singlets arise from coordinated and free hmpa respectively in the experimental spectra at the left of the Figure. Experimental temperatures appear at the left of the Figure, and calculated best-fit spectra and the corresponding τ_c(ms) values appear at the right.

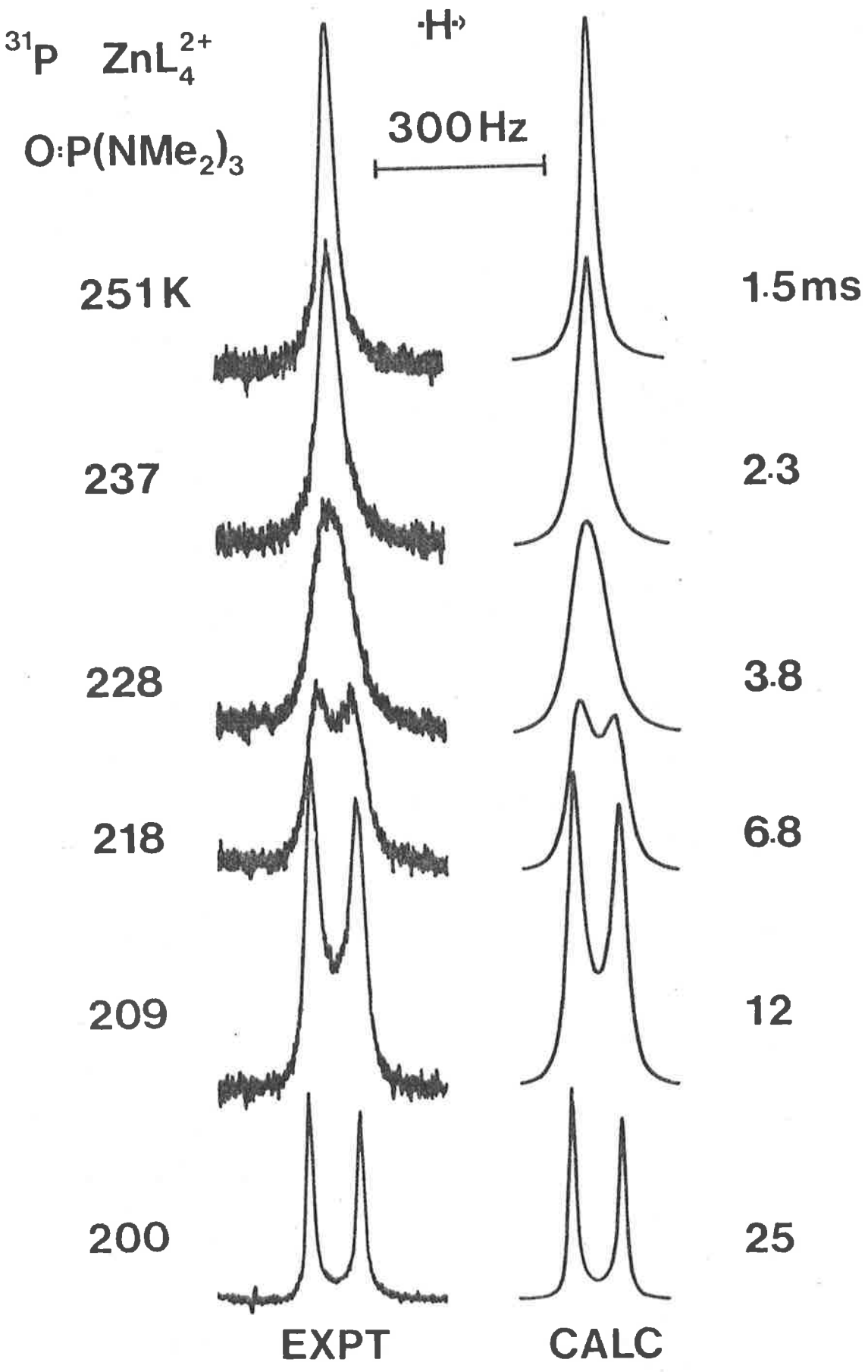
^{31}P ZnL_4^{2+}
O:P(NMe$_2$)$_3$
·H·
300 Hz
251 K
237
228
218
209
200
1.5 ms
2.3
3.8
6.8
12
25
EXPT
CALC

Table 3.2 Solution compositions and kinetic parameters for hmpa exchange on $[Zn(hmpa)_4]^{2+}$.

Solution	$[Zn(hmpa)_4]^{2+}$ mol dm $^{-3}$	$[hmpa]_{free}$ mol dm^{-3}	$[CD_2Cl_2]$ mol dm^{-3}	CN
(i)	0.0448	0.162	14.95	3.9 ± 0.1
(ii)	0.074	0.271	14.26	4.0 ± 0.1
(iii)	0.126	0.552	13.92	4.0 ± 0.1
(iv)	0.199	0.884	12.79	4.0 ± 0.1
(v)	0.225	0.988	9.45	4.0 ± 0.1
(vi)	0.337	1.493	8.27	4.0 ± 0.1

$k_2(240)$ dm^3 mol^{-1} s^{-1}	$\Delta H_2^{\neq}$ kJ mol^{-1}	$\Delta S_2^{\neq}$ J K^{-1} mol^{-1}
304 ± 17	22.7 ± 0.9	-101 ± 4

$k_1(240)$ s^{-1}	$\Delta H_1^{\neq}$ kJ mol^{-1}	$\Delta S_1^{\neq}$ J K^{-1} mol^{-1}
18 ± 5	13.9 ± 3.9	-161 ± 19

to a two term Eyring equation. The derived kinetic parameters are given in Table 3.2. The error in k_1 is such that the existence of the k_1 path is left in considerable doubt and accordingly only the k_2 exchange path is considered. So for hmpa exchange on $[Zn(hmpa)_4]^{2+}$ in CD_2Cl_2 solution a second order rate law is observed where

$$\text{rate} = 4k_2[\text{hmpa}]_{\text{free}}[Zn(hmpa)_4{}^{2+}]$$

and the mechanism of ligand exchange is of the associative type where the rate determining step is the formation of a reactive intermediate $[Zn(hmpa)_5]^{2+}$ where $k_{ex} = k_2[\text{hmpa}]_{\text{free}}$.

Hexamethylphosphoramide, probably as a consequence of its bulkiness and its high DN (38.8)[20], stabilises four coordination in the species $[M(hmpa)_4]^{n+}$ where $M^{n+} = Al^3$, Be^{2+}, Ni^{2+}, Mn^{2+} and Zn^{2+}, whereas with other oxygen donor solvents smaller in size and of lower DN, these metal ions commonly exhibit a coordination number of six[17,21,22] (except for Be^{2+} where CN = 4 is common).

Dissociative (D) and associative (A) ligand exchange mechanisms have been assigned to the $[Be(hmpa)_4]^{2+}$ and $[Al(hmpa)_4]^{2+}$[17,22] systems respectively on the basis of the ligand exchange rate laws (Table 3.3). Of these metal ions beryllium(II) is the smallest (r = 0.027 nm: this is the effective ionic radius for a tetrahedral environment as are the other quoted values)[23] and as a consequence steric crowding is probably an important factor leading to the operation of a D mechanism, whereas the larger (r = 0.039 nm)[23] aluminium(III) ion facilitates the operation of an A mechanism. On this basis an A mechanism is to be expected for the $[Zn(hmpa)_4]^{2+}$ system as zinc(II) is larger (r = 0.06 nm)[23] than aluminium(III). Further evidence supporting the steric crowding argument comes from considering the complexes of Al^{3+}, Be^{2+} and Zn^{2+} with the bidentate analogue of hexamethylphosphoramide, nonamethylimidodiphosphoramide (nipa).

Figure 3.3

The variation of $\tau_c T$ with $[hmpa]_{free}$ and temperature. The data sets arise from solutions (vi) - (i) in ascending order of magnitude of $\tau_c T$ at any given temperature. The line represents the simultaneous best fit of all of the datum points.

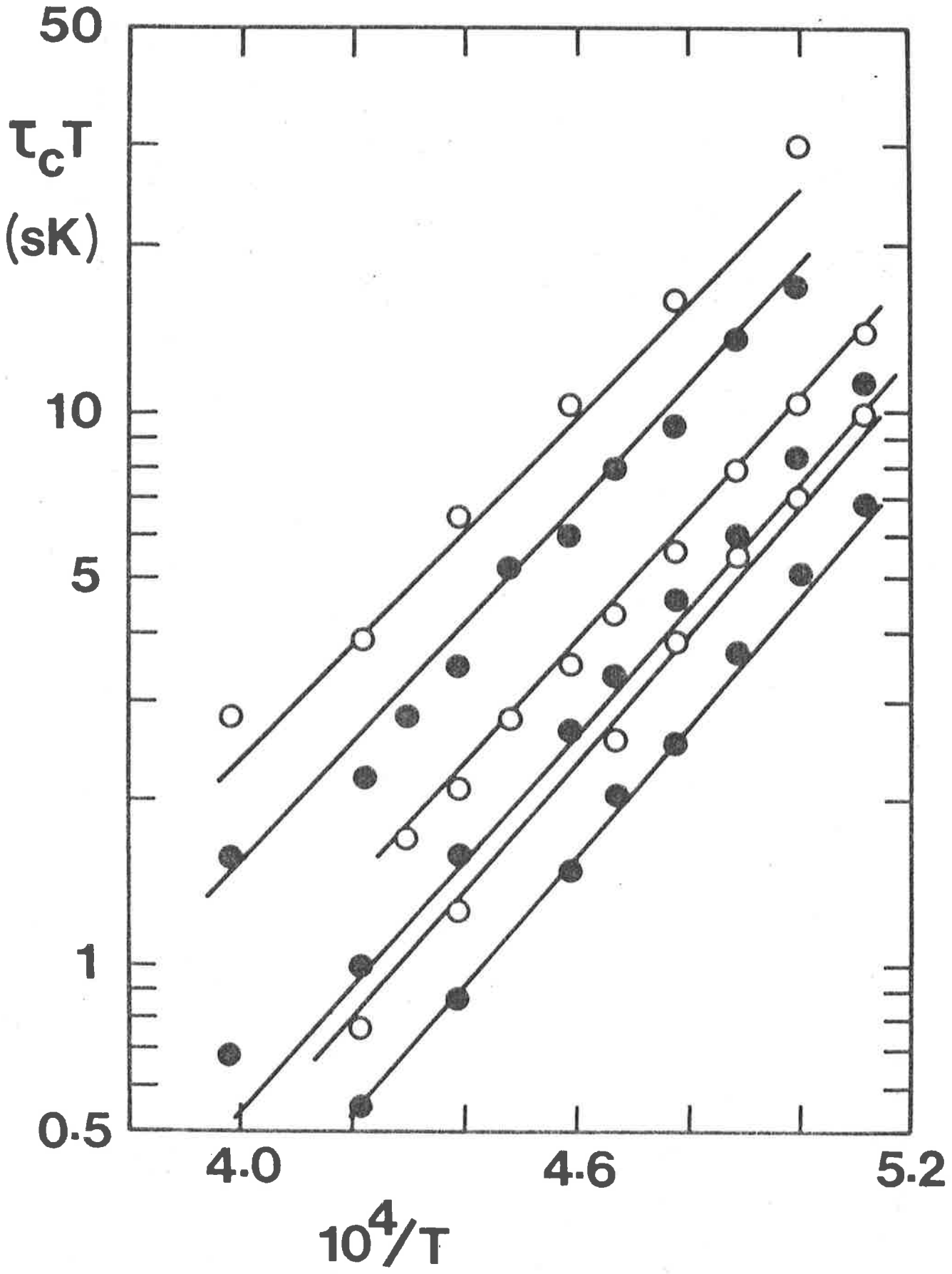
50
$\tau_c T$
(sK)
10
5
1
0·5
4·0
4·6
5·2
$10^4/T$

A comparison of the ground state coordination numbers for these metal ions when hmpa and nipa are coordinated shows that the coordination number for beryllium(II)[24,25] does not change from four, whereas for aluminium(III)[24,25] and zinc(II)[24.25] the coordination number increases from four to six.

These results confirm that steric crowding around beryllium(II) is considerable and the operation of a D ligand exchange mechanism is consistent with this. For aluminium(III) and zinc(II) steric crowding is less and the operation of an associative ligand exchange mechanism where the reactive intermediate is $[M(hmpa)_5]^{n+}$ is very plausible. A change in ligand results in a change to a D ligand exchange mechanism in the $[Zn(tmtu)_4]^{2+}$ system[26]. The overall size of hmpa is significantly larger than that of tmtu, the larger sulphur donor atom will result in more crowding in the immediate vicinity of the zinc(II) centre in $[Zn(tmtu)_4]^{2+}$ than in $[Zn(hmpa)_4]^{2+}$ and in consequence an assessment of the relative steric effects of the two ligands upon mechanism is difficult.

Secondly sulphur is more polarisable than oxygen (in consequence of which these donor atoms have been classified as soft and hard bases respectively)[27] and this may stabilise a zinc(II) (intermediate acid)[27] D reactive intermediate more than oxygen when acting as a donor atom.

From Table 3.3 it can be seen that $\Delta H^{\neq}$ is more important relative to $\Delta S^{\neq}$ in determining $\Delta G^{\neq}$ in the $[Zn(tmtu)_4]^{2+}$ system than is the case in the $[Zn(hmpa)_4]^{2+}$ system; a difference which clearly arises from the dissimilarities of the two ligands. When the ligand is hmpa and the metal is varied it is seen (Table 3.3) that $\Delta H^{\neq}$ for Al^{3+} and Zn^{2+}, on which ligand exchange occurs via an associative mechanism, is considerably less than that for Be^{2+} on which ligand exchange occurs through a D mechanism and further, that negative $\Delta S^{\neq}$ values characterise Al^{3+} and Zn^{2+} while a positive $\Delta S^{\neq}$ characterises Be^{2+}.

Table 3.3 Kinetic Parameters for ligand exchange on $[ML_4]^{n+}$ ions.

L	M^{n+}	k_1(298.2 K) (s^{-1})	k_2(298.2 K) $dm^3\ mol^{-1}\ s^{-1}$	$\Delta H^{\neq}$ $kJ\ mol^{-1}$	$\Delta S^{\neq}$ $J\ K^{-1}\ mol^{-1}$	Diluent	Ref.
hmpa	Zn^{2+}	-	3430 ± 460	22.7 ± 0.9	-101 ± 4	CD_2Cl_2	
hmpa	Be^{2+}	0.00027	-	117	78	B	17
hmpa	Al^{3+}	-	4800	32.2	-66.4	CH_3NO_2	13[A]

[A] $\Delta S^{\neq}$ quoted in this reference is -42.7 $J\ K^{-1}\ mol^{-1}$ which is in conflict with the values quoted for $\Delta H^{\neq}$ and k_2. The $\Delta S^{\neq}$ value has been recalculated on the assumption that k_2 and $\Delta H^{\neq}$ are correctly quoted in ref. 13.

[B] 4-Methyl-1,3-dioxolan-2-one, $O{=}\overline{COCH(CH_3)CH_2O}$.

It appears that the exchange of hmpa on M^{n+} is characterised by positive and negative $\Delta S^{\neq}$ values for D and A mechanisms, that $\Delta H^{\neq}$ is lower for an A mechanism than for a D mechanism and further that $\Delta H^{\neq}$ tends to decrease as the formal surface charge density ($m+/r^2$) of the metal ion decreases.

Care should be taken in attributing these observations solely to the factors considered above because, as a result of the characteristic dynamic temperature ranges, the beryllium(II), aluminium(III) and zinc(II) systems were studied in the non-coordinating diluents $O{=}\overline{COCH(CH_3)CH_2O}$, CH_3NO_2 and CD_2Cl_2 respectively and that the nature of the diluent can significantly affect activation parameters[17,18,28] and change rate laws[29].

3.5 Ligand exchange on pentakis(trimethylphosphate) zinc(II) and pentakis(dimethylmethylphosphonate) zinc(II)

The hygroscopic complexes $[Zn(tmp)_5](ClO_4)_2$ and $[Zn(dmmp)_5](ClO_4)_2$ were prepared following the procedure in section 6.2.

Solutions of $[Zn(tmp)_5](ClO_4)_2$ and $[Zn(dmmp)_5](ClO_4)_2$ and five fold excess concentrations of their respective free ligands, in CD_2Cl_2, exhibited only one ^{31}P nmr resonance in the temperature range 170 - 300 K. The results are consistent with ligand exchange being in the nmr fast exchange limit, and consequently it was not possible to determine the coordination numbers for the zinc(II) species in solution.

If the coordination number is greater than four in solution then the increased steric crowding at the zinc(II) centre would probably both labilise the ligand and result in a D mechanism operating.

3.6 Ligand exchange on tetrakis(triphenylphosphine oxide) zinc(II)

The white complex $[Zn(tppo)_4](ClO_4)_2$ was prepared by the method described in section 6.2. Cotton and Bannister[30] had previously reported the preparation of this complex however no kinetic study was undertaken.

Broad band ^{1}H decoupled ^{31}P nmr spectroscopy was used in this study due to the complex nature of the ^{1}H nmr spectrum of the ligand. Solutions containing $[Zn(tppo)_4](ClO_4)_2$ and tppo in CD_2Cl_2 were prepared under anhydrous conditions (see Table 3.4 for solution compositions). Over the eight fold concentration range of free tppo studied, the only detectable zinc(II) species in solution is $[Zn(tppo)_4]^{2+}$ as determined from a comparison of the integrated areas of the ^{31}P singlets of coordinated and free tppo over the temperature range 175 - 185 K.

Typically for solution (iv) (Table 3.4), the singlet for the coordinated tppo is observed 633 Hz downfield from that of free tppo. In the temperature range 185 - 220 K the tppo exchange rate increases from the slow exchange limit to the fast exchange limit of the nmr timescale and complete lineshape analysis of the spectra within this range at 5 K temperature intervals yielded the exchange rate constant k_{ex}. A comparison of the derived k_{ex}, $\Delta H^{\neq}$ and $\Delta S^{\neq}$ values for solutions (i) - (iv) shows that the results are virtually indistinguishable and are consistent with the rate determining step being the formation of a reactive intermediate of reduced coordination number characteristic of a (D) dissociative ligand exchange mechanism[11].

It is of interest at this point to compare these results with those obtained for tppo exchange on Mg^{2+}. Both four and five coordinate magnesium(II) species exist in CD_2Cl_2 solution as shown below

$$[Mg(tppo)_4]^{2+} + tppo \rightleftharpoons [Mg(tppo)_5]^{2+}$$

whereas in the solid state only $[Mg(tppo)_4](ClO_4)_2$ was found. (Crystal packing forces may cause $[Mg(tppo)_4]^{2+}$ to be more stable than $[Mg(tppo)_5]^{2+}$.) However the stability of the $[Mg(tppo)_5]^{2+}$ complex in solution is such that if $[[Mg(tppo)_5](ClO_4)_2]/[tppo]_{free} < 1$ then singlets arising from $[Mg(tppo)_5]^{2+}$ and tppo are observed, when this ratio > 1 then singlets arising from $[Mg(tppo)_5]^{2+}$ and $[Mg(tppo)_4]^{2+}$ are observed.

Table 3.4 Solution compositions and kinetic parameters for tppo exchange on $[Zn(tppo)_4]^{2+}$ in CD_2Cl_2 solution.

Solution	$[Zn(tppo)_4^{2+}]$ mol dm^{-3}	$[tppo]_{free}$ mol dm^{-3}	$[CD_2Cl_2]$ mol dm^{-3}	k_{ex}(200 K) s^{-1}	$\Delta H^{\neq}$ kJ mol^{-1}	$\Delta S^{\neq}$ J K^{-1} mol^{-1}	CN
(i)	0.0202	0.079	15.01	620 ± 19	31.7 ± 0.3	-29.6 ± 1.6	4.0 ± 0.2
(ii)	0.0427	0.167	14.75	610 ± 19	32.0 ± 0.3	-28.0 ± 1.7	4.1 ± 0.1
(iii)	0.0925	0.363	14.15	625 ± 27	31.6 ± 0.5	-29.8 ± 2.4	4.1 ± 0.1
(iv)	0.163	0.639	13.79	611 ± 37	31.9 ± 0.7	-28.2 ± 3.4	4.1 ± 0.1
	$[Mg(tppo)_5^{2+}]$	[tppo]		k_{ex}(220 K)	$\Delta H^{\neq}$	$\Delta S^{\neq}$	
(v)	0.0813	0.276		38 ± 4	73.7 ± 1.8	123 ± 8	
		$[Mg(tppo)_4^{2+}]$					
(vi)	0.050	0.050		[a] 200 ± 20	73.0 ± 1.6	[a] 133 ± 7	
				[b] 40 ± 4	73.0 ± 1.6	[b] 120 ± 7	

Quoted errors represent one standard deviation using ACTENG[32].

[a] k_{ex} and $\Delta S^{\neq}$ refer to the interconversion of $[Mg(tppo)_5]^{2+}$ to $[Mg(tppo)_4]^{2+}$ such that the ligand exchange rate = $\tau_{Mg}^{-1}[Mg(tppo)_5^{2+}]$.

[b] k_{ex} and $\Delta S^{\neq}$ refer to the exchange of one tppo ligand on $[Mg(tppo)_5]^{2+}$ such that the ligand exchange rate = $5\tau_c^{-1}[Mg(tppo)_5^{2+}]$.

The equilibrium constant K_{eq} is of the order 150 $dm^3\ mol^{-1}$ where

$$K_{eq} = \frac{[Mg(tppo)_5{}^{2+}]}{[Mg(tppo)_4{}^{2+}][tppo]_{free}}$$

It was shown that a dissociative mechanism[11] provides the predominant path for ligand exchange on $[Mg(tppo)_5]^{2+}$ (see Table 3.4).

The effective ionic radii of four coordinate magnesium(II) and zinc(II) are 0.067 nm and 0.068 nm respectively[23], from which it is concluded that steric effects are unlikely to cause the differences observed for the tppo complexes of magnesium(II) and zinc(II) in CD_2Cl_2 solution. Therefore an alternative origin of these differences must be sought.

Magnesium(II) has the neon electronic configuration while zinc(II) is characterized by [Ne] $3s^2 3p^6 3d^{10}$ which is reflected on an empirical basis by magnesium(II) behaving as a hard acid whilst zinc(II) exhibits characteristics which are borderline between those of a soft and hard acid[27]. Consequently magnesium(II) forms its most stable complexes with oxygen donor ligands whereas zinc(II) forms stable complexes with ligands bonding through sulphur or oxygen. These expectations may partly explain why zinc(II) achieves four coordination in $[Zn(tppo)_4]^{2+}$ in CD_2Cl_2 solution whilst magnesium(II) is five coordinate in $[Mg(tppo)_5]^{2+}$ under similar conditions.

From the study of zinc(II) a comparison of the activation parameters for the oxygen donor systems and the sulphur donor systems shows that $\Delta H^{\neq}$ and $\Delta S^{\neq}$ for the $[Zn(tmtu)_4]^{2+}$ system[26] increases markedly in magnitude relative to the oxygen donor systems. A quantitative comparison of tmtu and its oxygen donor analogue, tetramethylurea (in the $[Zn(tmu)_4]^{2+}$ system), was not possible as the latter system was in the fast exchange limit of the nmr timescale under the same conditions (concentrations and temperature) as the $[Zn(tmtu)_4]^{2+}$ system; nevertheless this observation demonstrates the marked effect of changing

the donor atom of the ligand. On the basis of the limited range of data it appears the greater $\Delta H^{\neq}$ value obtained for the $[Zn(tmtu)_4]^{2+}$ system compared with those obtained for the oxygen donor ligand systems may reflect the differences in bonding between zinc(II) and the soft base, sulphur and zinc(II) and the hard base oxygen.

REFERENCES: CHAPTER 3

1. M. Eigen, *Pure Appl. Chem.*, 6, 97 (1963).
2. M. Eigen and R.G. Wilkins, in "*Mechanisms of Inorganic Reactions*", Ed. R.F. Gould, American Chemical Society: Washington 1965.
3. J. Burgess, in "*Metal Ions in Solution*", Ellis Horwood Ltd., Chichester 1978.
4. H. Ohlaki, T. Yamaguchi and M. Maeda, *Bull. Chem. Soc. Jpn.*, 49, 701 (1976).
5. A. Fratiello, V. Kubo, S. Peak, B. Sanchez and R.E. Schuster, *Inorg. Chem.*, 10, 2552 (1971).
6. F. Fittipaldi and S. Petrucci, *J. Phys. Chem.*, 71, 3414 (1967).
7. M.W. Grant, *J. Chem. Soc., Faraday Trans. I*, 560 (1973).
8. S.A. Al-Baldawi and T.E. Gough, *Can. J. Chem.*, 47, 1417 (1969).
9. S.A. Al-Baldawi, M.H. Brooker, T.E. Gough and D.E. Irish, *Can. J. Chem.*, 48, 1202 (1970).
10. D.M.W. Buck and P. Moore, *J. Chem. Soc. (Dalton)*, 638 (1976).
11. C.H. Langford and H.B. Gray, "*Ligand Substitution Processes*", Benjamin: New York, 1966.
12. D.R. Eaton and K. Zaw, *J. Inorg. Nucl. Chem.*, 38, 1007 (1976).
13. L. Rodehüser, P.R. Rubini and J.-J. Delpuech, *Inorg. Chem.*, 16, 2827 (1977).
14. R. Vega, A. Lopez-Castro and R. Marquez, *Acta Cryst.*, B34, 2297 (1978).
15. E.F. Caldin and H.P. Bennetto, *J. Solution Chem.*, 2, 217 (1973).
16. H. Hoffman, *Pure Appl. Chem.*, 41, 327 (1975).
17. J.-J. Delpuech, A. Peguy, P. Rubini and J. Steinmetz, *Nouv. J. Chim.*, 1, 133 (1977).
18. J. Crea and S.F. Lincoln, *J. Chem. Soc. (Dalton)*, 2075 (1973).
19. J.T. Donoghue and R.S. Drago, *Inorg. Chem.*, 1, 866 (1962).
20. V. Meyer and V. Gutmann, *Struct. Bonding (Berlin)*, 12, 133 (1972).

21. S.F. Lincoln, *Coord. Chem. Rev.*, 6, 309 (1971).

22. J.-J. Delpuech, M.R. Khaddar, A.A. Peguy and P.R. Rubini, *J. Amer. Chem. Soc.*, 97, 3373 (1975).

23. R.D. Shannon and C.T. Prewitt, *Acta Cryst.*, B25, 925 (1969); B26, 1046 (1970).

24. J.-J. Delpuech, P.R. Rubini and L. Rodehüser, *Z. Naturforsch*, 33b, 684 (1978).

25. J.-J. Delpuech, P.R. Rubini and L. Rodehüser, *Inorg. Chem.*, 18, 2962 (1979).

26. Section 3.2.

27. F. Basolo and R.G. Pearson, "*Mechanisms of Inorganic Reactions*", J. Wiley: New York, 1967.

28. D.L. Pisaniello and S.F. Lincoln, *J. Chem. Soc. (Dalton)*, 699 (1980).

29. D.L. Pisaniello, S.F. Lincoln and E.H. Williams, *J. Chem. Soc. (Dalton)*, 1473 (1979).

30. E. Bannister and F.A. Cotton, *J. Chem. Soc.*, 1878 (1960).

31. F.A. Cotton and G. Wilkinson, "*Advanced Inorganic Chemistry*", Interscience: New York, 1972.

32. ACTENG Quantum Chemistry Program Exchange, 79.

CHAPTER 4: LIGAND EXCHANGE ON BERYLLIUM(II)

4.1 Introduction

The study of ligand exchange and substitution processes[1-11] on the beryllium(II) ion are of particular interest as a consequence of its small size (r = 0.027 nm)[12] and being one of the only tetrahedrally coordinated metal centres whose unidentate ligand exchange rate processes falls within experimentally accessible kinetic time scales.

In the earliest studies Connick *et al.*[13] and Alei *et al.*[14] determined the coordination number of beryllium(II) in aqueous solution utilising ^{17}O nmr and the molal shift method, and found four water molecules were coordinated to the beryllium(II) centre with $k_{ex}(298.2\ K) \approx 3000\ s^{-1}$. (Later studies[8] using ^{17}O and ^{1}H nmr spectroscopy separated the contributions of water exchange and protolysis to the kinetic process occurring at the Be^{2+} centre. Complete lineshape analysis methods gave more accurate values for water exchange, $k_{ex}(298.2\ K) = 1.8 \times 10^{3}\ s^{-1}$, $\Delta H^{\neq} = 41.5\ kJ\ mol^{-1}$ and $\Delta S^{\neq} = -44.0\ J\ K^{-1}\ mol^{-1}$.)

Matwiyoff and Movius[10] employed variable temperature ^{1}H nmr spectroscopy to obtain kinetic parameters for dmf exchange on $[Be(dmf)_4]^{2+}$ where $k_{ex}(298\ K) = 310\ s^{-1}$, $\Delta H^{\neq} = 61\ kJ\ mol^{-1}$ and $\Delta S^{\neq} = 11\ J\ K^{-1}\ mol^{-1}$. Ultrasonic studies[14] confirm $[Be(dmf)_4]^{2+}$ to be the predominant beryllium(II) species in dmf solution.

Two of the above investigations[4,5] determined the rate laws for ligand exchange with respect to the concentration of free ligand using an inert co-solvent or diluent. Crea and Lincoln[4] investigated the exchange of tmp on $[Be(tmp)_4]^{2+}$ in CH_2Cl_2 solution and assigned a D ligand exchange mechanism for the process as no variation in k_{ex} was observed when the $[tmp]_{free}$ was changed. Delpuech *et al.*[5] assigned D ligand exchange mechanisms for $[Be(hmpa)_4]^{2+}$, $[Be(tmdamp)_4]^{2+}$ and $[Be(dmadmp)_4]^{2+}$ systems in 4-methyl-1,3-dioxolan-2-one and nitromethane

solution for the first two and last complexes respectively on the same basis as Lincoln[4]. However A ligand mechanisms were assigned for the $[Be(tmp)_4]^{2+}$ and $[Be(dmmp)_4]^{2+}$ systems in CH_3NO_2 solution. As the results obtained for tmp exchange on $[Be(tmp)_4]^{2+}$ in CH_2Cl_2 and CH_3NO_2 solutions differ, it was considered desirable to augment these studies so that a greater understanding of the factors affecting the rates and mechanisms of the ligand exchange process on beryllium(II) species could be attained.

This chapter contains the results and conclusions of a systematic study of the ligand exchange process on beryllium(II).

4.2 Ligand exchange on tetrakis(dimethylsulphoxide) beryllium(II)

The complex $[Be(dmso)_4](ClO_4)_2$ was prepared by the method described in section 6.2. Solutions of the complex $[Be(dmso)_4](ClO_4)_2$ and dmso in nitromethane-d_3 were prepared (solution compositions given in Table 4.1). However it was found that the complex/ligand mixture is insoluble in the diluent acetonitrile-d_3.

Under slow exchange conditions the ^1H nmr spectra of the dmso solutions exhibit singlets arising from the methyl groups of the coordinated ligand downfield of those arising from the free ligand at frequencies which appear in Table 4.1.

A comparison of the integrated areas of the singlets indicates that 4.0 ± 0.1 dmso molecules are coordinated to beryllium(II) consistent with $[Be(dmso)_4]^{2+}$ being the predominant solvate species in solution. The temperatures below which slow ligand exchange conditions apply vary systematically from 280 K to 255 K for solutions (i) - (v) in Table 4.1. Under these conditions the only other resonances observed are those arising from the proton impurity of the CD_3NO_2 diluent, for which no resonances attributable to the CD_3NO_2 being coordinated are observed. From the above results it is concluded that the diluent CD_3NO_2 does not compete to any significant extent with dmso for first coordination

Figure 4.1

Typical experimental and calculated ^1H (90 MHz) nmr spectra arising from coordinated and free dmso in solution (ii) Table 4.1 in which $[Be(dmso)_4^{2+}]$, $[dmso]_{free}$ and $[CD_3NO_2]$ are 0.0432, 0.220 and 18.23 mol dm^{-3} respectively. The low field resonance arises from coordinated dmso. The corresponding experimental temperatures (K) are given to the left of each spectrum with the mean lifetimes τ_c(ms) of a single dmso ligand on $[Be(dmso)_4]^{2+}$ given on the right.

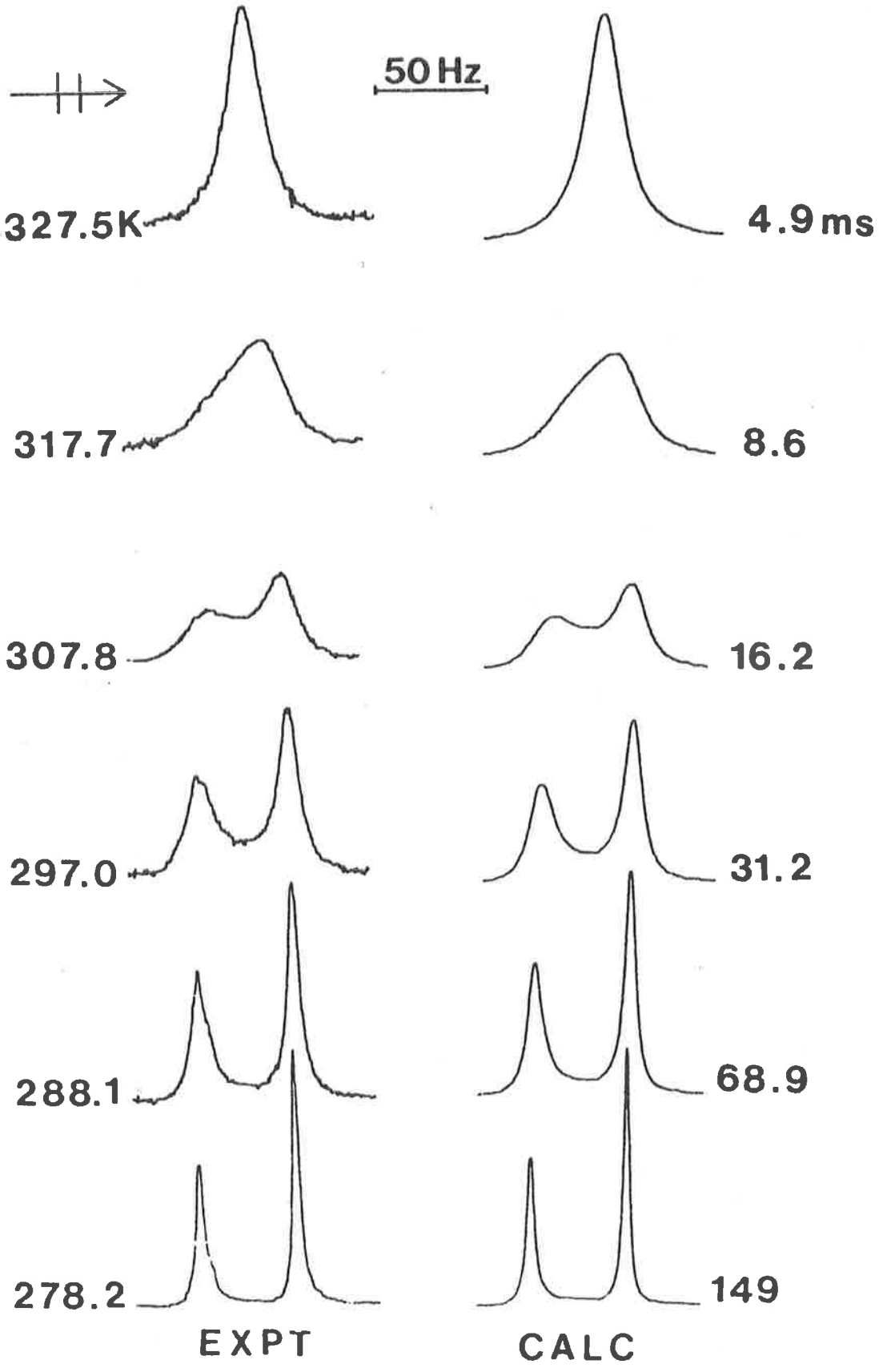
50 Hz
327.5K
4.9 ms
317.7
8.6
307.8
16.2
297.0
31.2
288.1
68.9
278.2
149
EXPT
CALC

Table 4.1 Solution compositions and kinetic parameters for dmso exchange on $[Be(dmso)_4]^{2+}$.

Solution	$[Be(dmso)_4^{2+}]$ / mol dm^{-3}	$[dmso]_{free}$ / mol dm^{-3}	$[CD_3NO_2]$ / mol dm^{-3}	CN	$\Delta\nu$[a] / ppm
(i)	0.0222	0.113	18.34	3.9 ± 0.1	0.471
(ii)	0.0432	0.220	18.23	4.0 ± 0.1	0.468
(iii)	0.0796	0.406	17.84	4.0 ± 0.1	0.464
(iv)	0.133	0.676	16.90	3.9 ± 0.1	0.462
(v)	0.335	1.37	14.26	4.0 ± 0.1	0.445

$k_2(298\ K)$[b] / $dm^3\ mol^{-1}\ s^{-1}$	$k_2(340)$[b] / $dm^3\ mol^{-1}\ s^{-1}$	$\Delta H_2^{\neq}$ / kJ mol^{-1}	$\Delta S_2^{\neq}$ / J $K^{-1}\ mol^{-1}$
140 ± 10	2030 ± 30	51.1 ± 0.6	-32.3 ± 2.2

[a] The chemical shift of the singlet of the coordinated dmso, downfield from that of the free dmso. The temperatures at which the shifts are quoted are 253.3 K.

[b] Derived from a best fit of 45 k_{ex} datum points to equation (2.12).

sphere sites on beryllium(II).

As the temperature is increased ligand exchange causes the singlets of the free and co-ordinated dmso to coalesce in the classical manner, (Figure 4.1) and complete lineshape analysis yields the lifetime, τ_c, of a single dmso molecule bound to beryllium(II). In general τ_c is related to the first order exchange rate constant k_{ex} by

$$\tau_c = \tau_F x_F / x_c = {}^{1}/_{k_{ex}} = 4[BeL_4{}^{2+}]/\text{exchange rate}$$

where τ_F is the lifetime of a solvent molecule in the free state x_F and x_c are the mole fractions of free and coordinated ligand respectively.

For the solutions studied, τ_c was obtained at nine or ten temperatures per solution in the range 260 - 360 K. These results indicate that the rate of dmso exchange is linearly dependent on $[dmso]_{free}$ as seen in Figure 4.2 consistent with a second order exchange process characterised by k_2 such that $k_{ex} = k_2[dmso]_{free}$.

In order to obtain k_2 the forty five τ_c values obtained were simultaneously fitted to equation (2.12) using DATAFIT[45]. The k_1 values obtained using this method were smaller than the experimental error in k_{ex} over the experimental temperature range studied and thus the predominant exchange path is kinetically second order.

The second order rate law observed for solvent exchange on $[Be(dmso)_4]^{2+}$ is consistent with the operation of an associative ligand exchange mechanism in which a five coordinate reactive intermediate is formed. (An alternative interpretation is that dmso exchanges on beryllium(II) through an interchange mechanism where no preferential occupation of the second coordination sphere occurs and consequently the exchange rate is directly dependent upon $[dmso]_{free}$ as the proportion of dmso increases in the second coordination sphere. However as the data obtained in this study provides no direct evidence for such an effect the operation of an I mechanism is not considered further.)

Figure 4.2

The variation of k_{ex} for dmso exchange on $[Be(dmso)_4]^{2+}$ with $[dmso]_{free}$ at selected temperatures. The solid lines represent the simultaneous best fit of the 45 individual k_{ex} datum points obtained in the temperature range 260.5 - 360.1 K to equation (2.12). Only 26 of the k_{ex} datum points are shown in this Figure.

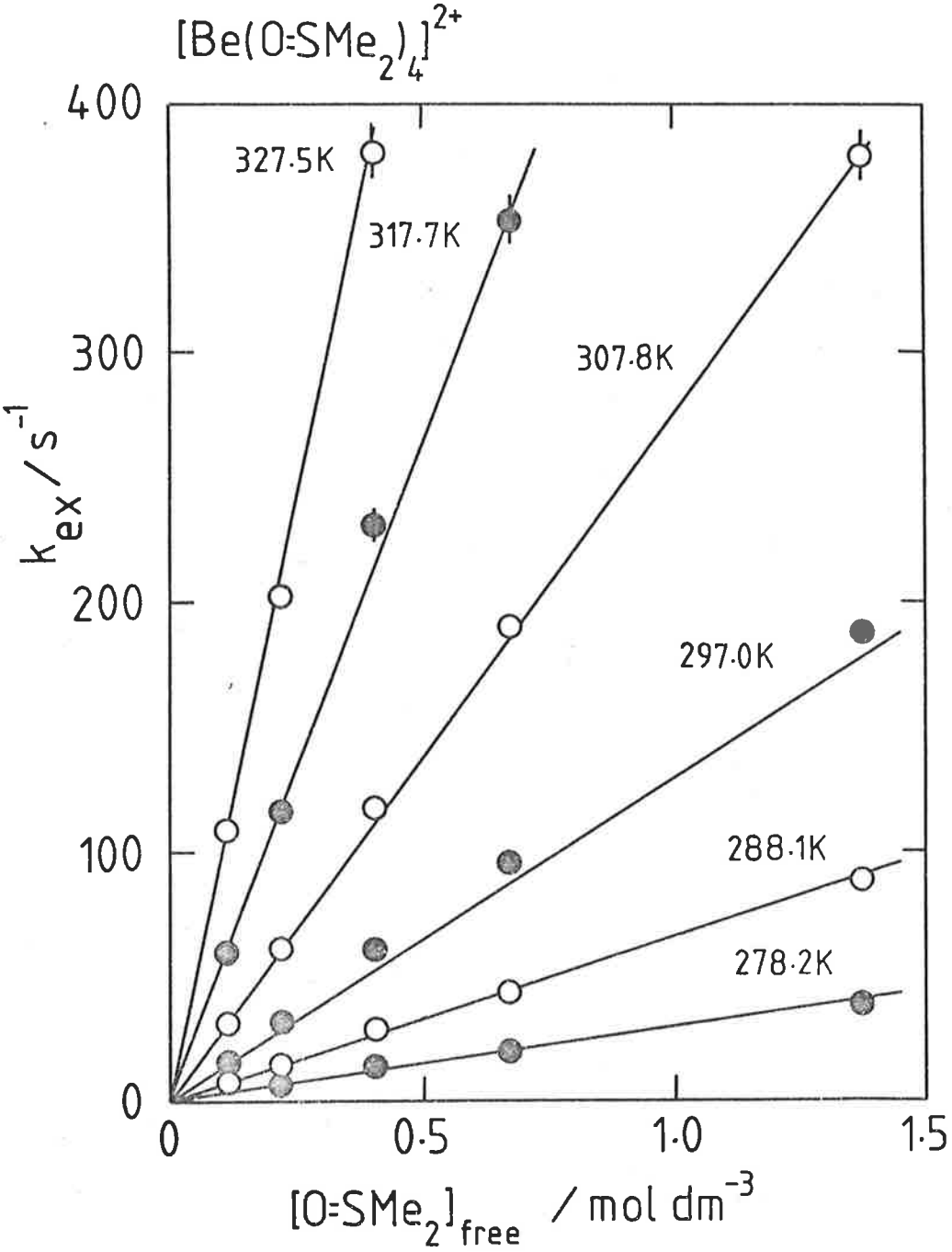
[Be(O=SMe2)4]2+
400
300
200
100
0
kex / s-1
327·5K
317·7K
307·8K
297·0K
288·1K
278·2K
0
0·5
1·0
1·5
[O=SMe2]free / mol dm-3

The activation parameters (Table 4.2) for dmso exchange on $[Be(dmso)_4]^{2+}$ in CD_3NO_2 and in dmso alone[6] differ significantly and may be symptomatic of differing exchange mechanisms. Over the twelve fold $[dmso]_{free}$ range studied in CD_3NO_2, $k_{ex}(298.2\ K) = 196 \pm 10\ s^{-1}$ observed at the high concentration extremes approaches that observed ($230 \pm 10\ s^{-1}$) in dmso alone[6]. It was not possible to study the $[dmso]_{free}$ range in between the highest concentration used, represented by solution (v), and dmso alone as the solubility of the solvate in such CD_3NO_2/dmso mixtures decreases below that required for accurate kinetic study. So while an A mechanism operates in CD_3NO_2 rich solutions, no conclusions regarding the type of mechanism operating in dmso alone may be drawn from this data.

4.3 Ligand exchange on tetrakis(1,1,3,3-tetramethylurea) beryllium(II)

The hygroscopic complex $[Be(tmu)_4](ClO_4)_2$ was soluble in CD_3NO_2 and CD_3CN, and the complex, free tmu and diluent concentrations for the solutions used in this study are given in Table 4.3.

The ^1H nmr spectra of the tmu solutions whose compositions appear in Table 4.3, exhibited singlets arising from the methyl groups of the coordinated tmu downfield of those arising from the free tmu (Figure 4.3) under slow exchange conditions. From a comparison of the integrated areas of these singlets it was found that the predominant beryllium(II) species in all the solutions studied was $[Be(tmu)_4]^{2+}$. (The observation of singlets for both free and coordinated tmu as seen in Figure 4.3 is a consequence of rotation about the C-N bonds being in the fast exchange limit of the nmr timescale down to the lowest temperature examined in solutions (i) - (vi) and (vii) - (xi) 265 K and 250 K respectively.

Figure 4.3

Typical experimental and calculated ^1H (90 MHz), nmr spectra arising from coordinated and free tmu in solution (xi), Table 4.3, in which $[Be(tmu)_4]^{2+}$, $[tmu]_{free}$ and $[CD_3CN]$ are 0.219, 0.945 and 14.7 mol dm^{-3} respectively. The low field resonance arises from the coordinated tmu in the experimental spectra in the left of the Figure. The experimental temperatures (K) and mean lifetimes τ_c(ms) of a single tmu ligand on $[Be(tmu)_4]^{2+}$ appear at the left and right sides of each spectrum in the Figure respectively.

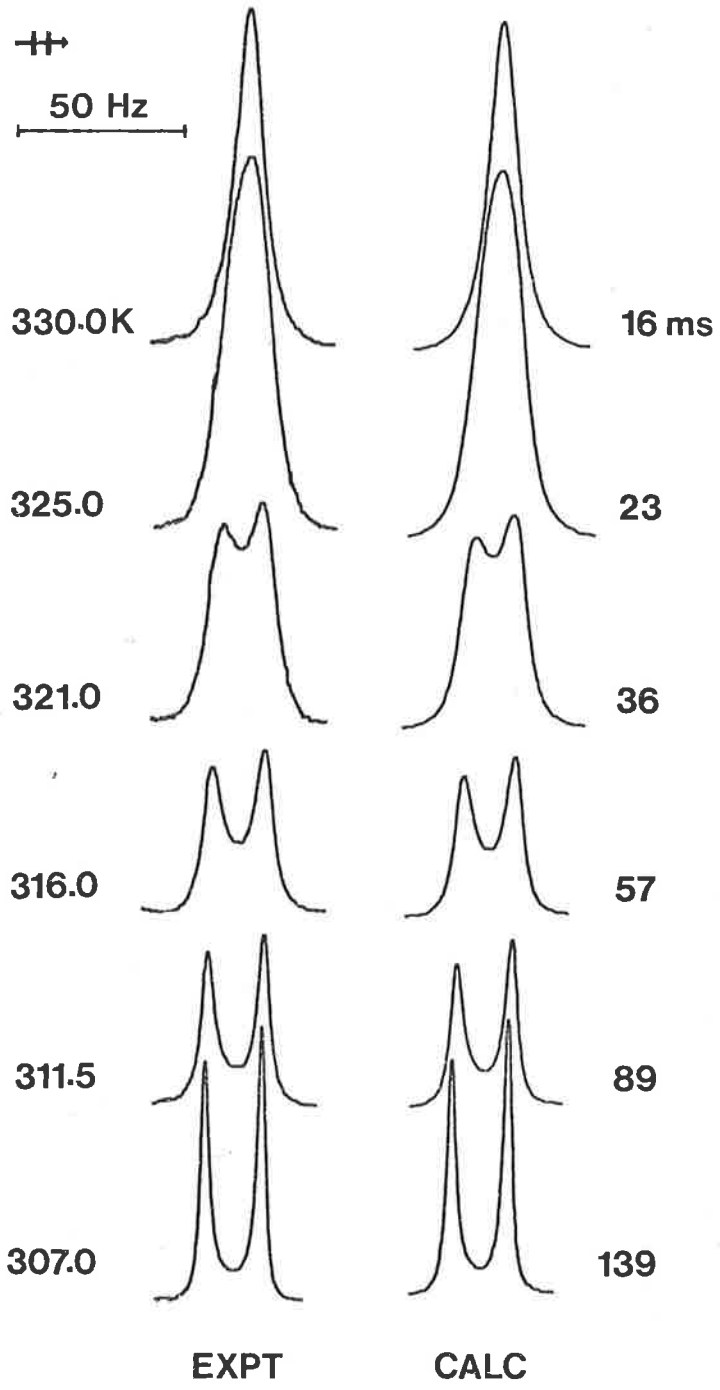
50 Hz
330.0K
325.0
321.0
316.0
311.5
307.0
16 ms
23
36
57
89
139
EXPT
CALC

Table 4.2 Kinetic Parameters for ligand exchange on $[BeL_4]^{2+}$.

L	Diluent	k_1(298 K) s^{-1}	k_2(298 K) $dm^3\ mol^{-1}\ s^{-1}$	$\Delta H^{\neq}$ $kJ\ mol^{-1}$	$\Delta S^{\neq}$ $J\ K^{-1}\ mol^{-1}$	Assigned Mechanism	Ref.
tmu	CD_3NO_2	1.39	-	77.1	16.4	D	Section 4.2
tmu	CD_3CN	2.47	-	79.8	30.2	D	Section 4.2
dmso	CD_3NO_2	-	140	51.1	-32.3	A	Section 4.1
dmso	$(CH_3)_2SO$	230	-	25	-110	I_d(?)	6
tmp	CH_2Cl_2	3.6	-	56.9	-43.9	D	4
tmp	$OP(CH_3)_3$	4.9	-	70.3	3.5	D(?)	4
tmp	CH_3NO_2	-	1.5	56.1	-54.0	A	5
dmmp	CH_3NO_2	-	0.81	60.2	-44.4	A	5
dmadmp	CH_3NO_2	0.0073	-	89.1	12.6	D	5
dmadmp	$OCOCH_2CHOCH_3$	0.09	-	77.4	-5.4	D	5
hmpa	$OCOCH_2CHOCH_3$	0.00027	-	116.7	78.2	D	5
H_2O	H_2O	1800	-	41.5	-44	I_d(?)	8
H_2O	$(CD_3)_2CO$	2100	-	34	-65	I_d(?)	9

Table 4.3 Solution compositions and kinetic parameters for tmu exchange on $[Be(tmu)_4]^{2+}$.

Solution	$[Be(tmu)_4^{2+}]$ mol dm^{-3}	$[tmu]_{free}$ mol dm^{-3}	$[CD_3NO_2]$ mol dm^{-3}	$[CD_3CN]$ mol dm^{-3}	CN	k_{ex}(340 K)[a] s^{-1}	$\Delta H^{\neq}$ [b] kJ mol^{-1}	$\Delta S^{\neq}$ [b] J K^{-1} mol^{-1}	$\Delta\nu$(288 K)[c] ppm
(i)	0.0074	0.0334	18.30	-	3.9 ± 0.1	73.5 ± 4.8	77.1 ± 1.4	16.4 ± 4.3	0.259
(ii)	0.0150	0.0676	18.17	-	4.0 ± 0.2	73.4 ± 4.3	76.5 ± 1.3	14.8 ± 3.8	0.256
(iii)	0.035	0.158	18.05	-	4.0 ± 0.1	81.0 ± 4.2	79.2 ± 1.1	23.6 ± 3.4	0.257
(iv)	0.0903	0.279	16.35	-	4.0 ± 0.2	86.1 ± 2.8	82.6 ± 0.7	34.0 ± 2.1	0.260
(v)	0.198	0.615	14.34	-	4.0 ± 0.1	88.1 ± 2.1	81.4 ± 0.5	30.7 ± 1.6	0.262
(vi)	0.328	1.48	12.39	-	4.0 ± 0.1	89.2 ± 2.2	79.9 ± 0.5	26.5 ± 1.7	0.263
(vii)	0.0116	0.0467	-	18.48	4.0 ± 0.1	149 ± 4	79.7 ± 0.7	30.2 ± 2.1	0.153
(viii)	0.0247	0.0999	-	18.37	4.0 ± 0.1	150 ± 6	79.3 ± 0.9	29.0 ± 2.7	0.157
(ix)	0.0525	0.227	-	18.06	4.0 ± 0.1	152 ± 4	80.0 ± 0.5	31.1 ± 1.7	0.163
(x)	0.0987	0.427	-	17.15	4.0 ± 0.1	155 ± 5	78.6 ± 0.6	27.3 ± 1.8	0.170
(xi)	0.219	0.945	-	14.7	4.0 ± 0.1	155 ± 9	79.7 ± 1.2	30.4 ± 3.7	0.182

[a] The quoted k_{ex} value is derived from the linear least squares fit of all the k_{ex} data in the experimental temperature range to the Eyring equation - errors represent one standard deviation.

[b] $\Delta H^{\neq}$ and $\Delta S^{\neq}$ are derived from ACTENG, a linear least squares fit to the Eyring equation - quoted errors represent one standard deviation.

[c] Chemical shift of the singlet for the coordinated tmu ligand downfield from that of the free tmu.

The temperatures below which the limiting condition of slow ligand exchange occurs are 300 K and 290 K for solutions (i) - (vi) and (vii) - (xi) respectively, and under these conditions the only other resonances observed were due to the ^1H impurities of the diluents, CD_3NO_2 and CD_3CN respectively with no evidence showing that either of the diluents were coordinated to the beryllium(II) species.

Complete lineshape analysis of the coalescence of the methyl group resonances of tmu yields the mean site lifetimes, τ_c, of a single ligand molecule coordinated to beryllium(II). A typical set of experimental and best-fit calculated nmr lineshapes for solution (xi) showing the coalescence of the coordinated and free tmu sites as the temperature is increased is seen in Figure 4.3.

For the $[Be(tmu)_4]^{2+}$ system in CD_3NO_2 and CD_3CN, τ_c and the related activation parameters vary very little over the respective 44 and 20 fold variations of $[tmu]_{free}$ as is seen from Table 4.3 and Figure 4.4, consistent with the rate of the predominant ligand exchange process being independent of $[tmu]_{free}$ such that the characteristic first order rate constant $k_1 = k_{ex}$.

The first order rate law observed for tmu exchange on $[Be(tmu)_4]^{2+}$ is consistent with the operation of a dissociative (D) mechanism in which a reactive three coordinate intermediate is formed. (The alternative interpretation is that tmu exchange on beryllium(II) operates through an interchange (I) mechanism where tmu preferentially occupies the second coordination sphere such that the exchange rate is independent of $[tmu]_{free}$. However from the data obtained there appears to be no direct evidence to suggest that such an effect occurs and thus an I mechanism is not considered in interpreting this data.)

Previous ligand exchange studies on beryllium(II)[4,5] have involved the assignment of ligand exchange mechanisms Dissociative or Associative[15] on the basis of first or second order rate laws respectively. An A mechanism was assigned to the exchange of tmp and dmmp[5] while a D

Figure 4.4

The variation of τ_c for tmu exchange on $[Be(tmu)_4]^{2+}$ with temperature, concentration and the nature of the diluent. The open and closed circles are datum points for the CD_3NO_2 solutions (vi) and (i) respectively and the open and closed triangles are datum points for the CD_3CN solutions (xi) and (vii) respectively. The solid and closed lines represent the linear regression fits of these data to the Eyring equation.

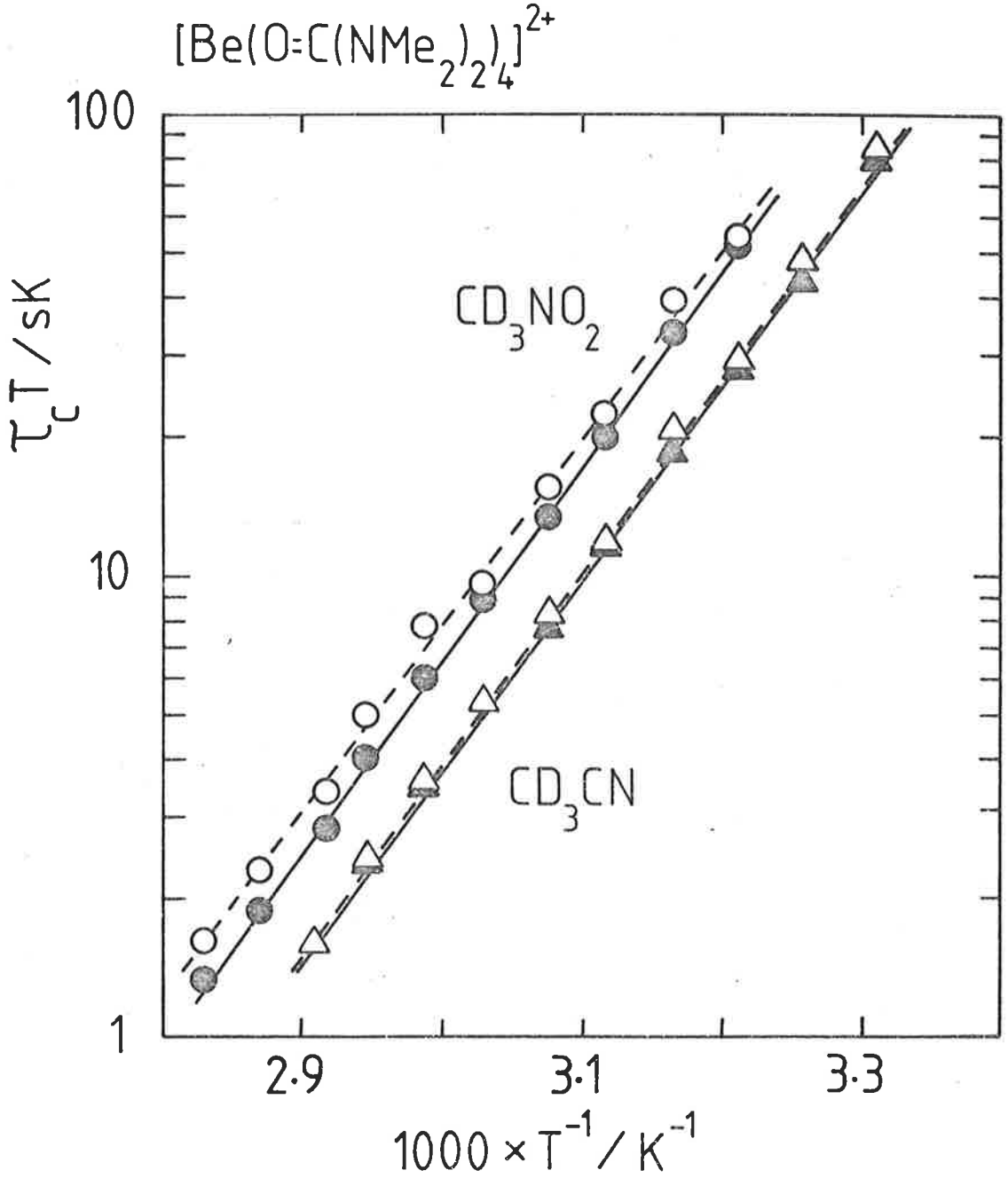
[Be(O=C(NMe2)2)4]2+
100
10
1
τcT / sK
CD3NO2
CD3CN
2·9
3·1
3·3
1000 × T−1 / K−1

mechanism was said to operate for the exchange of dmadmp in CH_3NO_2 solutions[5]. It has been argued that in the case of these phosphate based solvents the larger dmadmp molecule causes the greatest steric crowding on beryllium(II) and thus favours the operation of a D mechanism whereas the smaller tmp and dmmp molecules cause less steric crowding and as a result an A mechanism operates.

On this basis it is expected that the larger tmu molecule should favour the operation of a D mechanism to a greater extent than the smaller dmso molecule in accord with the observations made for these systems. In addition to the varying steric factors a variation in the structure of the ligand is expected to produce variations in their electron donor character which could be expected to influence the ligand exchange process. However a comparison of the available Gutmann donor numbers[17] which are 23.0, 29.6 and 29.8 for tmp, tmu and dmso respectively with the exchange mechanisms or magnitude of the exchange parameters shows no obvious correlation indicating that steric and donor strength effects upon mechanism are probably subtly interwoven.

The most direct mechanistic comparisons will be those made in the same diluent (it is assumed that the diluent properties of CD_3NO_2 and CH_3NO_2 do not differ significantly) as it is observed in this study that a change of the diluent from CD_3NO_2 to CD_3CN causes a small change in the solvent exchange parameters for $[Be(tmu)_4]^{2+}$ (Table 4.3 and Figure 4.4), and elsewhere that a change of diluent from CH_3NO_2 to 4-methyl-1,3-dioxolan-2-one causes major modification to the exchange parameters for $[Be(dmadmp)_4]^{2+}$ and that for $[Be(tmp)_4]^{2+}$ a change of diluent from CH_3NO_2 to CH_2Cl_2 causes the ligand exchange mechanism to change from A to D[4,5] respectively. (Similarly, modifications to the ligand exchange mechanism with changes in the nature of the diluent have been observed for six coordinate scandium(III)[18,19] systems.)

Because of the small size of beryllium(II) by comparison to that of the oxygen donor atoms in the first coordination sphere the

interactions between the latter atoms should have a major influence in determining the transition state dynamics for ligand exchange. For $[Be(H_2O)_4]^{2+}$ this effect is expected to be at a maximum, Strehlow and Knoche[3] (using an electrostatic model) have shown that a low energy path for H_2O exchange which approaches the experimental $\Delta H^{\neq}$ value is characterised by a transition state in which a water molecule is sited on the opposite faces of the trigonal planar entity $[Be(H_2O)_3]^{2+}$, so that water exchange occurs through a highly concerted movement of the entering and leaving water molecules along one of the C_3 axes of the $[Be(H_2O)_4]^{2+}$ tetrahedron which translates the leaving water molecule from a first coordination sphere site to a site in the second coordination sphere on a trigonal face of the new ground state $[Be(H_2O)_4]^{2+}$ species, and vice versa for the entering water molecule, in an apparent dissociative interchange (I_D) mechanism.

On the basis of this model it seems unlikely that the discrete reactive intermediate species $[Be(H_2O)_3]^{2+}$ required if a D mechanism is to operate will be formed in aqueous solution. However as the size and complexity of the ligand molecule increases then the dominance of the oxygen donor atoms in determining the electrostatic energies of the ground and transition states will diminish as the interactions between the other groups of the coordinated ligand molecules increases with the consequence that the stereochemistries of transition states and intermediates which are not energetically favoured in the aqueous system may become viable in non-aqueous systems. Thus for an A mechanism trigonal bypyramidal or square pyramidal (these five coordinate stereochemistries have been shown to be of similar energy) arrays of five oxygen donor atoms about beryllium(II) in transition states and intermediates are anticipated whereas a trigonal planar stereochemistry appears more probable for such species for a D mechanism. An additional effect is that a general Born solvation energetic contribution which was

found to be important in the aqueous system should decrease in importance as the ligand molecule increases in size. Nevertheless as the diluent has been shown to modify both activation parameters and mechanisms for solvent exchange processes it appears that interactions occurring outside the first coordination sphere, for which a number of models have been proposed, can have significant effects upon transition state dynamics. The small variation of k_{ex} with concentration of free ligand observed for tmu exchange on $[Be(tmu)_4]^{2+}$ in both CD_3CN and CD_3NO_2 can possibly be explained by changes in the interactions outside the first coordination sphere as the $[diluent]/[tmu]_{free}$ is varied.

4.4 Ligand exchange on tetrakis(dimethylmethylphosphonate) beryllium(II)

Delpuech *et al.*[5] have reported the preparation of the complex $[Be(dmmp)_4](ClO_4)_2$ and investigated the exchange of dmmp on $[Be(dmmp)_4]^{2+}$ in CH_3NO_2 solution using variable temperature ^1H nmr spectroscopy. From the observed rate law where the rate of dmmp exchange was dependent on $[dmmp]_{free}$ an associative (A) mechanism was assigned. Furthermore similar results for tmp exchange on $[Be(tmp)_4]^{2+}$ in CH_3NO_2 solution were observed, i.e. an associative ligand mechanism was said to operate.

However Crea and Lincoln[4] had previously observed that the rate law for tmp exchange on $[Be(tmp)_4]^{2+}$ in CH_2Cl_2 solution was independent of $[tmp]_{free}$ and as such a D ligand exchange mechanism was proposed. As a result studies of dmmp exchange on $[Be(dmmp)_4]^{2+}$ in the diluents CD_3CN and CD_3NO_2 were initiated to further the understanding of the processes occurring in solution and these results are reported in this section.

The complex $[Be(dmmp)_4](ClO_4)_2$ was prepared by the method described in section 6.2. Solutions of the complex $[Be(dmmp)_4](ClO_4)_2$ and dmmp without any diluent, and in the diluents CD_2Cl_2 and CD_3CN were prepared whose compositions are given in Table 4.4.

Table 4.4 Solution compositions and kinetic parameters for dmmp exchange on $[Be(dmmp)_4]^{2+}$.

Solution	$[Be(dmmp)_4^{2+}]$ mol dm^{-3}	$[dmmp]_{free}$ mol dm^{-3}	$[CD_2Cl_2]$ mol dm^{-3}	CN[a]	$k_{ex}(340)$[b] s^{-1}	$\Delta H^{\neq}$[b] kJ mol^{-1}	$\Delta S^{\neq}$[b] J K^{-1} mol^{-1}	$\Delta\nu(280\ K)$[c] ppm
(i)	0.346	0.582	11.66	4.1 ± 0.2	68.9 ± 2.3	75.8 ± 0.8	12.1 ± 2.5	0.217
(ii)	0.267	0.954	11.59	4.0 ± 0.1	79.7 ± 4.2	77.8 ± 1.5	19.2 ± 4.7	0.226
(iii)	0.574	2.05	7.44	4.0 ± 0.1	82.9 ± 3.7	77.8 ± 1.2	19.4 ± 3.9	0.238
(iv)	0.458	2.68	9.06	4.0 ± 0.2	80.0 ± 2.4	76.8 ± 1.0	16.3 ± 3.1	0.239
(v)	0.817	4.77	3.23	4.1 ± 0.1	88.0 ± 1.0	78.0 ± 0.3	20.7 ± 1.0	0.258
(vi)	0.595	5.91	-	4.1 ± 0.1	114 ± 4	73.2 ± 0.6	8.5 ± 2.0	0.282

Solution	$[Be(dmmp)_4^{2+}]$ mol dm^{-3}	$[dmmp]_{free}$ mol dm^{-3}	$[CD_3CN]$ mol dm^{-3}	CN[a]	$\Delta\nu(280\ K)$[c] ppm
(vii)	0.00213	0.115	18.32	4.0 ± 0.1	0.197
(viii)	0.0405	0.291	18.04	3.9 ± 0.2	0.204
(ix)	0.0995	0.441	16.10	4.0 ± 0.1	0.208
(x)	0.176	0.783	15.06	4.0 ± 0.1	0.217
(xi)	0.373	1.66	11.76	4.0 ± 0.1	0.230

Table 4.4 (Continued)

Diluent	k_1(340 K) s^{-1}	k_2(340 K) mol dm^{-3} s^{-1}	$\Delta H^{\neq}$ kJ mol^{-1}	$\Delta S^{\neq}$ J K^{-1} mol^{-1}
CD_3CN	26.3 ± 0.6	-	64.3 ± 1.2	29.7 ± 3.7
CD_3CN	-	11.7 ± 1.0	69.4 ± 4.4	-21.3 ± 13.1

[a] The mean number of ligands per beryllium(II) ion as determined from a comparison of the integrated areas of the resonances of the coordinated and free ligands in the temperature range 260 - 290 K.

[b] The individual k_{ex} values were derived from the complete lineshape analysis of the coalescing doublets of the coordinated and free ligands over the temperature range 300 - 350 K (solutions (i) - (v) and (vii) - (x) and 310 - 370 K (for solution (vi)). The quoted k_{ex} values are derived from a linear least squares fit for all the k_{ex} data for each solution to the Eyring equation. The errors in k_{ex}, $\Delta H^{\neq}$ and $\Delta S^{\neq}$ represent one standard deviation.

[c] $\Delta\nu$(280 K) is the chemical shift of the O-Me doublet of the coordinated ligand downfield from that of the free ligand. The analogous P-Me shifts show a similar systematic trend encompassed within the following ranges; solutions (i) - (v) 0.400 - 0.433, (vi) 0.467, (vii) - (xi) 0.317 - 0.383 ppm. The chemical shifts of the O-Me and P-Me doublets of the coordinated ligand from the proton impurity resonance of CD_2Cl_2 for solutions (i) - (v) vary systematically in the ranges 1.48 - 1.63 ppm and 3.48 - 3.68 ppm respectively. In CD_3CN solution the proton impurity was too close to the P-Me doublets to allow accurate shift measurements.

Under the limiting conditions of slow exchange the ^1H nmr spectra of the dmmp solutions exhibited O-Me doublets for coordinated dmmp ($J(^1H - ^{31}P)$ = 11.5 Hz) downfield of the doublets of free dmmp ($J(^1H - ^{31}P)$ = 11.1 Hz) at frequencies which appear in Table 4.4.

A comparison of the integrated areas of the doublets at temperatures below which slow exchange conditions apply (see Table 4.4) indicates that $[Be(dmmp)_4]^{2+}$ is the predominant species in solutions (i) - (xi). At higher temperatures coalescence of the doublets arising from the coordinated and free ligands occurs, consistent with intermolecular exchange (Figure 4.5) and complete lineshape analysis yields the lifetime of a ligand coordinated to beryllium(II), τ_c which is related to the observed first order rate constant k_{ex} as shown previously.

In CD_2Cl_2 solution the k_{ex}, $\Delta H^{\neq}$ and $\Delta S^{\neq}$ values obtained characterising ligand exchange on $[Be(dmmp)_4]^{2+}$ show a small variation with concentration of free dmmp over the 8.2 fold range studied, however the first order term seems to dominate the exchange rate law, and as such a dissociative ligand exchange mechanism has been assigned. Whereas in CD_3CN solution the variation of k_{ex} (Figure 4.6) with $[dmmp]_{free}$ over a 14.4 fold concentration range is of the form

$$k_{ex} = k_1 + k_2 [dmmp]_{free}$$

Activation parameters for the latter system were obtained using DATAFIT[45] which simultaneously fitted all k_{ex} data for solutions (vii) - (xi) to equation (2.12).

The two term rate law observed suggests that associative and dissociative ligand exchange mechanisms operate simultaneously.

Figure 4.5

The experimental ^1H (90 MHz) nmr spectra and best-fit calculated lineshapes for solution (vii) in which $[Be(dmmp)_4^{2+}]$, $[dmmp]_{free}$ and $[CD_3CN]$ are 0.00213, 0.115 and 18.32 mol dm^{-3} respectively. The doublet arising from the coordinated dmmp appears downfield. Experimental temperatures appear at the left of each spectrum in the Figure and the best fit τ_c values appear to the right of each lineshape.

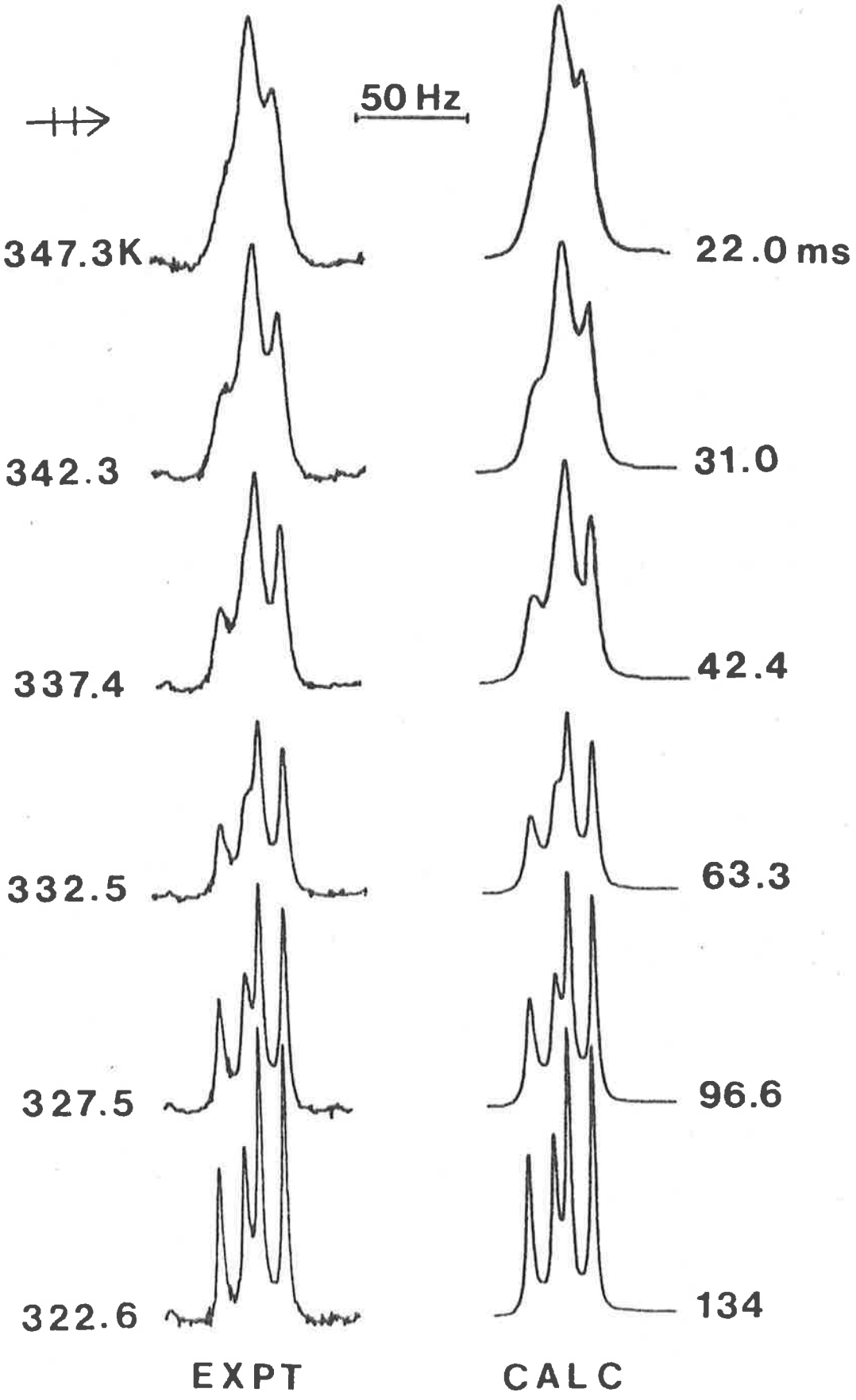
50 Hz
347.3K
342.3
337.4
332.5
327.5
322.6
22.0 ms
31.0
42.4
63.3
96.6
134
EXPT
CALC

Figure 4.6

The variation of k_{ex} for ligand exchange on $[Be(dmmp)_4]^{2+}$ with $[dmmp]_{free}$ and temperature in CD_3CN solution. The temperatures (K) for each curve are given, the curves represent the simultaneous best fit for all of the data for the $[Be(dmmp)_4]^{2+}$ system to equation (2.12).

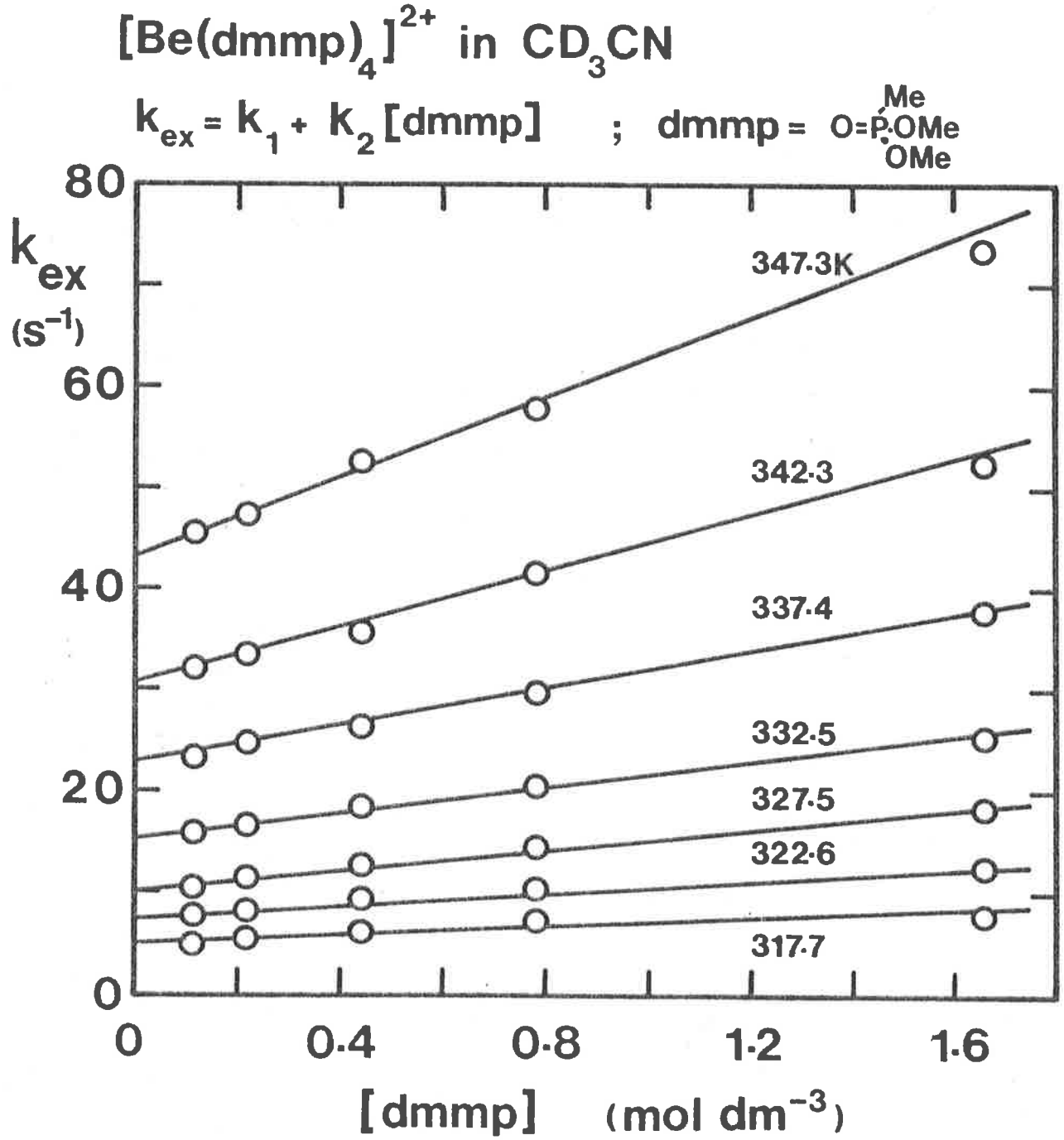
[Be(dmmp)4]2+ in CD3CN
kex = k1 + k2[dmmp] ; dmmp = O=P(Me)(OMe)OMe
kex (s−1)
80
60
40
20
0
347·3K
342·3
337·4
332·5
327·5
322·6
317·7
0
0·4
0·8
1·2
1·6
[dmmp] (mol dm−3)

4.5 Ligand exchange on tetrakis(methylmethylphenylphosphinate)

The complex $[Be(mmpp)_4](ClO_4)_2$ was prepared by the method described in section 6.2. Solutions of the complex $[Be(mmpp)_4](ClO_4)_2$ and free mmpp alone or in CD_2Cl_2, CD_3CN and CD_3NO_2 were prepared, the compositions of which are given in Table 4.5 and 4.6.

Under slow exchange conditions the ^1H nmr spectra of the mmpp solutions (i) - (xv) (Tables 4.5 and 4.6) exhibit O-Me and P-Me doublets (Figure 4.7) arising from the coordinated mmpp downfield from those of the free mmpp. A comparison of the integrated areas of the coordinated and free mmpp doublets indicated that within experimental error the predominant beryllium(II) species in solution is $[Be(mmpp)_4]^{2+}$.

Tables 4.5 and 4.6 give the temperatures below which slow exchange conditions apply. (Broad band ^1H decoupled ^{31}P nmr spectra of these solutions confirmed that $[Be(mmpp)_4]^{2+}$ was the only beryllium(II) species in solution, Figure 4.8 is typical of the results obtained. Coalescence of the coordinated and free mmpp doublets occurred as the temperature was raised consistent with intermolecular site exchange, and complete lineshape analysis (Figure 4.9) yielded, τ_c the mean site lifetime of a single mmpp molecule coordinated to beryllium(II). Data from individual solutions were collected at 8 - 10 temperatures at approximately 5 K temperature intervals within the temperature ranges indicated in Tables 4.5 and 4.6.

In CD_3CN and CD_2Cl_2 solutions the values of k_{ex}, $\Delta H^{\neq}$ and $\Delta S^{\neq}$ characterising ligand exchange (Table 4.5) on $[Be(mmpp)_4]^{2+}$ are virtually invariant over the 53.6 and 10.3 fold free mmpp concentration ranges studied respectively, consistent with a first order exchange rate law, whereas in CD_3NO_2 solution k_{ex} is linearly dependent upon the free mmpp concentration over a 20.5 fold range consistent with a second order exchange rate law, where $k_{ex} = k_2[mmpp]_{free}$.

Figure 4.7

^1H (90 MHz) nmr spectrum at 300 K of solution (vi) (Table 4.5) in which $[Be(mmp)_4^{2+}]$, $[mmpp]_{free}$ and $[CD_2Cl_2]$ are 0.0623, 0.261 and 13.87 mol dm^{-3} respectively. The peaks in region (a) are due to the protons of the phenyl groups in the bound and free environments of mmpp on beryllium(II). The peaks in region (b) are due to the ^1H impurity of the diluent CD_2Cl_2. The doublets in region (c) and (d) are due to the O-Me and P-Me groups of the mmpp ligand with the doublets of the coordinated ligand downfield from those of the free ligand in both cases respectively.

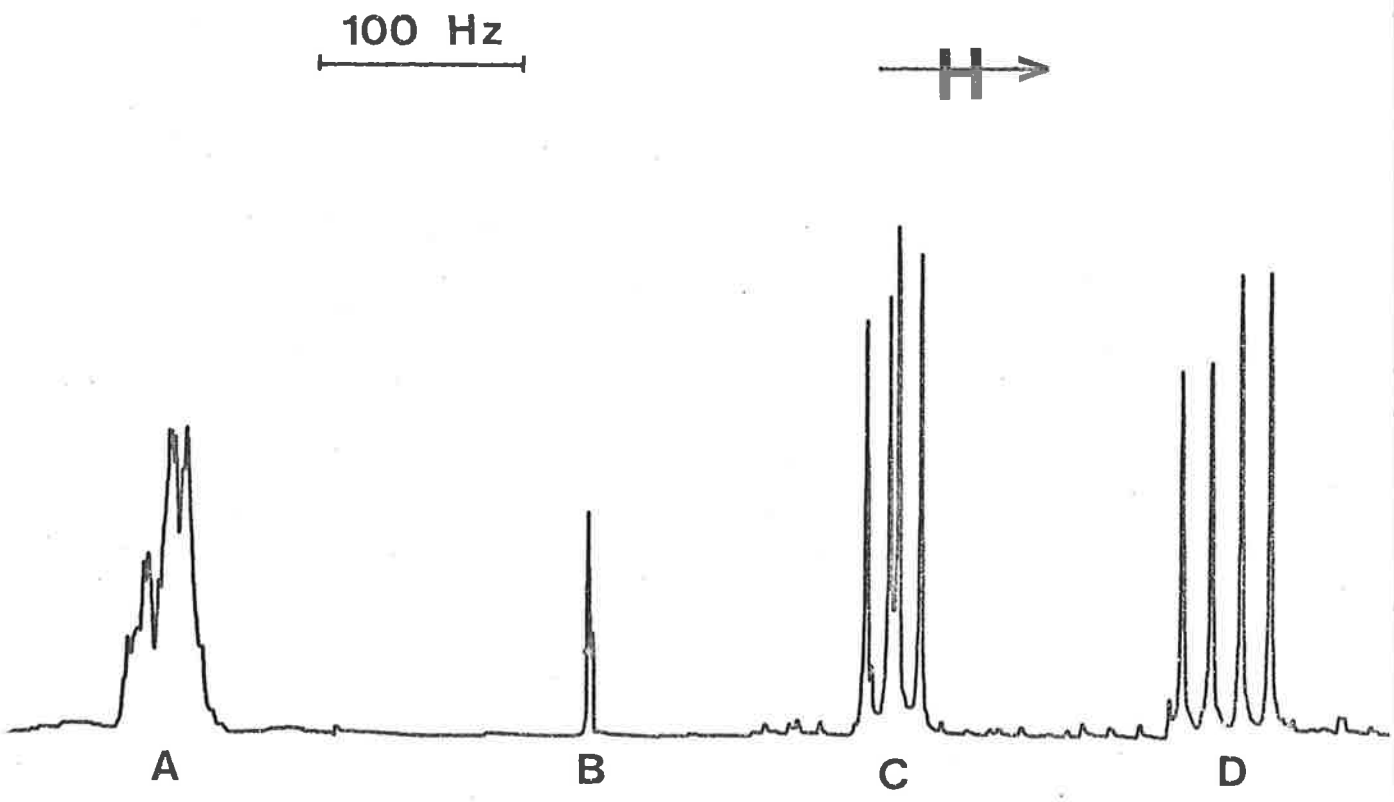
100 Hz
H
A
B
C
D

Figure 4.8

Broad band ^{1}H decoupled ^{31}P (36.43 MHz) nmr spectrum at 300 K of solution (iii) in which $[Be(mmpp)_4^{2+}]$, $[mmpp]_{free}$ and $[CD_3CN]$ are 0.0477, 0.209 and 17.43 mol dm^{-3} respectively. $J(^{9}Be - ^{31}P)$ = 3.5 Hz and the chemical shift difference between the centre of quartet (a) due to $[Be(mmpp)_4]^{2+}$ and the singlet (b) (due to free mmpp) is 11.78 ppm.

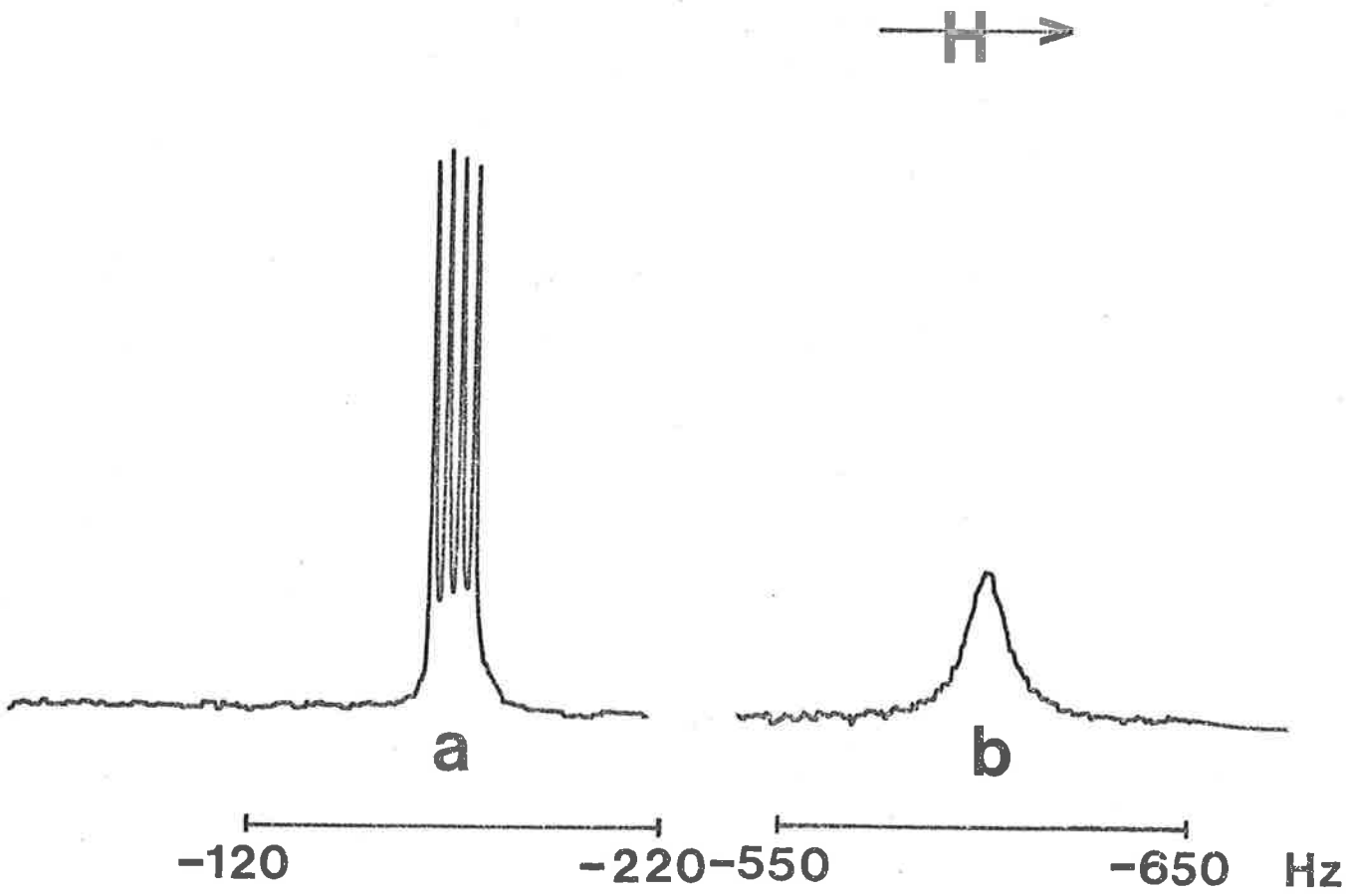
H
a
b
-120
-220
-550
-650
Hz

Figure 4.9

Experimental ^1H (90 MHz) nmr spectra and calculated best-fit lineshapes arising from a solution in which $[Be(ummpp)_4^{2+}]$, $[mmpp]_{free}$ and $[CD_3NO_2]$ were 0.487, 2.37 and 5.71 mol dm^{-3} respectively. The P-Me resonances of $[Be(mmpp)_4]^{2+}$ are downfield, the experimental temperatures (K) and best-fit lifetimes, τ_c(ms), appear to the left and right of the Figure respectively.

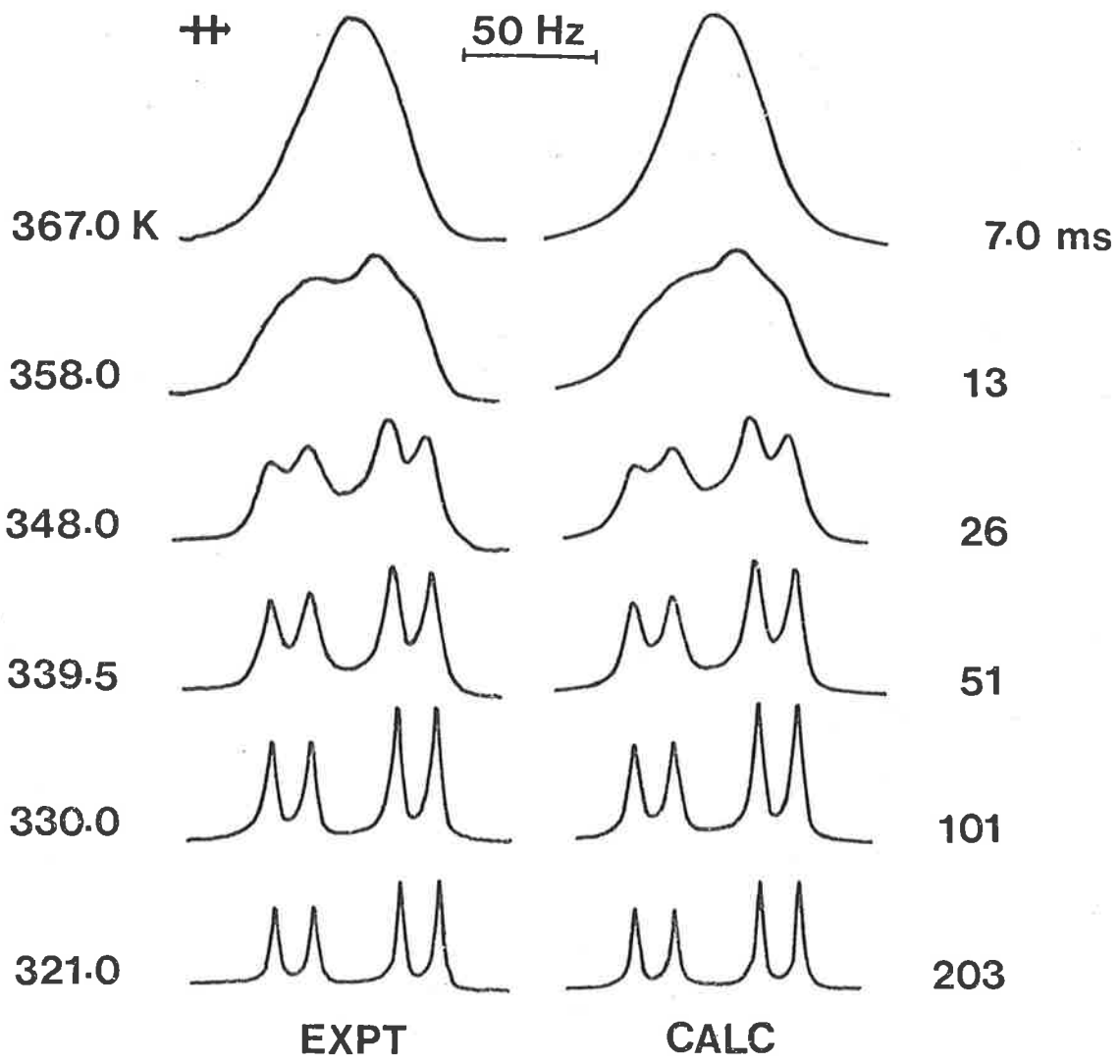
50 Hz
367.0 K
358.0
348.0
339.5
330.0
321.0
7.0 ms
13
26
51
101
203
EXPT
CALC

Table 4.5 Solution compositions and kinetic parameters for mmpp exchange on $[Be(mmpp)_4]^{2+}$.

Solution	$[Be(mmpp)_4^{2+}]$ mol dm^{-3}	$[mmpp]_{free}$ mol dm^{-3}	$[CD_3CN]$ mol dm^{-3}	$[CD_2Cl_2]$ mol dm^{-3}	CN[a]	k_{ex}(340 K)[b] s^{-1}	$\Delta H^{\neq}$ [b] kJ mol^{-1}	$\Delta S^{\neq}$ [b] J K^{-1} mol^{-1}	$\Delta\nu$(280 K)[d] ppm
(i)	0.0055	0.0243	18.16	-	3.9 ± 0.1	21.2 ± 0.5	62.6 ± 0.8	-36.4 ± 2.3	0.200
(ii)	0.0143	0.0626	18.08	-	4.0 ± 0.1	21.2 ± 0.5	62.9 ± 0.5	-35.4 ± 1.5	0.203
(iii)	0.0477	0.209	17.43	-	4.0 ± 0.1	20.9 ± 0.4	62.6 ± 0.5	-36.6 ± 1.4	0.210
(iv)	0.121	0.529	15.88	-	4.0 ± 0.1	21.3 ± 0.3	63.3 ± 0.4	-34.4 ± 1.2	0.221
(v)	0.296	1.30	11.11	-	4.0 ± 0.1	21.3 ± 0.5	63.2 ± 0.6	-34.7 ± 1.9	0.250
(vi)	0.0623	0.261	-	13.87	3.9 ± 0.1	43.5 ± 0.9	59.7 ± 0.8	-38.9 ± 2.4	0.182
(vii)	0.128	0.538	-	12.79	3.9 ± 0.1	42.3 ± 0.8	59.8 ± 0.7	-38.6 ± 2.2	0.195
(viii)	0.286	1.53	-	8.64	4.0 ± 0.1	42.8 ± 1.0	59.3 ± 0.6	-40.2 ± 1.8	0.256
(ix)	0.502	2.69	-	4.19	4.0 ± 0.1	42.7 ± 0.8	59.5 ± 0.6	-39.8 ± 1.7	0.319
(x)	0.305	5.47	-	-	4.0 ± 0.1	-	-	-	0.383

Table 4.6 Solution compositions and kinetic parameters for mmpp exchange on $[Be(mmpp)_4]^{2+}$ continued.

Solution	$[Be(mmpp)_4^{2+}]$ mol dm^{-3}	$[mmpp]_{free}$ mol dm^{-3}	$[CD_3NO_2]$ mol dm^{-3}	CN[a]	$\Delta\nu$(280 K)[d] ppm
(xi)	0.0261	0.115	17.21	3.9 ± 0.1	0.250
(xii)	0.0663	0.294	16.18	3.9 ± 0.1	0.258
(xiii)	0.144	0.639	14.73	3.9 ± 0.1	0.270
(xiv)	0.304	1.35	11.32	4.0 ± 0.1	0.294
(xv)	0.487	2.37	5.71	4.0 ± 0.1	0.333

k_2(340 K)[c] mol dm^{-3} s^{-1}	$\Delta H_2^{\neq}$[c] kJ mol^{-1}	$\Delta S_2^{\neq}$[c] J K^{-1} mol^{-1}
8.5 ± 0.1	68.7 ± 0.9	-26.1 ± 2.7

Tables 4.5 and 4.6

[a] The mean number of ligands per beryllium(II) ion as determined from a comparison of the integrated areas of the ^1H resonances of the coordinated and free ligands in the temperature ranges 270 - 300 K (for solutions (i) - (v)), 260 - 300 K (for solutions (vi) - (x)) and 270 - 300 K (for solutions (xi) - (xv)).

[b] The individual k_{ex} values were derived from the complete lineshape analysis of the coalescing doublets of the coordinated and free ligands over the temperature ranges 310 - 345 K (for solutions (i) - (x)) and 310 - 375 K (for solutions (xi) - (xv)). The quoted k_{ex} values were derived from a linear least squares fit to the Eyring equation, where the errors quoted for k_{ex}, $\Delta H^{\neq}$ and $\Delta S^{\neq}$ represent one standard deviation.

[c] The quoted k_2, $\Delta H_2^{\neq}$ and $\Delta S_2^{\neq}$ values are derived from a non linear least squares fit of all the k_{ex} data to Equation (2.12) using DATAFIT[45].

[d] $\Delta\nu$(280 K) is the chemical shift of the O-Me doublet of the coordinated ligand downfield from that of the free ligand. The analogous P-Me shifts show a similar trend encompassed within the following ranges; for solution (i) - (v) 0.303 - 0.420, (vi) - (ix) 0.333 - 0.483, (x) 0.633 and (xi) - (xv) 0.414 - 0.524 ppm. The chemical shifts of the O-Me and P-Me doublets of the coordinated ligand from the proton impurity of CD_2Cl_2 vary systematically in the ranges 1.60 - 1.70 and 3.39 - 3.44 respectively. Similarly, chemical shift measurements of the O-Me and P-Me doublets from the ^1H impurity signal of CD_3NO_2 for solution (xi) - (xv) cover the ranges 0.500 - 0.517 and 2.23 - 2.20 ppm respectively.

The activation parameters (Table 4.6) were derived through the simultaneous fit of all k_{ex} data for solutions (xi) - (xv) (Table 4.6) to equation (2.12) using the program DATAFIT[45]. These results obtained for mmpp exchange on $[Be(mmpp)_4]^{2+}$ in CD_2Cl_2 and CD_3CN solutions are consistent with the operation of a D ligand exchange mechanism where a three coordinate reactive intermediate $[Be(mmpp)_3]^{2+}$ is formed. Whereas in CD_3NO_2 solution the second order rate law observed is consistent with the operation of an A mechanism where a five coordinate reactive intermediate is formed.

4.6 Ligand exchange on tetrakis(triphenylphosphine oxide) beryllium(II)

The complex $[Be(tppo)_4](ClO_4)_2$ was prepared by the method described in section 6.2.

The ^1H nmr spectra of free and coordinated tppo is too complex to use complete lineshape analysis methods and ^{31}P nmr spectroscopy was used in this study.

The broad band ^1H decoupled ^{31}P nmr spectra of CD_3NO_2 solutions of $[Be(tppo)_4](ClO_4)_2$ and free tppo exhibited a quartet ($J(^9Be - ^{31}P) = 4.3$ Hz) arising from $[Be(tppo)_4]^{2+}$ downfield from the free tppo singlet (Figure 4.10) over the temperature range 280 - 370 K consistent with an estimated $k_{ex}(370\ K) < 3 \times 10^{-3}\ s^{-1}$. (At 370 K the ^{31}P nmr spectrum was still in the slow exchange limit.)

A comparison of the integrated areas of the coordinated and free tppo signals indicates that $[Be(tppo)_4]^{2+}$ is the predominant beryllium(II) species in solution. Typically the quartet appears 510 Hz downfield from the singlet at 300 K in a solution in which $[Be(tppo)_4{}^{2+}]$, $[tppo]_{free}$ and $[CD_3NO_2]$ are 0.0105, 0.0482 and 17.41 mol dm^{-3} respectively.

Figure 4.10

A broad band ^{1}H decoupled ^{31}P (36.43 MHz) nmr spectrum at 300 K of a solution of $[Be(tppo)_4](ClO_4)_2$ and tppo in CD_3NO_2 where the concentrations of the above components are 0.0105, 0.0482 and 17.41 mol dm^{-3} respectively. The quartet (A) arises from $[Be(tppo)_4]^{2+}$ ($J(^{9}Be - ^{31}P)$ = 4.3 Hz) downfield of a singlet (B) due to the free tppo.

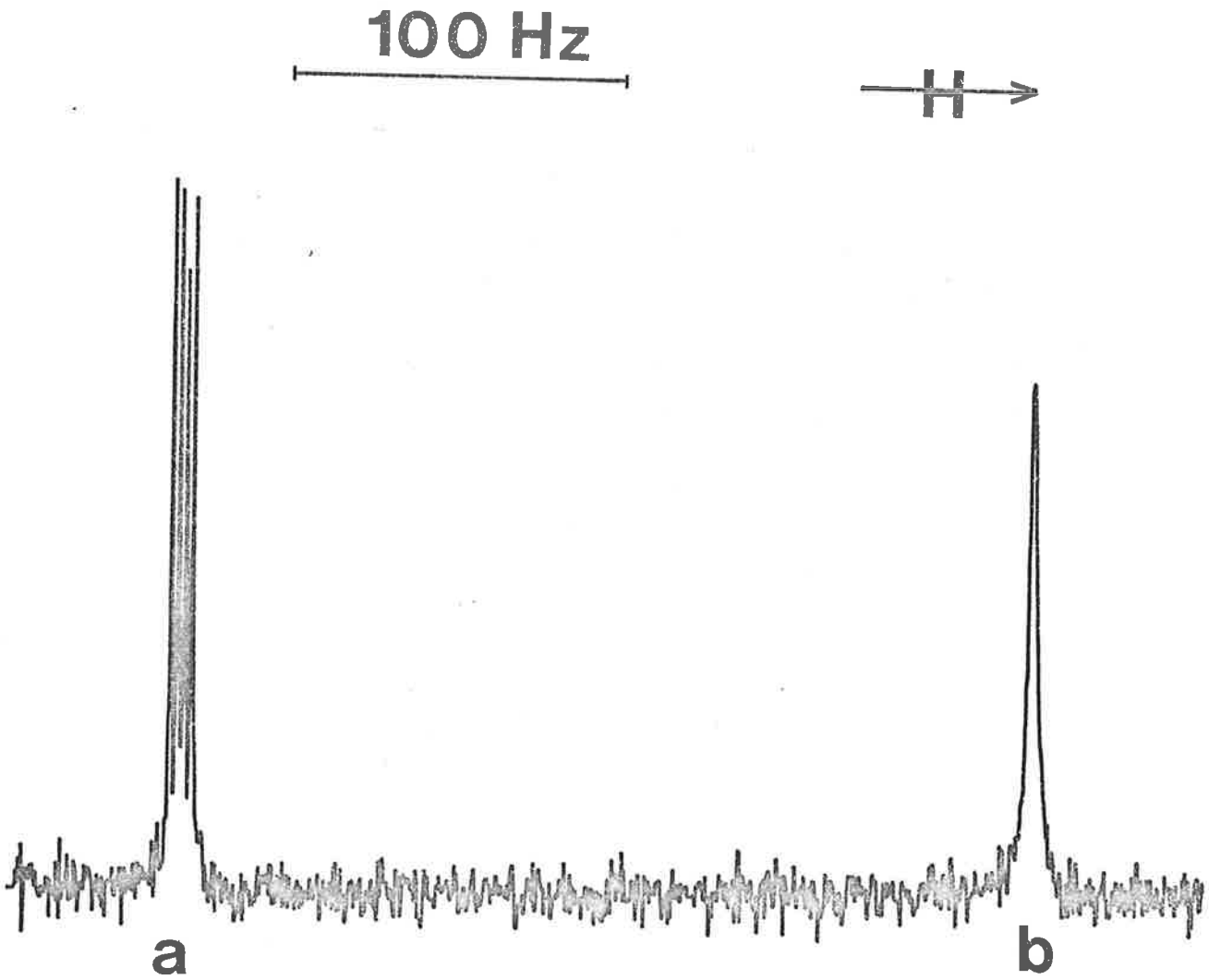
100 Hz
H
a
b

4.7 Ligand exchange on beryllium(II) for the phosphate systems

At this point it is worth considering the earlier reported beryllium(II) ligand exchange studies and also those of some six coordinate trivalent species as they provide informative mechanistic comparisons for the new beryllium(II) data reported herein.

It was found that in CH_3NO_2 or CD_3NO_2 solution the rate of tmp exchange on $[M(tmp)_6]^{3+}$, where M = Al^{21}, Ga^{22}, In^{22} or Sc^{19} was independent of, and linearly dependent on the free ligand concentration, $[tmp]_{free}$, for the first two and second two species respectively. Accordingly a D ligand exchange mechanism was assigned to $[Al(tmp)_6]^{3+}$ and its gallium(III) analogue whereas A mechanisms were assigned to the indium(III) and scandium(III) species. These differences in mechanism are attributed to the larger ionic radii[12] of In^{3+} (0.080 nm) and Sc^{3+} (0.074 nm) facilitating an increase in coordination number in the transition state whereas the greater steric crowding of Al^{3+} (0.053 nm) and Ga^{3+} (0.062 nm) leads to a transition state of reduced coordination number being favoured.

Similarly in CH_3NO_2 solution ligand exchange on $[Be(tmp)_4]^{2+}$ and $[Be(dmmp)_4]^{2+}$ have been assigned A ligand exchange mechanisms, and $[Be(dmadmp)_4]^{2+}$ a D mechanism on the basis of the linear dependence of their ligand exchange rates on free ligand concentration in the first two systems and the rate independence of free ligand concentration for the latter system[5]. Once again for these cases the change in mechanism has been attributed to steric interaction effects but here it is the size of the ligand which determines in which direction the coordination number will change in the transition state. On the basis of these rationalisations the linear exchange rate dependence on free ligand concentration (Table 4.7) exhibited by $[Be(mmpp)_4]^{2+}$ in CD_3NO_2 solution is attributed to the operation of an A mechanism, whereas the rate independence of free ligand concentration exhibited in CD_2Cl_2 and CD_3CN

Table 4.7 Kinetic Parameters[a] for Ligand Exchange on $[BeL_4]^{2+}$.

Species	Diluent	Assigned Ligand Exchange Mechanism	10^3 k_1(298.2 K) s^{-1}	10^3 k_2(298.2 K) $dm^3\ mol^{-1}\ s^{-1}$	$\Delta H^{\neq}$ kJ mol^{-1}	$\Delta S^{\neq}$ J K^{-1} mol^{-1}	Ref.
$[Be(mmpp)_4]^{2+}$	CD_3NO_2	A	-	220 ± 10	68.7 ± 0.9	-26.1 ± 2.7	Section 4.5
"	CD_3CN	D	810 ± 15	-	62.6 ± 0.5	-36.6 ± 1.4	"
"	CD_2Cl_2	D	1930 ± 40	-	59.8 ± 0.7	-38.6 ± 2.2	"
$[Be(dmmp)_4]^{2+}$	CH_3NO_2	A	-	810 ± 50	60.2 ± 0.8	-44.4 ± 3.0	5
"	CD_3CN	D	930 ± 40	-	64.3 ± 1.2	-29.7 ± 3.7	Section 4.4
"	CD_3CN	A	-	330 ± 50	69.4 ± 4.4	-21.3 ± 13.1	"
"	CD_2Cl_2	D	1440 ± 80	-	77.8 ± 1.2	19.4 ± 3.9	"
"	dmmp	D(?)	2600 ± 90	-	73.1 ± 0.6	8.5 ± 2.0	"
$[Be(tmp)_4]^{2+}$	CH_3NO_2	A	-	1500 ± 200	56.0 ± 1.8	-54.0 ± 5.4	5
"	CH_3NO_2	A	-	1750	60.1	-36.8	5
"	CH_2Cl_2	D	3600 ± 600	-	56.9 ± 4.2	-43.9 ± 12.6	4
"	tmp	D(?)	4900 ± 180	-	70.3 ± 8.4	3.5 ± 24.6	4
$[Be(dmadmp)_4]^{2+}$	CH_3NO_2	D	7.3 ± 1.7	-	89.1 ± 2.5	12.6 ± 5.9	5
"	$\overline{OCOCH(Me)CH_2O}$	D	0.91	-	77.4	-5.4	5
$[Be(tmdamp)_4]^{2+}$	"	D	6.9 ± 2.0	-	89.1 ± 4.2	12.6 ± 11.7	5
$[Be(hmpa)_4]^{2+}$	"	D	0.27 ± 0.04	-	117 ± 1.2	78 ± 3.8	5
$[Be(H_2O)_4]^{2+}$	H_2O	D(?)	(1800 ± 100) x 10^3	-	41.5 ± 2.0	-44 ± 15	8
"	$H_2O(CD_3)_2CO$	D(?)	(2100 ± 600) x 10^3	-	34 ± 5	-65 ± 15	9

[a] Determined using ^1H nmr studies with the exception of the second set of $[Be(tmp)_4]^{2+}/CH_3NO_2$ data and the $[Be(H_2O)_4]^{2+}/H_2O$ data which were determined from ^9Be and ^{17}O nmr studies respectively.

solution (Table 4.6) indicates a change to a D mechanism in these diluents. Similarly the rate independence of free ligand concentration for ligand exchange on $[Be(dmmp)_4]^{2+}$ in CD_2Cl_2 solution is consistent with the operation of a D mechanism whereas the two term rate law observed in CD_3CN solution suggests the simultaneous operation of D and A mechanisms.

The kinetic parameters characterising ligand exchange in the various diluents may be viewed as modifications of those characterising the ligand exchange process in solutions of the complex and free ligand alone. Unfortunately the solubility of the complex in the liquid ligand is usually too low for reliable kinetic parameters to be derived but in the case of $[Be(dmmp)_4]^{2+}$ this is not so (Table 4.5) and comparisons can be made between the kinetic parameters derived in CD_2Cl_2, CD_3CN and CD_3NO_2 diluents and in their absence. Over the concentration range studied k_{ex}(340 K) characterising the CD_2Cl_2 solutions (i) - (v) (Table 4.4) differs least from that observed in the presence of dmmp alone whereas that observed in CH_3NO_2 [5] (Table 4.7) shows a marked variation with the concentration of free dmmp.

The minor variations of the ligand exchange parameters over a 17.9 fold variation of $[dmmp]_{free}/[CD_2Cl_2]$ suggest that the overall kinetic influence of the environment external to the first coordination sphere is virtually constant despite the variation in the chemical composition of the environment. A similar conclusion can be drawn from the invariance of the kinetic parameters characterising ligand exchange on $[Be(mmpp)_4]^{2+}$ over a 87.6 and 34.2 fold variation in $[mmpp]_{free}/[CD_3CN]$ and $[mmpp]_{free}/[CD_2Cl_2]$ respectively in solutions (i) - (v) and (vi) - (ix) in Table 4.5. The invariance of the kinetic parameters characterising these systems could arise from a preferential occupation of the second coordination sphere by either the free ligand or the diluent but the chemical shifts (Tables 4.4, 4.5 and 4.6) of the doublets characterising the coordinated and free ligands indicate that the relative magnetic environments of the ligand in these two sites change systematically for

the five systems investigated irrespective of the diluent and the observed rate law and appear to provide no evidence for preferential occupation of the second coordination sphere by either the ligand or diluent.

Hence it seems that, despite their structural dissimilarity, CD_2Cl_2 and dmmp outside the first coordination sphere exert similar influences upon the energetics of the D transition state and that in view of this and the similarities of the kinetic parameters characterising solutions (i) - (v) and (vi) (Table 4.4) ligand exchange on $[Be(dmmp)_4]^{2+}$ in the presence of free dmmp alone may also occur through a D mechanism. It was previously noted that the kinetic data characterising CH_3NO_2 solutions are most consistent with the operation of an A mechanism, but clearly as $[CH_3NO_2]$ decreases the exchange process will eventually become that operating in the absence of diluent and at some intermediate stage it is probable that two mechanisms may operate simultaneously.

Following this line of argument it can be expected that if the diluent influences the relative energies of A and D transition states then the possibility arises that the energies of these transition states may become sufficiently similar in a given diluent for both mechanisms to operate simultaneously. This is evidently the case for $[Be(dmmp)_4]^{2+}$ in CD_3CN for which the observed ligand exchange rate constant: $k_{ex} = k_1 + k_2[dmmp]_{free}$ where k_1 and k_2 are assigned to D and A mechanisms respectively.*

---

* Alternative explanations of the two term rate law are:-

(a) A D mechanism operates alone over the concentration range studied and the variation of k_{ex} reflects the changing dynamics of the transition state as the environment outside the first coordination sphere is varied. This explanation seems unlikely, however as in solutions (ix) - (xi) (Table 4.4) the $[CD_3CN]$ is in considerable excess over $[dmmp]_{free}$.

(b) A mechanism for ligand substitution analogous to that proposed for platinum(II) species[23] operates, where the k_1 term may characterise a process in which CD_3CN displaces dmmp from beryllium(II) via an A mechanism and that the resultant $[Be(dmmp)_3(CD_3CN)]^{2+}$ species is particularly labile towards the displacement of CD_3CN by dmmp through an A mechanism. If the first process is rate determining for the

(b) (continued)

overall, indirect, dmmp exchange then the result will be the k_1 term in the expression $k_{ex} = k_1 + k_2[dmmp]_{free}$ where k_2 characterises the the direct dmmp exchange. However attempts to detect the $[Be(dmmp)_3(CD_3CN)]^{2+}$ species in solution through the CD_3CN ^1H impurity resonance have not been successful.

As the nature of the diluent can be a major factor determining the ligand exchange mechanism it is to be expected that it will also have a significant influence on the magnitudes of the kinetic parameters characterising a given mechanism. This is seen to some extent for the D mechanism in the differences between the kinetic parameters characterising ligand exchange on $[Be(mmpp)_4]^{2+}$ in CD_2Cl_2 and CD_3CN, and to a greater extent in those characterising $[Be(dmadmp)_4]^{2+}$ in CH_3NO_2 and $\overline{OCOCH(CH_3)CH_2O}$,4-methyl-1,3-dioxolan-2-one (Table 4.7). (The observed $\Delta H^{\neq}$ and $\Delta S^{\neq}$ data probably include varying contributions from outside the first coordination sphere and thus the sign of $\Delta S^{\neq}$ for a D mechanism is expected to depend on the system as illustrated by $[Be(dmmp)_4]^{2+}$ and $[Be(mmpp)_4]^{2+}$ in CD_2Cl_2 where $\Delta S^{\neq}$ is positive and negative respectively (Table 4.7) and as a consequence mechanistic assignments based on the sign of $\Delta S^{\neq}$ are of dubious value. Such comparisons for the A mechanism are not possible as this mechanism only operates alone in CD_3NO_2, nevertheless by comparison to other diluents it becomes apparent that CD_3NO_2 favours the A mechanism for ligand exchange on beryllium(II) as is also the case for scandium(III)[19,20].

The origin of the varying kinetic effects of the different diluents on ligand exchange processes at the beryllium(II) centre does not appear to arise from differences in dielectric constants or dipole moments.

For $[Be(mmpp)_4]^{2+}$, D ligand exchange mechanisms operate in CD_2Cl_2 and CD_3CN solutions whereas an A mechanism operates in CD_3NO_2 solutions and yet from the dielectric constants or dipole moments[41] of CH_3NO_2, CH_3CN and CH_2Cl_2 which are; 35.8 (3.56), 37.5 (3.44) and 8.93 (1.14) at

298.2 K respectively (where the values in parentheses are the dipole moments (Debyes)). It would be anticipated that the kinetic effects of CD_3CN and CD_3NO_2 should be similar if the dielectric constants or dipole moments are important factors in determining the operational mechanism. (It should be noted that the dielectric constants are expected to vary with temperature and as such the choice of room temperature as the standard compared with the range of temperatures used in the dynamic nmr studies could alter their significance.)

Similarly the Reichardt E_T[25] parameters and the Gutmann donor numbers[17,18,26] which are 46.3 and 2.7 for CH_3NO_2, 46.0 and 14.1 for CH_3CN and 41.1 and $\sim$ 0 for CH_2Cl_2 respectively do not show any obvious correlation with the kinetic diluent effects. (These parameters which represent measures of Lewis acidity and basicity have been shown to correlate with solvent effects in some ionisation and solvolysis reactions of organic species[27,28].

Clearly extensive solvent properties such as dielectric constants will be modified by the solutes, particularly in some of the more concentrated solutions examined here and in other studies[4,5], and it appears that specific interactions between the first and second coordination spheres of the beryllium(II) species may be a more probable source of the differing solvent kinetic effects. The maximum difference between the interactions of CD_3NO_2 and CD_3CN with the array of methyl and phenyl groups presented by $[Be(dmmp)_4]^{2+}$ and $[Be(mmpp)_4]^{2+}$ (and also $[Be(tmp)_4]^{2+}$ arises if the $-NO_2$ and $-CN$ groups of these solvents are oriented towards the beryllium(II) centre. The electrostriction of the first and second coordination spheres may cause the geometries of CD_3NO_2, CD_3CN and CD_2Cl_2 to be critical in determining the time averaged orientation of the methyl and phenyl groups at the surface of the first coordination sphere and in consequence, the relative energies of the $[Be(ligand)_4^{2+}]$ ground state and the potential A and D transition states also.

A simple model suggests that if steric crowding in the first coordination sphere is either low or high the effect of the solvent is less likely to be critical in determining the mechanism that operates (although modification of the kinetic parameters characterising ligand exchange may occur) and that A and D mechanisms should operate respectively. In intermediate cases of steric crowding, which $[Be(mmpp)_4]^{2+}$, $[Be(dmmp)_4]^{2+}$ and $[Be(tmp)_4]^{2+}$ evidently are, a change in solvent may lead to modifications in the relative transition state energetics and produce a change in mechanism.

The results of the study of tppo exchange on $[Be(tppo)_4]^{2+}$ in CD_3NO_2 did not yield the ligand exchange mechanism operating, however it is predicted that a D mechanism would operate. To qualify this statement one needs to consider the results obtained for the $[Zn(hmpa)_4]^{2+}$ system and those of the $[Zn(tppo)_4]^{2+}$ system (see section 3.4 and 3.6) where A and D mechanisms were found to operate respectively, and the results for ligand exchange on $[Be(hmpa)_4]^{2+}$ in CH_3NO_2 where a D ligand exchange mechanism was assigned[5].

In the case of the zinc(II) ion steric crowding was used to explain the operation of the D mechanism for tppo exchange whereas, with hmpa the zinc(II) ion (r = 0.060 nm)[12] could accommodate the fifth molecule to form the $[Zn(hmpa)_5]^{2+}$ transition state intermediate as was exemplified by the ground state $[Zn(nipa)_3]^{2+}$ complex[37]. For the exchange of hmpa on $[Be(hmpa)_4]^{2+}$ in CH_3NO_2 a D ligand exchange mechanism was assigned, where steric crowding by the hmpa[5] ligand about the smaller beryllium(II) ion was said to be the cause, therefore tppo which is larger than hmpa is expected to have a similar effect on the beryllium(II) species and result in a D ligand exchange mechanism operating.

4.8 Ligand exchange on tetrakis(N,N-dimethylformamide) beryllium(II)

The complex $[Be(dmf)_4](ClO_4)_2$ which had previously been prepared by Matwiyoff and Movius[10] was prepared by the method given in section 6.2. Matwiyoff and Movius[10] measured the temperature dependence of the proton relaxation rates (linewidths) to obtain kinetic parameters characterising dmf exchange on $[Be(dmf)_4]^{2+}$. However the results from this method lack in accuracy compared with those obtained using the total lineshape analysis method and as such the experiment was repeated and the results reported herein for ligand exchange on $[Be(dmf)_4]^{2+}$ in dmf alone.

Solutions of the complex $[Be(dmf)_4](ClO_4)_2$ and dmf alone and in CD_3NO_2, CD_3CN and CD_2Cl_2 diluents were prepared, the compositions of which are given in Table 4.8(a).

The ^1H resonances of free dmf appear upfield from those of dmf coordinated to beryllium(II) when ligand exchange is slow on the nmr timescale (Table 4.8(a)). A comparison of the integrated areas of these resonances (N-Me resonances for solutions (i) - (x) and (xvi) and formyl protons for solutions (xi) - (xvi)) indicates that within experimental error the predominant beryllium(II) species in solution is $[Be(dmf)_4]^{2+}$. As the temperature is increased ligand exchange between the coordinated and free sites results in coalescence of the ^1H resonances of the coordinated and free dmf.

Complete lineshape analysis of the exchange modified spectra allow τ_c, the best-fit mean site lifetime of a single dmf ligand directly coordinated to beryllium(II), to be calculated. The variation of $k_{ex}(= {}^1/\tau_c)$ with $[dmf]_{free}$ and temperature in all three diluents CD_3NO_2, CD_3CN and CD_2Cl_2 is best described by the operation of a two term ligand exchange rate law where $k_{ex} = k_1 + k_2[dmf]_{free}$. The kinetic parameters in Table 4.8(b) were derived from a simultaneous non-linear least squares fit of all the k_{ex} data for each diluent to equation (2.12) using DATAFIT[45]. For solution (xvi) the k_{ex} data was fitted to the Eyring equation using ACTENG. The k_1 and k_2 terms of the observed ligand

Table 4.8(a) Solution compositions for dmf exchange on $[Be(dmf)_4]^{2+}$.

Solution	$[Be(dmf)_4^{2+}]$ mol dm^{-3}	$[dmf]_{free}$ mol dm^{-3}	$[CD_3NO_2]$ mol dm^{-3}	$[CD_3CN]$ mol dm^{-3}	$[CD_2Cl_2]$ mol dm^{-3}	CN[a]	$\Delta\nu$[b](288.1 K) ppm
(i)	0.0286	0.129	18.59	-	-	4.0 ± 0.1	0.293
(ii)	0.0538	0.243	18.09	-	-	4.0 ± 0.1	0.293
(iii)	0.0972	0.438	17.56	-	-	4.0 ± 0.1	0.295
(iv)	0.172	0.774	16.33	-	-	4.0 ± 0.1	0.298
(v)	0.325	1.46	14.59	-	-	4.0 ± 0.1	0.303
(vi)	0.0286	0.118	-	18.25	-	4.0 ± 0.1	0.266
(vii)	0.0514	0.213	-	17.84	-	4.0 ± 0.1	0.269
(viii)	0.0941	0.391	-	17.17	-	3.9 ± 0.1	0.269
(ix)	0.186	0.772	-	15.55	-	4.0 ± 0.1	0.274
(x)	0.359	1.49	-	13.95	-	4.0 ± 0.1	0.276
(xi)	0.0212	0.0904	-	-	15.25	4.0 ± 0.1	0.104*
(xii)	0.0452	0.193	-	-	14.68	4.0 ± 0.1	0.102*
(xiii)	0.0981	0.418	-	-	14.22	4.0 ± 0.1	0.102*
(xiv)	0.212	0.903	-	-	12.78	4.0 ± 0.1	0.111*
(xv)	0.442	1.885	-	-	9.98	4.0 ± 0.1	0.137*
(xvi)	0.894	8.55	-	-	-	4.0 ± 0.1	0.254[c]*
						4.0 ± 0.2	0.299[d]*

Table 4.8(a)

[a] The number of dmf ligands in the first coordination sphere of beryllium(II) as determined by the integration of the areas of the free and coordinated dmf resonances under slow exchange conditions. The temperature ranges from which these values were determined were for solutions (i) - (v) 260 - 290 K, for solutions (vi) - (x) 250 - 290 K, for solutions (xi) - (xv) 220 - 250 K and for solution (xvi), 240 - 260 K.

[b] $\Delta\nu$ is the chemical shift between the ^1H resonances of the coordinated and free dmf. These were the N-Me resonances for solutions (i) - (x) and (xvi) and the formyl resonances for solutions (xi) - (xvi). The proton impurity resonances of; CD_3NO_2 varied systematically from 1.12 - 1.18 ppm downfield of the coordinated ligand resonance for solutions (i) - (v), CD_3CN varied systematically from 0.883 - 0.853 ppm upfield of the coordinated ligand resonance for solutions (xi) - (x) respectively and CD_2Cl_2 varied systematically from 2.64 - 2.52 ppm upfield of the coordinated ligand resonance for solutions (xi) - (xv) respectively.

[*] $\Delta\nu$(258.1 K).

[c] Chemical shift difference for the formyl protons in their free and bound environments.

[d] Chemical shift differences for the N-Me group in their free and bound environments.

Table 4.8(b) Kinetic Parameters for dmf exchange on $[Be(dmf)_4]^{2+}$.

Solutions	Diluent	k_1(298.2 K) s^{-1}	$\Delta H_1^{\neq}$ kJ mol^{-1}	$\Delta S_1^{\neq}$ J K^{-1} mol^{-1}	k_2(298.2 K) mol dm^{-3} s^{-1}	$\Delta H_2^{\neq}$ kJ mol^{-1}	$\Delta S_2^{\neq}$ J K^{-1} mol^{-1}
(i) - (v)	CD_3NO_2	0.10 ± 0.03	83.6 ± 6.3	16.3 ± 17.6	-	-	-
(i) - (v)	"	-	-	-	8.5 ± 0.1	58.1 ± 0.5	-32.0 ± 1.6
(vi) - (x)	CD_3CN	1.56 ± 0.04	62.9 ± 0.8	-29.8 ± 2.7	-	-	-
(vi) - (x)	"	-	-	-	7.98 ± 0.07	60.2 ± 0.4	-25.6 ± 1.3
(xi) - (xv)	CD_2Cl_2	2.54 ± 0.06	40.7 ± 1.0	-100.4 ± 3.1	-	-	-
(xi) - (xv)	"	-	-	-	10.3 ± 0.2	44.0 ± 0.6	-77.8 ± 1.9
(xvi)[a]	dmf	66.3 ± 2.8	53.9 ± 2.0	-29.3 ± 0.6			
(xvi)[b]	dmf	70 ± 11	55.7 ± 2.1	-22.9 ± 7.2			

[a] Results from lineshape analysis of formyl protons of free and coordinated dmf.

[b] Results from lineshape analysis of N-Me signals of free and coordinated dmf.

exchange rate law are considered to characterise D and A ligand exchange mechanisms respectively.

4.9 Ligand exchange on tetrakis(N-methylacetamide) beryllium(II)

The complex $[Be(nma)_4](ClO_4)_2$ was prepared by the method described in section 6.2. Solutions of the complex $[Be(nma)_4](ClO_4)_2$ and nma in CD_3NO_2 and CD_3CN were prepared, the compositions of which are given in Table 4.9.

The $[Be(nma)_4]^{2+}$ system is somewhat complicated by the existence of isomers. La Planche and Rogers[29] did not observe any peaks attributable to the *cis* isomer of nma in the ^1H nmr spectrum whereas Barker and Bordeaux[30] showed that ∿ 3% of the *cis*-nma isomer (II) was present at ∿ 308 K.

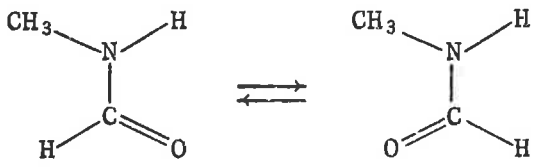

(I) (II)

(It is not clear what the solution compositions used to obtain these results were.) From a solution of nma in CD_3CN the ^1H (90 MHz) nmr spectra indicate that ∿ 3% of the *cis*-nma isomer is present at 300 K.

For $[Be(nma)_4]^{2+}$ the *cis*-nma isomer proportion increases to ∿ 5% (see Figure 4.12) and as a consequence ∿ 20% of this complex exists as $[Be(trans\text{-}nma)_3(cis\text{-}nma)]^{2+}$ in CD_3CN solution at 300 K.

Similar results have been observed for the nma complexes of scandium(III), ∿ 8% *cis* isomer[31], aluminium(III) ∿ 15% *cis* isomer[32], zinc(II) ∿ 4% *cis* isomer[33] and magnesium(II) ∿ 2% *cis* isomer[31]. In CD_3CN solution the N-methyl and acetyl ^1H nmr resonances of *cis*-nma in $[Be(nma)_4]^{2+}$ appear 0.082 and 0.183 ppm downfield from the analogous *trans* nma peaks at 300 K (see Figure 4.12). Similar chemical shifts are observed in CD_3NO_2 solution. (The observation of the ^1H nmr signal

Table 4.9 Solution compositions and kinetic parameters for nma exchange on $[Be(nma)_4]^{2+}$.

Solution	$[Be(nma)_4^{2+}]$ mol dm^{-3}	$[nma]_{free}$ mol dm^{-3}	$[CD_3NO_2]$ mol dm^{-3}	$[CD_3CN]$ mol dm^{-3}	CN[a]	$\Delta\nu$(290 K)[b] ppm
(i)	0.0206	0.0879	18.06	-	4.1 ± 0.1	0.440
(ii)	0.0438	0.180	17.96	-	4.0 ± 0.1	0.427
(iii)	0.0930	0.383	17.17	-	4.0 ± 0.1	0.404
(iv)	0.184	0.758	16.15	-	4.1 ± 0.1	0.386
(v)	0.405	1.67	13.97	-	4.1 ± 0.1	0.365
(vi)	0.957	3.94	6.31	-	4.0 ± 0.1	0.339
(vii)	0.0177	0.058	-	18.58	3.9 ± 0.1	0.282
(viii)	0.0382	0.153	-	17.19	4.0 ± 0.1	0.283
(ix)	0.104	0.342	-	16.36	4.0 ± 0.1	0.280
(x)	0.231	0.758	-	16.20	4.0 ± 0.1	0.275
(xi)	0.550	1.80	-	11.55	4.0 ± 0.1	0.276
(xii)	1.032	4.59	-	4.99	4.0 ± 0.1	0.311

Table 4.9 (Continued)

Diluent	k_1(340 K) s^{-1}	k_2(340 K) $dm^3\ mol^{-1}\ s^{-1}$	$\Delta H^{\neq}$ $kJ\ mol^{-1}$	$\Delta S^{\neq}$ $J\ K^{-1}\ mol^{-1}$
CD_3NO_2	9.2 ± 0.2	-	71.5 ± 0.9	-17.3 ± 2.6
CD_3NO_2	-	16.3 ± 0.3	76.8 ± 0.9	3.1 ± 2.9
CD_3CN	38.6 ± 0.6	-	74.7 ± 0.9	4.0 ± 2.6
CD_3CN	-	19.3 ± 0.7	82.9 ± 2.1	22.6 ± 6.2

[a] The number of ligands in the first coordination sphere of beryllium(II) as determined by integration of the free and bound acetyl resonances of *trans* nma under slow exchange conditions on the ^1H nmr timescale. The temperatures at which these determinations were made were 260 - 290 K for solutions (i) - (vi) and 250 - 290 K for solutions (vii) - (xii).

[b] $\Delta\nu$ is the ^1H chemical shift between the coordinated and free *trans* nma acetyl resonances. For solutions (i) - (vi) the ^1H impurity resonance of CD_3NO_2 varies systematically from 2.000 - 2.050 ppm downfield of the coordinated peak and for solutions (vii) - (xii) the ^1H impurity resonance of CD_3CN varies systematically from 0.176 - 0.208 ppm upfield of the coordinated peak.

Figure 4.11

^1H (90 MHz) nmr spectra for a solution of $[Be(nma)_4](ClO_4)_2$ (0.957 mol dm^{-3}) and nma (3.94 mol dm^{-3}) in the diluent CD_3NO_2 (6.31 mol dm^{-3}). The acetyl singlet arising from the coordinated nma appears downfield. Experimental temperatures (K) appear to the left of each spectrum in the Figure, while the mean site lifetime of a single nma ligand on beryllium(II), τ_c(ms), appears to the right of each calculated lineshape.

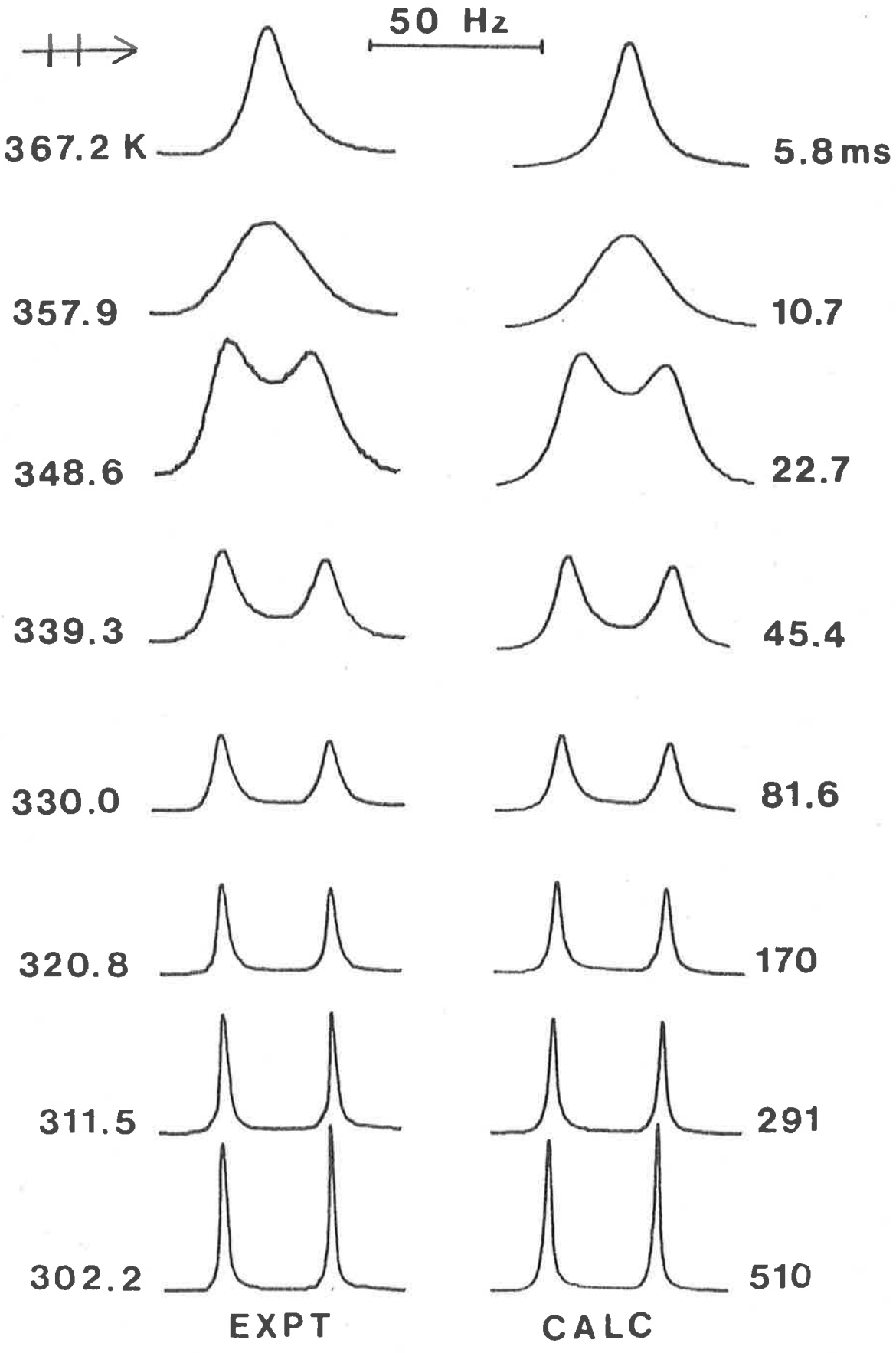
50 Hz
367.2 K
5.8 ms
357.9
10.7
348.6
22.7
339.3
45.4
330.0
81.6
320.8
170
311.5
291
302.2
510
EXPT
CALC

Figure 4.12

A ^1H (90 MHz) nmr spectrum of $[Be(nma)_4](ClO_4)_2$ in CD_3CN at 300 K. The N-Me resonances of *cis* and *trans* nma are labelled (A) and (B), the acetyl resonances (C) and (D) and the proton impurity resonances of the diluent CD_3CN (E) respectively.

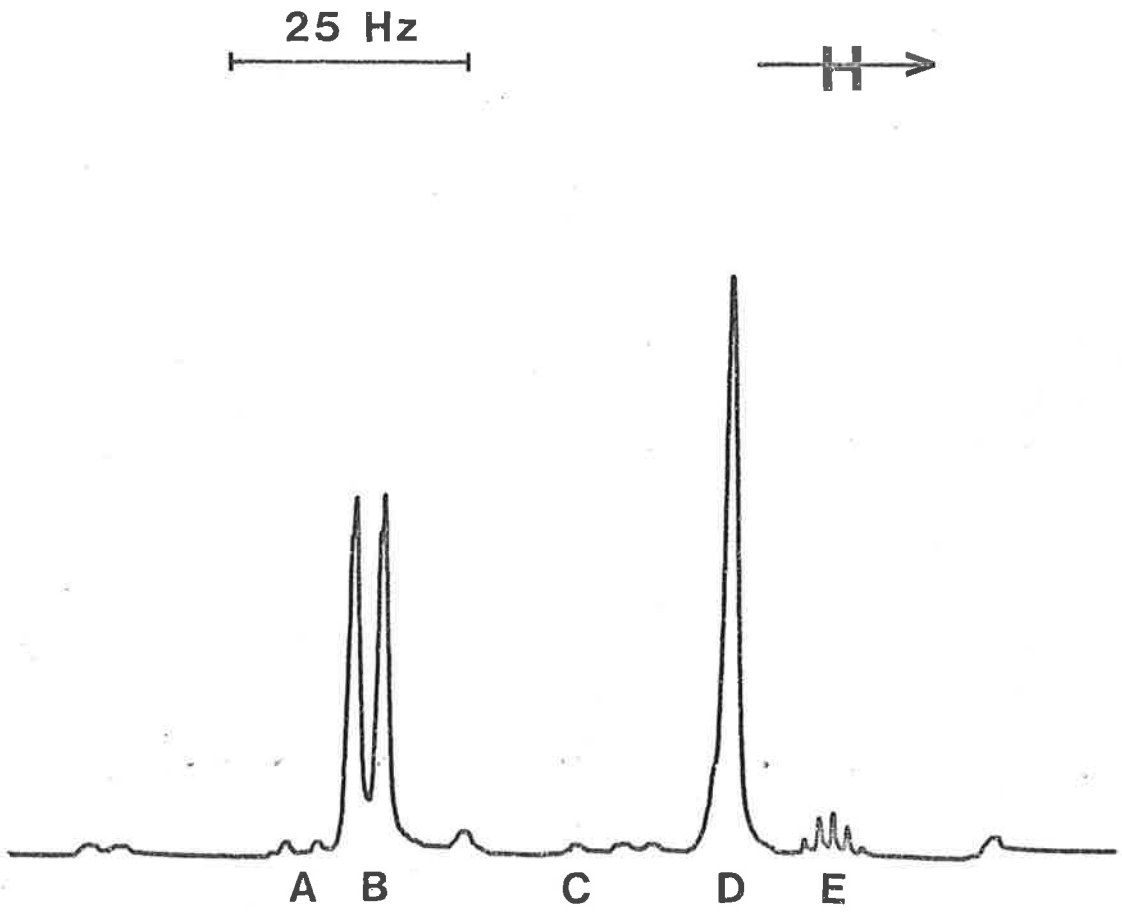
25 Hz
H
A
B
C
D
E

Figure 4.13

Semilogarithmic plot of $\tau_c T$ (sK) against T^{-1} (K^{-1}) for nma exchange on $[Be(nma)_4]^{2+}$ in CD_3NO_2. The solid lines represent the non-linear least squares best-fit of all the data points shown to equation (2.12), for solutions (vi) - (i) (Table 4.9) in ascending order of magnitude of $\tau_c T$ at any temperature respectively.

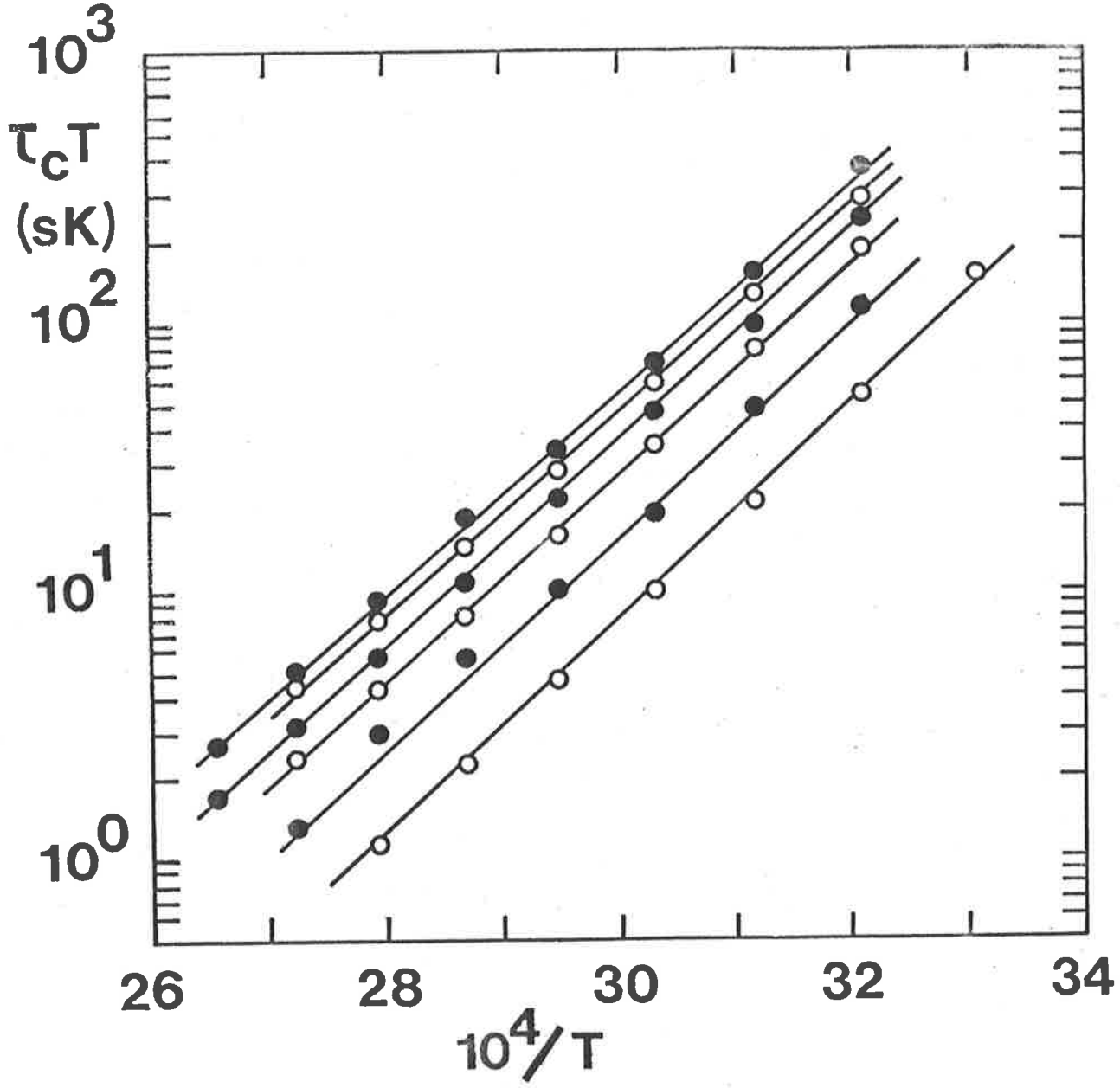
10^3
$\tau_c T$
(sK)
10^2
10^1
10^0
26
28
30
32
34
$10^4/T$

of the less stable *cis* isomer of nma downfield of the major *trans* isomer peaks is in agreement with the expected shielding of an alkyl group *cis* to a carbonyl group compared with that of a *trans* group[34-36].)

As a consequence of the existence of *cis* and *trans* isomers for nma there will be several paths by which ligand exchange can occur on $[Be(nma)_4]^{2+}$. The probability of direct intermolecular exchange of *cis*-nma between the coordinated and free states (path (a)) is relatively low compared with the *cis-trans* (path (b) and (c)) and *trans-trans* (path (d)) exchange probabilities.

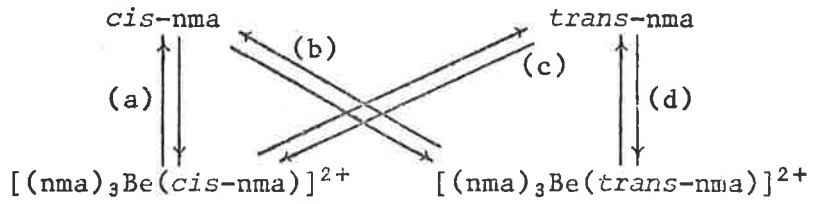

Hence coalescence of the *cis*-nma resonances occurs as a consequence of direct (path (a)) and indirect (path (b) and (c)) intermolecular exchange but because these resonances are superimposed on those of the *trans*-nma isomer resonances it was not possible to obtain accurate kinetic data for the *cis*-nma intermolecular exchange process. Hence the procedure adopted was to subtract the superimposed *cis* coalescence lineshape from that of the *trans* coalescence lineshape for the acetyl resonances to obtain exchange parameters characterising the exchange of *trans*-nma between free and coordinated sites.

Under slow exchange conditions (see Table 4.9) the predominant beryllium(II) species in CD_3CN and CD_3NO_2 solution obtained from a comparison of the integrated areas of free and coordinated acetyl resonances of *trans*-nma was $[Be(nma)_4]^{2+}$. As the temperature was increased coalescence of the acetyl singlets of the free and coordinated *trans*-nma occurred, Figure 4.11 shows the coalescence phenomena observed for solution (vi) Table 4.9. .

Complete lineshape analysis of the acetyl resonances was used to derive kinetic parameters for the predominantly *trans*-nma exchange at

7 - 10 temperatures per solution in the temperature ranges 300 - 370 K for solutions (i) - (vi) and 300 - 350 K for solutions (vii) - (xii) in Table 4.9.

In both CD_3NO_2 and CD_3CN solutions the variation of the observed rate constant with $[nma]_{free}$ is best characterised by a two term rate law where $k_{ex} = k_1 + k_2[nma]_{free}$. Figure 4.13 shows that τ_c decreases systematically as $[nma]_{free}$ increases and as such the activation parameters were derived from a simultaneous non-linear least squares best-fit of all the k_{ex} data to equation (2.12). For the two term rate law which describes nma exchange on $[Be(nma)_4]^{2+}$ the k_1 term is assigned to a D mechanism whilst the k_2 term is assigned to an A mechanism.

4.10 Ligand exchange on tetrakis(N,N-dimethylacetamide) beryllium(II)

The complex $[Be(dma)_4](ClO_4)_2$ was prepared by the method described in section 6.2. Solutions of the complex $[Be(dma)_4](ClO_4)_2$ and dma in CD_3NO_2 and CD_3CN were prepared, the compositions of which are given in Table 4.10.

Under the limiting conditions of slow exchange (below 300 K) the ^1H (90 MHz) nmr spectra of the dma solutions (i) - (xi) exhibited acetyl singlets (the N-Me doublets which appear downfield of the acetyl singlets were not used to obtain kinetic information as rotation about the C-N bond occurs in the temperature range studied) for coordinated dma downfield of those for free dma (see Table 4.10 for the relative chemical shifts) and a comparison of the integrated areas of the coordinated and free acetyl singlets of dma show that within experimental error four dma ligands are bound per beryllium(II) ion, i.e. $[Be(dma)_4]^{2+}$ is the predominant beryllium(II) species in solution.

As the temperature was increased the acetyl singlets of the coordinated and free dma coalesced (see Figure 4.14) consistent with an increased rate of ligand exchange and complete lineshape analysis yielded

Figure 4.14

^1H (90 MHz) nmr spectra of the acetyl resonances of free and coordinated dma for a solution where $[Be(dma)_4^{2+}]$, $[dma]_{free}$ and $[CD_3NO_2]$ are 0.486, 1.90 and 11.88 mol dm^{-3} respectively. The acetyl singlet arising from coordinated dma appears downfield. The experimental temperatures (K) appear to the left, and the best-fit τ_c(ms) values appear to the right of the Figure respectively.

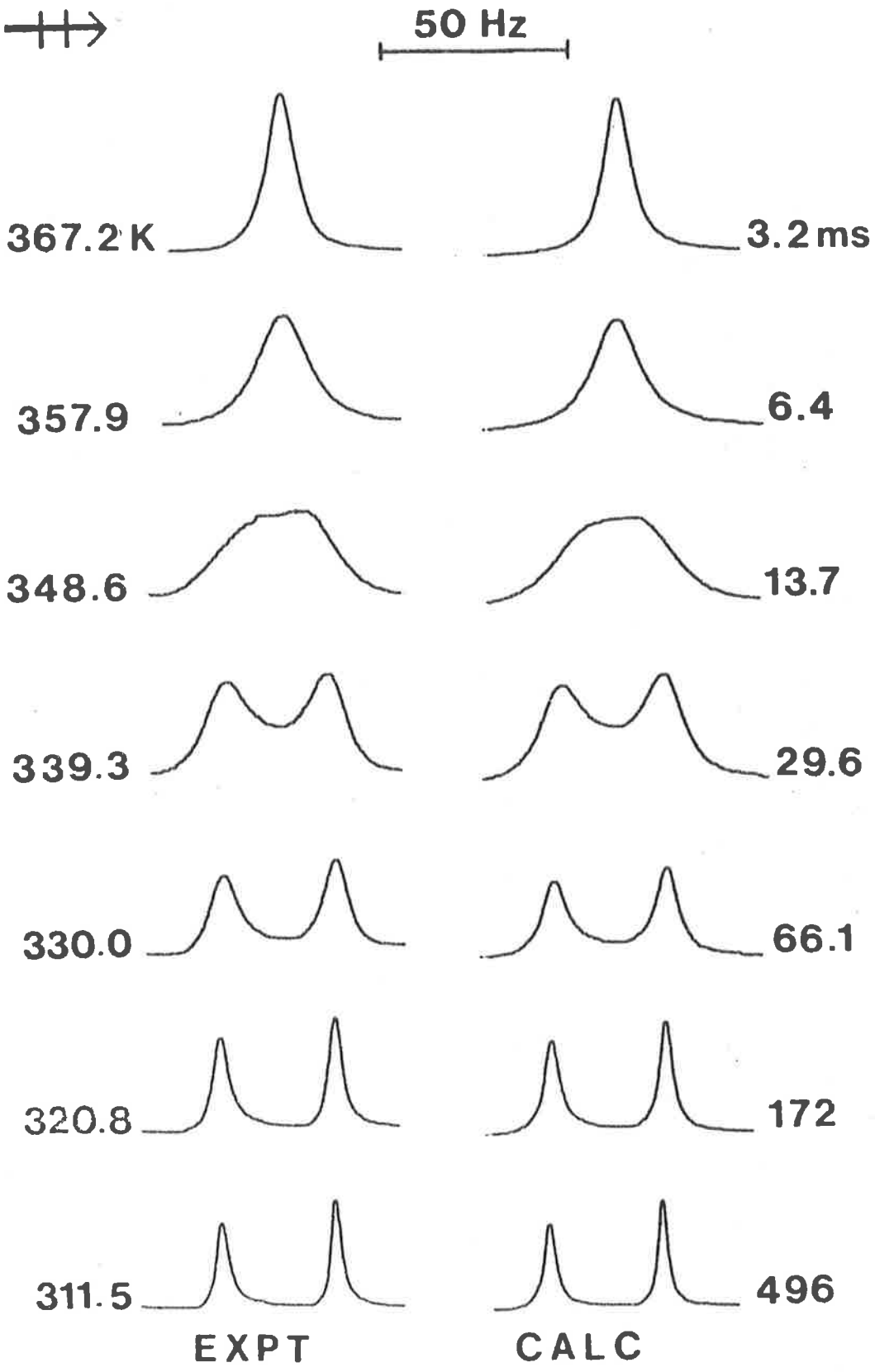
50 Hz
367.2 K
3.2 ms
357.9
6.4
348.6
13.7
339.3
29.6
330.0
66.1
320.8
172
311.5
496
EXPT
CALC

Table 4.10 Solution compositions and kinetic parameters for dma exchange on $[Be(dma)_4]^{2+}$.

Solution	$[Be(dma)_4^{2+}]$ mol dm^{-3}	$[dma]_{free}$ mol dm^{-3}	$[CD_3NO_2]$ mol dm^{-3}	$[CD_3CN]$ mol dm^{-3}	CN[a]	$\Delta\nu$[b](290 K) ppm
(i)	0.0169	0.0663	19.07	-	4.0 ± 0.1	0.365
(ii)	0.0416	0.163	18.37	-	3.9 ± 0.1	0.363
(iii)	0.0941	0.367	18.24	-	3.9 ± 0.1	0.362
(iv)	0.216	0.842	15.56	-	3.9 ± 0.1	0.359
(v)	0.486	1.90	11.88	-	4.0 ± 0.1	0.355
(vi)	0.00752	0.0274	-	18.82	4.0 ± 0.1	0.200
(vii)	0.0176	0.0639	-	18.45	3.9 ± 0.1	0.208
(viii)	0.0426	0.155	-	18.10	4.0 ± 0.1	0.210
(ix)	0.0901	0.328	-	17.32	4.0 ± 0.1	0.219
(x)	0.197	0.716	-	15.92	4.1 ± 0.1	0.232
(xi)	0.422	1.54	-	12.69	3.9 ± 0.1	0.254

Table 4.10 (Continued)

Diluent	k_1(340 K) s^{-1}	k_2(340 K) $dm^3\ mol^{-1}\ s^{-1}$	$\Delta H^{\neq}$ $kJ\ mol^{-1}$	$\Delta S^{\neq}$ $J\ K^{-1}\ mol^{-1}$
CD_3NO_2	7.33 ± 0.29	-	56.9 ± 1.5	-62.1 ± 4.6
"	-	10.6 ± 0.6	66.7 ± 2.5	-30.1 ± 7.4
CD_3CN	18.2 ± 0.2	-	78.0 ± 0.6	+7.5 ± 1.9
"	-	10.5 ± 0.4	67.8 ± 2.2	-26.9 ± 6.4

[a] The number of ligands in the first coordination sphere beryllium(II) as determined by a comparison of the integrated areas of the acetyl resonances of coordinated and free dma under slow exchange conditions on the ^1H nmr timescale. The temperature ranges used in these determinations were 260 - 290 K for solutions (i) - (v) and 250 - 290 K for solutions (vi) - (xi).

[b] The ^1H (90 MHz) nmr chemical shifts between the acetyl resonances of the coordinated and free dma. The proton impurity peaks of CD_3NO_2 varied systematically from 1.98 - 1.93 ppm downfield of the coordinated ligand resonances in solutions (i) - (v). The proton impurity peaks of CD_3CN varied systematically from 0.241 - 0.263 ppm upfield of the coordinated dma resonance for solutions (vi) - (xi).

τ_c, the mean site lifetime of a single dma molecule coordinated to beryllium(II). Spectra were collected at 7 - 10 temperatures for individual solutions over the temperature ranges 300 - 370 K for solutions (i) - (v) and 300 - 350 K for solutions (vi) - (xi).

In both CD_3NO_2 and CD_3CN solution the variation of k_{ex} with $[dma]_{free}$ over 28.6 and 56.2 fold concentration ranges respectively is of the form;

$$k_{ex} = k_1 + k_2[dma]_{free}.$$

The kinetic parameters were derived from the simultaneous best-fit of all the k_{ex} data for each diluent to equation (2.12) using DATAFIT[45]. The observed two term rate laws for dma exchange on $[Be(dma)_4]^{2+}$ can be rationalised in terms of the simultaneous operation of both D and A ligand exchange mechanisms, where the k_1 term is assigned to the operation of a D mechanism and the k_2 term is assigned to the operation of an A mechanism.

For scandium(III) similar results were obtained for the exchange of dma on $[Sc(dma)_6]^{3+}$ in both CD_3CN and CD_3NO_2 solutions[20], i.e. the rate law observed was of the form $k_{ex} = k_1 + k_2[dma]_{free}$ and these results were interpreted in terms of the simultaneous operation of D and A mechanisms.

4.11 Ligand exchange on tetrakis(N,N-diethylacetamide) beryllium(II)

The complex $[Be(dea)_4](ClO_4)_2$ was prepared by the method described in section 6.2. Solutions containing dea and $[Be(dea)_4](ClO_4)_2$ in CD_3NO_2 and CD_3CN solutions were prepared, the compositions of which are given in Table 4.11.

The ^1H nmr acetyl peaks of the coordinated dea appear downfield from those of the free dea (see Table 4.11 for the relative chemical shifts) and a comparison of the integrated areas of these resonances under slow exchange conditions shows that $[Be(dea)_4]^{2+}$ is the predominant

Table 4.11 Solution compositions and kinetic parameters for dea exchange on $[Be(dea)_4]^{2+}$.

Solution	$[Be(dea)_4^{2+}]$ mol dm^{-3}	$[dea]_{free}$ mol dm^{-3}	$[CD_3NO_2]$ mol dm^{-3}	$[CD_3CN]$ mol dm^{-3}	CN[a]	$\Delta\nu$[b](290 K) ppm
(i)	0.0204	0.0754	18.29	-	4.1	0.380
(ii)	0.0442	0.163	17.85	-	3.9	0.380
(iii)	0.0782	0.289	17.25	-	4.0	0.380
(iv)	0.104	0.479	16.47	-	4.0	0.380
(v)	0.195	0.898	13.90	-	4.0	0.380
(vi)	0.356	1.64	10.38	-	4.0	0.380
(vii)	0.0215	0.0911	-	17.95	4.0	0.202
(viii)	0.0320	0.130	-	17.51	4.0	0.206
(ix)	0.0666	0.271	-	17.10	4.0	0.215
(x)	0.117	0.474	-	16.42	4.0	0.226
(xi)	0.219	1.18	-	11.94	4.0	0.258

Table 4.11 (Continued)

Diluent	k_1(340 K) s^{-1}	k_2(340 K) $dm^3\ mol^{-1}\ s^{-1}$	$\Delta H^{\neq}$ $kJ\ mol^{-1}$	$\Delta S^{\neq}$ $J\ K^{-1}\ mol^{-1}$
CD_3NO_2	2.29 ± 0.09	-	76.4 ± 2.2	-14.6 ± 6.4
CD_3NO_2	-	19.9 ± 0.3	68.5 ± 0.8	-19.6 ± 2.4
CD_3CN	17.5 ± 0.1	-	75.2 ± 0.5	-1.0 ± 1.5
CD_3CN	-	18.6 ± 0.3	69.5 ± 1.0	-17.2 ± 3.1

[a] The number of ligands in the first coordination sphere of beryllium(II) as determined by a comparison of the integrated areas of the acetyl resonances for free and coordinated dea. The error in the CN is ±0.1.

[b] The ^1H chemical shifts of the acetyl resonances of $[Be(dea)_4]^{2+}$ downfield of that of free dea. In CD_3NO_2 solutions (i) - (vi) the free ligand chemical shift varies systematically from 2.320 - 2.420 ppm upfield from the diluent proton impurity signal, and in CD_3CN solutions (vii) - (xi) the free ligand chemical shift varies systematically from 0.037 - 0.011 ppm downfield of the proton impurity signal of the diluent.

beryllium(II) species in solution. The ^1H nmr acetyl peaks were used to obtain kinetic information about the ligand exchange process on $[Be(dea)_4]^{2+}$ as the N-$C\underline{H}_2$ and N-CH_2-$C\underline{H}_3$ ^1H resonances are too complex (Figure 4.16).

As the temperature is increased coalescence of the acetyl resonances of free and coordinated dea occurs, (Figure 4.15 shows the coalescence pattern observed and the simulated lineshapes for solution (v) Table 4.11) and complete lineshape analysis of these exchange modified spectra give best-fit values of the mean site lifetimes of one dea molecule bound to beryllium(II), τ_c which is related to $k_{ex} = P_F/\tau_c$ (where P_F = relative population of free dea). The variation of k_{ex} with $[dea]_{free}$ is found to be consistent with the operation of a two term ligand exchange rate law where $k_{ex} = k_1 + k_2[dea]_{free}$. The kinetic parameters quoted in Table 4.11 have been derived from a simultaneous best-fit of all k_{ex} data for solutions with the same diluent to equation (2.12).

The k_1 and k_2 terms of the ligand exchange rate law observed for dea exchange on $[Be(dea)_4]^{2+}$ are considered to characterise D and A ligand exchange mechanisms respectively.

4.12 Ligand exchange on tetrakis(N-phenylacetamide) beryllium(II)

The complex $[Be(npa)_4](ClO_4)_2$ was prepared by the method described in section 6.2, and was found to be soluble in CD_3CN and virtually insoluble in CD_2Cl_2 and CD_3NO_2. The solubility of $[Be(npa)_4](ClO_4)_2$ and npa in CD_3CN was limited to $\sim$ 20 mg/cm^3 and $\sim$ 14 mg/cm^3 of the above respectively, larger quantities of free npa resulted in precipitation occurring at the lower temperatures, npa was soluble in CD_3CN ($\sim$ 25 mg/cm^3 < 260 K).

The ^1H nmr spectra of npa in CD_3CN were consistent with only one isomer (*trans*) being present as was observed in $CDCl_3$ [39] and pyridine[40].

Figure 4.15

^1H (90 MHz) nmr spectra of the acetyl group characterising dea exchange on $[Be(dea)_4]^{2+}$ in a solution where $[Be(dea)_4{}^{2+}]$, $[dea]_{free}$ and $[CD_3NO_2]$ are 0.195, 0.898 and 13.90 mol dm^{-3} respectively. The acetyl singlet of coordinated dea is the downfield singlet. The experimental temperatures (K) and the mean site lifetimes τ_c(ms) appear to the left of the experimental spectra, and the right of the calculated lineshapes respectively in the Figure.

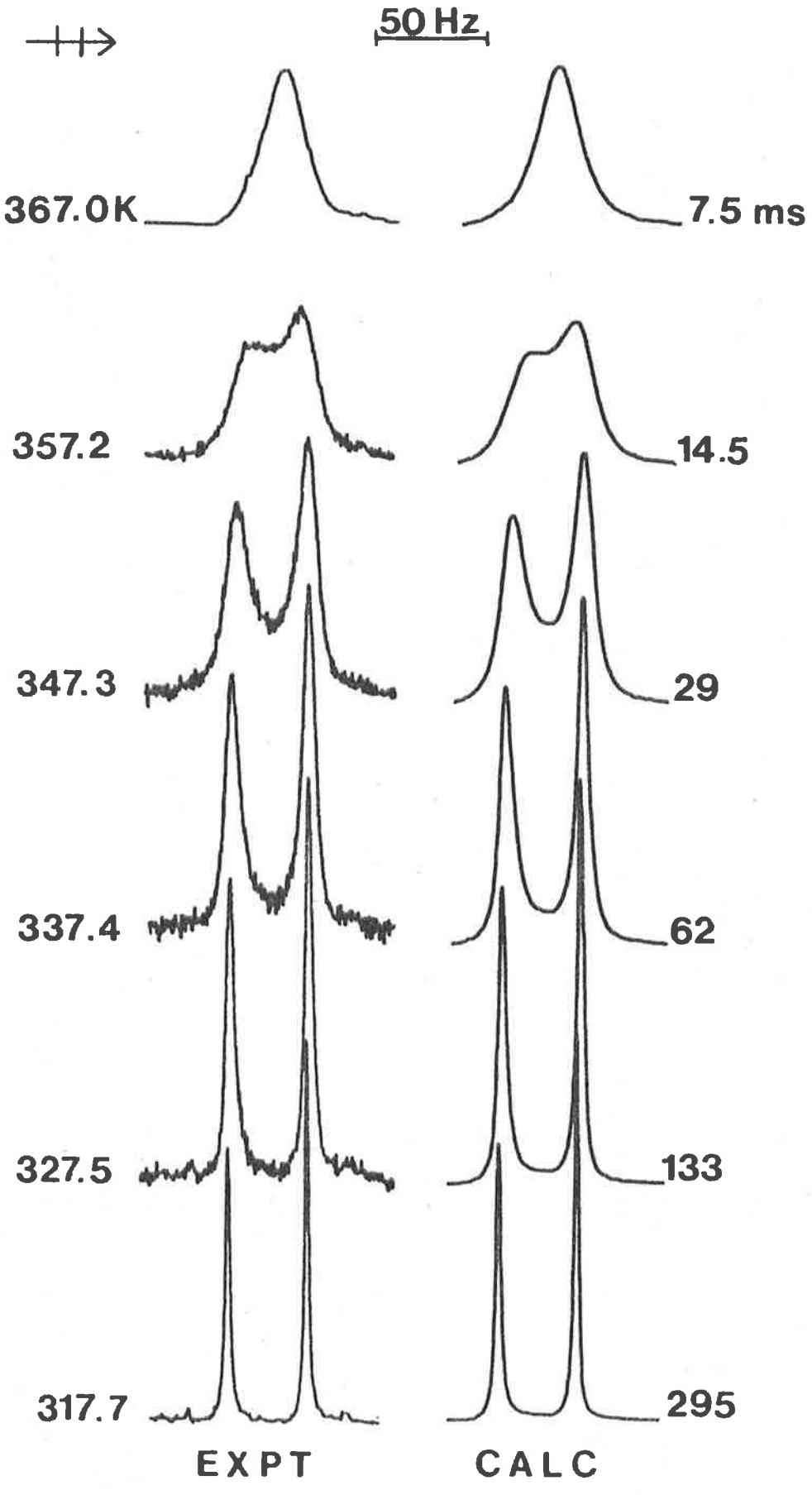
50 Hz
367.0K
7.5 ms
357.2
14.5
347.3
29
337.4
62
327.5
133
317.7
295
EXPT
CALC

Figure 4.16

^1H (90 MHz) nmr spectrum of $[Be(dea)_4]^{2+}$ in CD_3CN at 300 K. The proton impurity resonances of the diluent are labelled (A), the N-$\underline{CH}_2$ resonances (B), the acetyl resonances (C) and the N-CH_2-$\underline{CH}_3$ resonances (D) respectively.

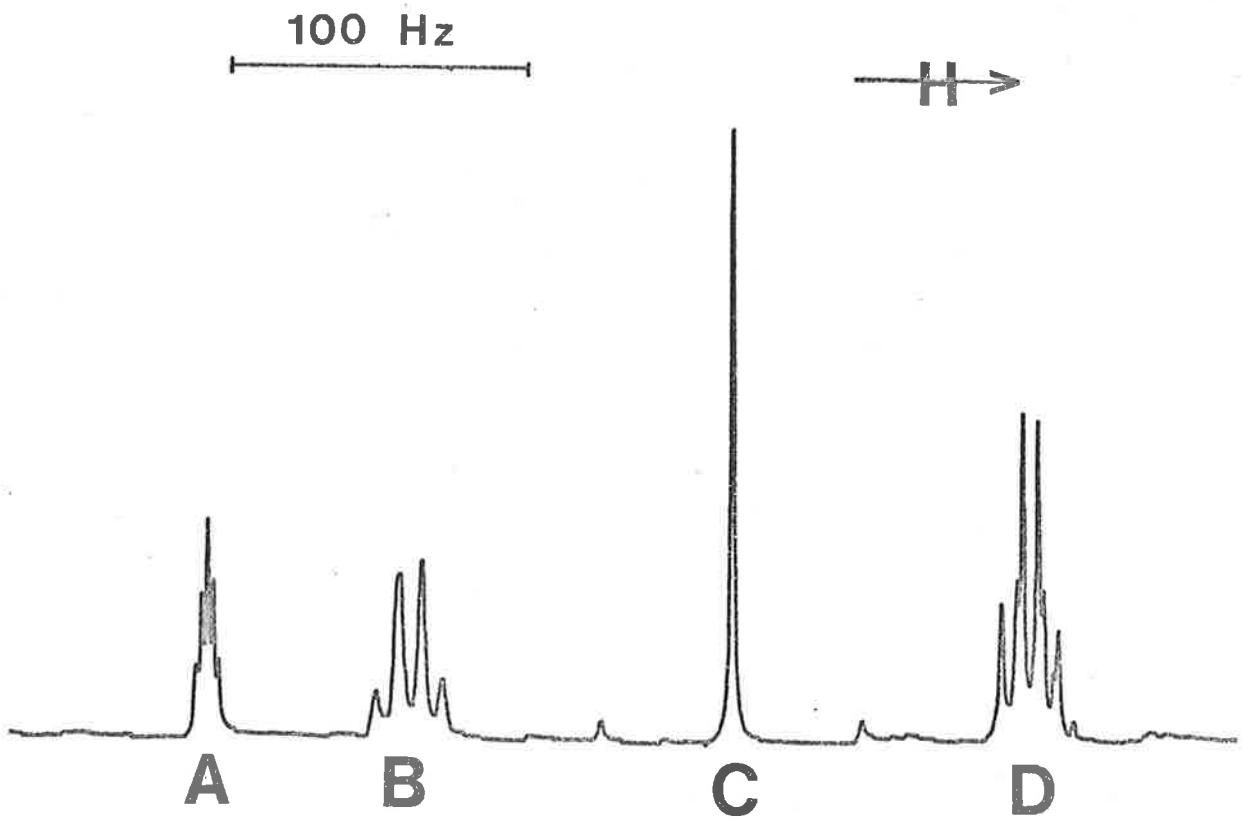
100 Hz
H
A
B
C
D

The ^1H (90 MHz) nmr spectra of $[Be(npa)_4](ClO_4)_2$ in CD_3CN ($\sim$ 50 mg/cm^3) in the acetyl region consisted of one sharp major singlet and two minor singlets 9 and 15 Hz downfield of the major singlet (see Figure 4.17) and in the N-H region one major singlet was observed downfield of a minor singlet at 260 K.

On increasing the temperature to 320 K, coalescence of the minor and major singlets in the acetyl and N-H regions occurs respectively, at 320 K only one singlet is observed in both regions above with the N-H singlet being considerably broadened (see Figure 4.16).

The ^1H (90 MHz) nmr spectra of a solution of $[Be(npa)_4](ClO_4)_2$ and npa in CD_3CN in the acetyl region consisted of one major singlet and two minor singlets downfield of the major singlet as observed for the ^1H nmr spectra of the complex alone (as described above) and the proton impurity signal of the diluent CD_3CN slightly upfield, at 260 K. In the N-H region two peaks are observed, a sharp singlet (assigned as the bound N-H peak) is $\sim$ 120 Hz downfield of a broad peak (assigned as the free N-H peak) at 260 K. On increasing the temperature coalescence of the singlets in the N-H region occurs and at 300 K the two peaks can still be distinguished.

From the low temperature spectra $\lesssim$ 260 K the coordination number of beryllium(II) in CD_3CN solution is 4.0 $\pm$ 0.2.

However as a result of (i) the broadening of the N-H peaks due to differing ^{14}N relaxation times, (ii) the low concentration range which can be examined and (iii) the problems of spinning side bands interfering with the free N-H singlet of npa no qualitative kinetic data was obtained regarding npa exchange on $[Be(npa)_4]^{2+}$.

Figure 4.17

^1H (90 MHz) nmr spectra of; (i) $[Be(npa)_4](ClO_4)_2$ in CD_3CN at 260 K ($\sim$ 50 mg/cm^3), (ii) same as (i) but at 300 K, (iii) a solution of $[Be(npa)_4](ClO_4)_2$ and npa in CD_3CN at 260 K containing $\sim$ 19/13 mg/cm^3 of each component respectively. Peak; (a) is due to the formyl proton of the bound npa ligand and on increasing the temperature from spectrum (i) to (ii) shows broadening, (b) is the signal due to the formyl group of free npa, (c) is the ^1H signal due to the phenyl group and (d) consists of the *cis* and *trans* isomer peaks of the acetyl group of npa plus the proton impurity peaks of the diluent CD_3CN.

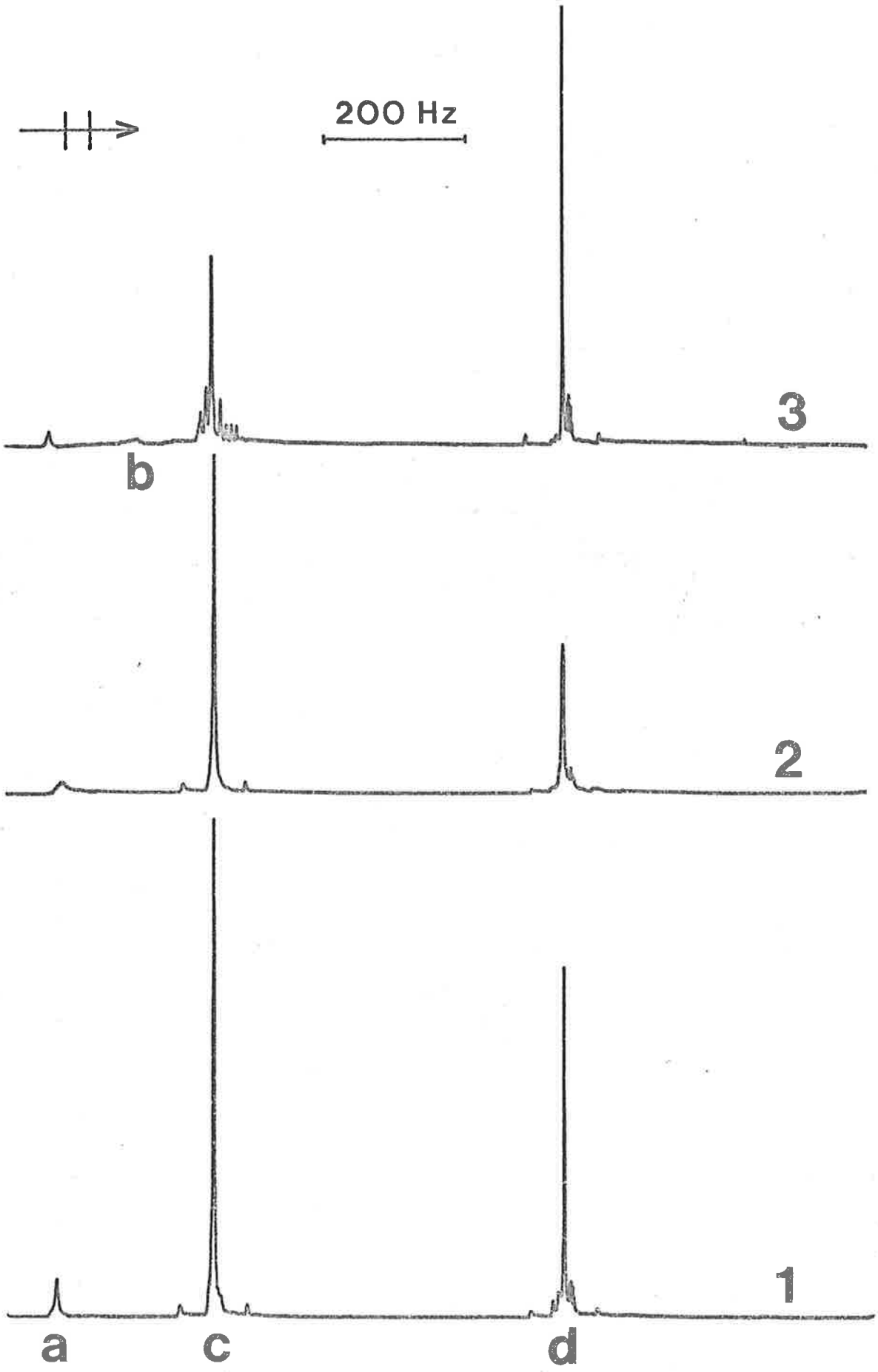
200 Hz
3
b
2
1
a
c
d

4.13 Ligand exchange on beryllium(II) amide systems

The ligand exchange data for $[Be(dmf)_4]^{2+}$ and its nma, dma, dea and tmu analogues (Table 4.12) suggest that the steric character of the ligand is important in determining the relative magnitudes of k_1 and k_2 terms in the observed rate law $k_{ex} = k_1 + k_2[L]_{free}$ (where L is any of the above amides) in which these parameters are considered to characterise D and A ligand exchange mechanisms respectively. Unfortunately in the cases of npa (lack of solubility and lack of chemical shift between the free and coordinated acetyl resonances, see section 4.12) and def (no solid complex formed with beryllium(II), see section 6.2) no kinetic data was obtained.

[An alternative explanation for the two term rate law found is that a D ligand exchange mechanism operates alone over the concentration range studied and the variation of τ_c with concentration merely reflects the influence of the changing environment outside the first coordination sphere on the transition state dynamics. A direct measure of this changing environment is the systematic variation of the chemical shifts with concentration (see Tables 4.8(a), 4.9, 4.10 and 4.11) characterising each system.

The $[Be(tmu)_4]^{2+}$ system exhibits similar chemical shift variations (see Table 4.3) however, τ_c shows no variation with concentration as is the case for the $[Be(mmpp)_4]^{2+}$ system (see section 4.7) which is characterised by first and second order ligand exchange rate laws (see section 4.5) depending on the diluent. That no obvious correlation exists between the chemical shifts and the observed rate law for a given diluent suggests that either the chemical shift variations bear no relevance to the exchange process or that the chemical shift variation is very much dependent on the nature of the ligand itself. As the data presented for the amide systems will not provide an unequivocal choice between the above suggestions or the

Table 4.12 Kinetic parameters for ligand (L) exchange on $[BeL_4]^{2+}$.

L	Diluent	k_1(340 K) s^{-1}	k_2(340 K) $dm^3\ mol^{-1}\ s^{-1}$	$\Delta H^{\neq}$ kJ mol^{-1}	$\Delta S^{\neq}$ J $K^{-1}\ mol^{-1}$	Assigned Mechanism	k_1/k_2(340 K) ratio
dmf	CD_3NO_2	7.4 ± 0.8	-	83.6 ± 6.3	16.3 ± 17.6	D	0.042
"	"	-	176 ± 4	58.1 ± 0.5	-32.0 ± 1.6	A	
dma	"	7.3 ± 0.7	-	56.9 ± 1.5	-62.1 ± 4.6	D	0.695
"	"	-	10.5 ± 1.0	66.7 ± 2.6	-30.1 ± 7.4	A	
nma	"	9.2 ± 0.9	-	71.5 ± 0.9	3.1 ± 2.9	D	0.564
"	"	-	16.3 ± 1.6	76.8 ± 0.9	16.3 ± 17.6	A	
dea	"	2.3 ± 0.1	-	76.4 ± 2.2	-14.6 ± 6.4	D	0.115
"	"	-	19.9 ± 0.3	68.5 ± 0.8	-19.6 ± 2.4	A	
tmu	"	72.6	-	77.1 ± 1.5	16.3 ± 4.3	D	

Table 4.12 (Continued)

L	Diluent	k_1(340 K) s^{-1}	k_2(340 K) $dm^3\ mol^{-1}\ s^{-1}$	$\Delta H^{\neq}$ kJ mol^{-1}	$\Delta S^{\neq}$ J $K^{-1}\ mol^{-1}$	Assigned Mechanism	k_1/k_2(340 K) ratio
dmf	CD_3CN	41.6 ± 0.9	-	63.0 ± 0.8	-29.8 ± 2.4	D	0.227
"	"	-	183 ± 3	60.2 ± 0.4	-25.6 ± 1.3	A	
dma	"	18.1 ± 1.8	-	78.0 ± 0.6	7.5 ± 1.9	D	1.72
"	"	-	10.5 ± 1.0	67.8 ± 2.2	-26.9 ± 6.4	A	
nma	"	38.3 ± 4.0	-	74.7 ± 0.9	4.0 ± 2.6	D	1.98
"	"	-	19.3 ± 2.0	82.9 ± 2.1	22.6 ± 6.2	A	
dea	"	17.5 ± 0.1	-	75.2 ± 0.5	-1.0 ± 1.5	D	0.940
"	"	-	18.6 ± 0.3	69.5 ± 1.0	-17.2 ± 3.1	A	
tmu	"	147	-	79.8 ± 0.7	30.2 ± 2.1	D	
dmf	CD_2Cl_2	22.0 ± 1.0	-	40.8 ± 1.0	-100 ± 3	D	0.209
	"	-	105 ± 4	44.0 ± 0.6	-77.8 ± 1.9	A	

simultaneous operation of D and A mechanisms one must look at other metal ions.

For the four systems $[M(tmp)_6]^{3+}$ (where M = Al^{21}, Ga^{22}, In^{22} and Sc^{20}) in CH_3NO_2 and CD_3NO_2 whose sizes, geometries and surface charge densities and therefore interactions outside the first coordination sphere are very similar first and second order ligand exchange rate laws characterise the first two and second two species respectively which is compelling evidence for a mechanistic difference arising from the nature of the interaction of the different metal centres and the entering and leaving ligands. From which a D ligand exchange mechanism has been assigned where M = Al or Ga and an A mechanism where M = In or Sc. Hence a logical extension of the assignments made for the $[M(tmp)_6]^{3+}$ species is the assignment of D and A mechanisms for ligand exchange on beryllium(II) species.

For tmu exchange on $[Be(tmu)_4]^{2+}$ (section 4.2) D ligand exchange mechanisms operate alone, whereas for dea, dma, nma and dmf exchange D and A mechanisms operate simultaneously, and for the dmf systems the A mechanism predominates particularly in CD_3NO_2 (see Table 4.12).

A comparison of the data for ligand exchange of the isomeric ligands dmf and nma on beryllium(II) suggests that steric crowding by the R1 group which is in close proximity to the beryllium(II) centre

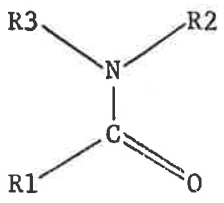

inhibits the operation of an A mechanism, i.e. when R1 = H, the case for dmf, steric crowding is small and the A mechanism predominates whilst for nma where R1 = CH_3, the methyl group with larger steric crowding inhibits the operation of an A mechanism.

Such simple steric arguments should only be applied to a given class of ligands and the influence of any variation in the

beryllium(II)-ligand bonding with the nature of the ligand should also be considered. It is probable that such variations in bonding will occur as a consequence of changes in the electron donating ability of the ligand of which the Gutmann donor number[17,18,26], DN (kcal mol^{-1}) is a measure. It is seen that as the DN decreases in the sequence tmu (DN = 29.6, R1 = $N(CH_3)_2$), dma (DN = 27.9, R1 = CH_3) and dmf (DN = 26.6, R1 = H) which is the same sequence as the trend for ligand exchange to occur via a D mechanism decreases and the size of the ligand decreases (or alternatively the steric crowding around the beryllium(II) centre decreases). (No DN is available for nma.) Then on the basis of this data it appears that an increase in the electron donating ability and size both stabilise the D transition state relative to the A transition state, however no attempt will be made to apportion the above ligand characteristics as the nature of the diluent also affects the mechanisms operating.

If in light of the above one compares the k_1/k_2(340 K) ratios for ligand exchange on the beryllium(II) centre where the ligands considered are dea (DN = 32.2, R1 = CH_3, R2 = R3 = CH_2CH_3), dma and dmf in the diluent CD_3NO_2 and CD_3CN then this ratio for the $[Be(dea)_4]^{2+}$ is greater than that for $[Be(dmf)_4]^{2+}$ but less than that obtained for the $[Be(dma)_4]^{2+}$ system respectively, which is further evidence showing that interactions outside the first coordination sphere can make significant contributions to the kinetic parameters obtained. [For all the beryllium(II)-amide systems reported herein no evidence was found to suggest that the inert diluents (CD_3NO_2, CD_3CN or CD_2Cl_2) resided in the first coordination sphere of the beryllium(II)-ligand species.]

The two term ligand exchange rate law observed for the amide systems is also observed for the $[Be(dmmp)_4]^{2+}$ system in CD_3CN solution (see section 4.4) which suggests that the D and A transition state energetics are quite similar. As D and A mechanisms can operate alone for ligand exchange on beryllium(II) depending on the nature of the ligand (see Table 4.7) it should be expected that circumstances may arise

where both mechanisms operate in parallel.

So far the discussion has ignored the possibility of ligand exchange occurring through an interchange (I) mechanism[16] in which the ligands interchange between the first and second coordination spheres of beryllium(II), and in which the activation mode may vary from predominantly dissociative (I_D) to predominantly associative (I_A), but does not produce the reactive intermediates characterising the D and A mechanisms. The interchange mechanism necessarily proceeds through an encounter complex in which the entering ligand resides in the second coordination sphere of $[BeL_4]^{2+}$ which is formed in a rapid pre-equilibrium characterised by a formation constant K_o[16,23]. On this basis the k_2 term of equation (2.12) may be taken as an indication that the proportion of $[BeL_4]^{2+}$ existing in the encounter complex form is a small proportion of its total concentration such that $k_2 = k_i K_o$ where k_i is the rate constant characterising ligand exchange between the first and second coordination spheres of $[BeL_4]^{2+}$. Thus the k_2 term of equation (2.12) may be attributed to the operation of an I mechanism in parallel to a D mechanism characterised by k_1. The variation in the magnitude of the k_2 term (Table 4.12) can thus arise as a consequence of variation in k_i, K_o, or both of these parameters simultaneously. If this variation arises solely as a consequence of k_i then the involvement of the entering ligand in the formation of the transition state is significant and an I_a mechanism operates. For this mechanism the same steric arguments proposed previously for the A mechanism will rationalise the relative magnitudes of k_1 and k_2. However this study provides no kinetic evidence for or against the formation of an encounter complex. In principle the systematic variations of the chemical shifts of the coordinated and free ligands with concentration observed in this study (Tables 4.8(a), 4.9, 4.10 and 4.11) and also for the dmso, tmu, mmpp and dmmp systems should reflect the changing proportions of the free ligand concentration residing in the first coordination sphere of beryllium(II). These variations probably

also reflect the overall change of solution composition and thus are unlikely to provide a specific probe for the formation of encounter complexes. In any event the formation of an encounter complex does not require the operation of an I mechanism. The basic difference between assigning the k_2 term of equation (2.12) to an I or A mechanism is that the involvement of the entering ligand in the formation of the transition state is less in the former mechanism than in the latter. (There is no involvement of the entering ligand in the transition state in the D mechanism.) Whilst an unequivocal choice between an I or an A mechanism cannot be made for the k_2 term of equation (2.12) on the basis of the present data it is probable that k_2 characterises an associative mode of activation.

That the diluent is important in determining the relative importance of D and A mechanisms for ligand exchange is indicated from the data in Table 4.7. For the exchange of dea, dma, nma and dmf on the beryllium(II) centre the operation of the D mechanism is enhanced when the diluent is changed from CD_3NO_2 to CD_3CN, and similarly CD_2Cl_2 enhances the operation of the D mechanism. [For the $[Be(mmpp)_4]^{2+}$ system changing the diluent from CD_3NO_2 to CD_3CN causes the mechanism to change from A to D, and for CD_2Cl_2 a D mechanism also operates.]

In section 4.7 it was noted that on the basis of dielectric constants, dipole moments, DN's and Reichardt parameters, CD_3NO_2 and CD_3CN should influence the ligand exchange mechanism in a similar manner than is the case for CD_3CN and CD_2Cl_2. This suggests that the interaction of the diluent with $[BeL_4]^{2+}$ is specific in nature and the variation of the chemical shifts for dea, dma, nma, dmf and tmu (Tables 4.11, 4.10, 4.9, 4.8(a) and 4.3 respectively) systems demonstrates this. The maximum difference in chemical shift and kinetic effects will arise if the $-NO_2$ and -CN groups of the diluents are oriented towards $[BeL_4]^{2+}$ however the present data does not allow elucidation of these orientations.

If the data for dmf exchange on $[Be(dmf)_4]^{2+}$ in dmf alone is considered little or no mechanistic information can be obtained. However a comparison of the activation parameters for the exchange process for the $[Be(dmf)_4]^{2+}$ systems (in the diluents CD_3NO_2, CD_3CN and CD_2Cl_2) with the above does allow mechanistic inferences to be made.

The observed first order exchange rate constant for ligand exchange on $[Be(dmf)_4]^{2+}$ in dmf alone is considerably greater than the k_1 term for dmf exchange in the inert diluents and as such suggests that either an A mechanism operates alone or A and D mechanisms operate simultaneously for the former system. The activation enthalpy and entropy do not provide an easy means for comparing the data as contributions from outside the first coordination sphere will be incorporated into these parameters and as such will be expected to vary as the diluent is changed. Such contributions to $\Delta H^{\neq}$ and $\Delta S^{\neq}$ emanating from interactions outside the first coordination sphere have been considered by Hoffman *et al.*[42]. These workers suggest that intramolecular ligand rotational motions may vary significantly between the coordinated and free states and in consequence it is probable that a variation in the nature of the diluent will produce a corresponding variation in the contributions to $\Delta H^{\neq}$ and $\Delta S^{\neq}$. Caldin and Bennetto[43] have postulated a more extensive model which also envisages contributions to $\Delta H^{\neq}$ and $\Delta S^{\neq}$ originating from outside the first coordination sphere, which is based on the structure of the solvated metal ion proposed by Frank and Wen[44] as described in section 1.1. Reiterating, Frank and Wen[44] envisaged a region (a) of relatively ordered solvent outside the first coordination sphere which merges into a region (b) of disordered solvent which in turn merges into the normal solvent structure region (c). According to Caldin and Bennetto[43] the movement of solvent or ligand between any of these three regions synchronously with the formation of the transition state may result in positive or negative contributions to the observed $\Delta H^{\neq}$ and $\Delta S^{\neq}$ values for the solvent or ligand

exchange process. The structure of the solvated metal ion proposed by Frank and Wen[44] is more appropriate for dilute solutions in water and in similarly structured liquids rather than for quite concentrated solutions in aprotic diluents used in this study. Thus the transfer of diluent or ligand between regions (a) - (c) envisaged in the Caldin and Bennetto[43] model are unlikely to apply strictly in the systems considered here, nevertheless both the diluent and the free ligand will experience a range of environments as their proximity to the beryllium(II) species varies through the solution and it is possible that movement between the environments may be an origin of contributions to $\Delta H^{\neq}$ and $\Delta S^{\neq}$.

REFERENCES: CHAPTER 4

1. M. Eigen, *Pure Appl. Chem.*, 6, 97 (1963).
2. W.G. Baldwin and D.R. Stranks, *Aust. J. Chem.*, 21, 2161 (1968).
3. H. Strehlow and W. Knoche, *Ber. Bunsenges. Phys. Chem.*, 73, 427 (1969).
4. J. Crea and S.F. Lincoln, *J. Chem. Soc. (Dalton)*, 2075 (1973).
5. J.-J. Delpuech, A. Peguy, P. Rubini and J. Steinmetz, *Nouv. J. Chim.*, 1, 133 (1977).
6. H.-H. Füldner, D.H. Devia and H. Strehlow, *Ber. Bunsenges. Phys. Chem.*, 82, 499 (1978).
7. D.H. Devia and H. Strehlow, *Ber. Bunsenges. Phys. Chem.*, 83, 627 (1979).
8. J. Frahm and H.-H. Füldner, *Ber. Bunsenges. Phys. Chem.*, 84, 173 (1980).
9. J. Frahm, *Ber. Bunsenges. Phys. Chem.*, 84, 754 (1980).
10. N.A. Matwiyoff and W.G. Movius, *J. Amer. Chem. Soc.*, 89, 6077 (1967).
11. H. Strehlow, D.H. Devia, S. Dagnall and G. Busse, *Ber. Bunsenges. Phys. Chem.*, 85, 281 (1981).
12. R.D. Shannon and C.T. Prewitt, *Acta Cryst.*, B25, 925 (1969); B26, 1046 (1970).
13. R.E. Connick and D.N. Fiat, *J. Chem. Phys.*, 39, 1349 (1963).
14. M. Alei Jr. and J.A. Jackson, *J. Chem. Phys.*, 41, 3403 (1964).
15. C.V. Chaturvedi and S. Parkash, *Ind. J. Chem.*, 10, 669 (1972).
16. C.H. Langford and H.B. Gray, "*Ligand Substitution Processes*", W.A. Benjamin, New York, 1966.
17. V. Gutmann, "*Coordination Chemistry in Non-aqueous Solutions*", Springer-Verlag, Wien, 1968.
18. V. Gutmann and E. Wychera, *Inorg. Nucl. Chem. Letts.*, 2, 257 (1966).
19. D.L. Pisaniello, S.F. Lincoln and E.H. Williams, *J. Chem. Soc. (Dalton)*, 1473 (1979).
20. D.L. Pisaniello and S.F. Lincoln, *J. Chem. Soc. (Dalton)*, 699 (1980).
21. J.-J. Delpuech, M.R. Khaddar, A.A. Peguy and P.R. Rubini, *J. Amer. Chem. Soc.*, 97, 3373 (1975).

22. L. Rodehüser, P.R. Rubini and J.-J. Delpuech, *Inorg. Chem.*, 16, 2837 (1977).

23. R.G. Wilkins in "*The study of Kinetics and Mechanisms of Reactions of Transition Metal Complexes*", Allyn and Bacon, Boston, 1974.

24. J. Burgess in "*Metal Ions in Solution*", Ellis Horwood Ltd., Chichester, 1978.

25. C. Reichardt in "*Losungsmittel Effekte in der Organischen Chemie*", Verlag Chemie, Weinheim, 1973.

26. V. Gutmann and R. Schmeid, *Coord. Chem. Rev.*, 12, 263 (1974).

27. T.M. Krygowski and W.R. Fawcett, *J. Amer. Chem. Soc.*, 97, 2143 (1975).

28. T.M. Krygowski and W.R. Fawcett, *Aust. J. Chem.*, 28, 2115 (1975).

29. L.A. LaPlanche and M.T. Rogers, *J. Amer. Chem. Soc.*, 86, 337 (1964).

30. R.H. Barker and G.J. Bordeaux, *Spectrochim. Acta*, 23A, 727 (1967).

31. D.L. Pisaniello, *Ph.D. Dissertation*, University of Adelaide, 1980.

32. J.A. Carver, Private communication.

33. M.N. Tkaczuk, Unpublished data.

34. J.V. Hatton and R.E. Richards, *Mol. Phys.*, 5, 139 (1962).

35. L.A. LaPlanche and M.T. Rogers, *J. Amer. Chem. Soc.*, 85, 3728 (1963).

36. B.B. Wayland, R.S. Drago and H.F. Henneike, *J. Amer. Chem. Soc.*, 88, 2455 (1966).

37. J.-J. Delpuech, P.R. Rubini and L. Rodehüser, *Inorg. Chem.*, 18, 2962 (1979).

38. W.E. Stewart and T.H. Sidall III, *Chem. Rev.*, 70, 517 (1970).

39. H. Kessler and A. Rieker, *Justus Liebigs. Ann. Chem.*, 708, 57 (1967).

40. B.F. Pedersen and B. Pedersen, *Tetrahedron Lett.*, 2995 (1965).

41. J.A. Riddick and W.B. Bugner in "*Techniques of Chemistry Vol. II, Organic Solvents. Physical properties and methods of purification.*", 3rd ed., Wiley Interscience, 1970.

42. P. Fischer, H. Hoffman and G. Platz, *Ber. Bunsenges. Phys. Chem.*, 76, 1060 (1972).

43. E.F. Caldin and H.P. Bennetto, *J. Soln. Chem.*, 2, 217 (1973).

44. H.S. Frank and W.Y. Wen, *Discuss. Far. Soc.*, 24, 133 (1957).

45. T. Kurucsev, Unpublished data.

CHAPTER 5: The Correlation between Activation Enthalpy and Entropy for Ligand Exchange on Metal Ions, An Isokinetic Relationship.

5.1 Introduction

Several authors[1,5,6] have shown that plots of activation enthalpy against activation entropy for a specific type of ligand exchange process (i.e. a dissociative ligand exchange process) on metal centres are approximately linear.

Such linear relationships between $\Delta H^{\neq}$ and $\Delta S^{\neq}$ for both organic and inorganic reactions have been discussed by Hoffman[3] and Krug[7] *et al.* Hoffman suggests that the restrictive timescale of equipment used to obtain activation parameters for the ligand substitution process may limit the range of values obtained and thus the correlations will be fortuitous and unrelated to any chemical property. Krug[7] *et al.* have approached the problem of whether the $\Delta H^{\neq}/\Delta S^{\neq}$ correlation is real by employing a statistical method to determine its validity and have tested the correlation for a number of organic reactions.

The kinetic data reported herein and elsewhere for ligand exchange on a number of beryllium(II) unidentate oxygen donor complexes provides a means of testing for a $\Delta H^{\neq}/\Delta S^{\neq}$ correlation using Krug's[7] statistical analysis method.

5.2 Results and Discussion

The lability of beryllium(II) complexes towards ligand exchange varies by a factor $> 10^6$ at 298.2 K (Table 4.7) and a linear least squares analysis of the experimental $\Delta H^{\neq}/\Delta S^{\neq}$ values gives a line of best fit as seen in figure 5.1. Over a small range of $\Delta H^{\neq}/\Delta S^{\neq}$ values, experimental error can produce an apparent linear relationship and to some extent the variations in the activation parameters characterising the $[Be(tmp)_4]^{2+}$ system in CH_3NO_2, determined in the same laboratory

using ^{1}H and ^{9}Be nmr spectroscopy reflect the likely magnitude of such experimental variability. However, in view of the large $\Delta H^{\neq}/\Delta S^{\neq}$ range covered and the different origins of the data it appears that the data plotted in Figure 5.1 does reflect an isokinetic relationship for ligand exchange on beryllium(II) rather than an experimental artefact.

A linear regression fit of the data to the relationship (5.1), in which each system was weighted in direct proportion to the number of

$$\Delta G^{\neq} = \Delta H^{\neq} - \hat{T}\Delta S^{\neq} \qquad (5.1)$$

solutions studied, yields $\Delta G^{\neq} = 74.4 \pm 1.0$ kJ mol^{-1} and an isokinetic temperature $\hat{T} = 440.7 \pm 58.3$. (A statistical method for assessing the significance of the linearity of isokinetic plots has been proposed by Krug[7] *et al.*, according to which this linearity may be attributed to chemical origins with 95% certainty if the harmonic mean of the experimental temperatures, $T_{hm} = \langle T^{-1} \rangle^{-1}$, lies outside the 95% confidence interval for the isokinetic temperature, $\hat{T}$. This is the case for unidentate oxygen donor ligand exchange on six coordinate magnesium(II)[6] and scandium(III)[6,11], but in the case of beryllium(II) such a complete assessment is not possible as all the experimental temperatures are not available from the literature.

However, for the five systems reported in this thesis where the ligand exchange mechanism on beryllium(II) was found to be dissociative this test was applied. The plot of $\Delta H^{\neq}$ against $\Delta S^{\neq}$ for the twenty five sets of values yielded $\Delta G^{\neq} = 71.9 \pm 0.2$ and an isokinetic temperature, $\hat{T} = 282.8$ K with the 95% confidence interval being 276.6 - 289.0 K. From the 226 temperatures used to obtain the activation parameters $T_{hm} = 326.7$ K which is well outside the 95% confidence interval for the isokinetic temperature and suggests that the isokinetic plot has chemical significance. However as the range of activation parameters used in this test is small these results do not conclusively prove the significance of the above correlation.

For the forty four sets of $\Delta H^{\neq}/\Delta S^{\neq}$ values used to obtain the results (given in Table 5.1) the highest temperature used in any of the studies of ligand exchange on beryllium(II) was 388 K (for the $[Be(hmpa)_4]^{2+}$ system in 4-methyl-1,3-dioxolan-2-one[12]) which is just inside the lower 95% confidence interval for the isokinetic temperature obtained and T_{hm} will be lower than this value. Therefore without even calculating T_{hm} one can say that the linear correlation between $\Delta H^{\neq}$ and $\Delta S^{\neq}$ has chemical significance.

The isokinetic parameters ($\hat{T}$ and $\Delta G^{\neq}$) for the four coordinate beryllium(II) systems are similar to those of the trivalent metal ions scandium(III) and aluminium(III) compared with those for magnesium(II) (see Table 5.1). These results indicate that the large values of $\Delta G^{\neq}$ and $\hat{T}$ are characteristic of the high surface charge densities of the ions concerned. The proximity of the data characterising A ligand exchange mechanisms to the beryllium(II) isokinetic line suggests that surface charge density is also important in determining the dynamics of the A mechanisms.

Strictly, the beryllium(II) data should be compared with that of other divalent metal ions however only the three zinc(II) systems whose data is plotted in Figure 5.1 are available for comparison. That the zinc(II) data lies considerably closer to the magnesium(II) isokinetic line is not unexpected and lends further support to the earlier suggested relationship between the surface charge density of the metal centre and $\Delta G^{\neq}$ and $\hat{T}$. All the data with one exception, the $[Zn(tmtu)_4]^{2+}$ system (section 3.2), refer to oxygen donor ligands and the different electronic configurations of the metal centres will cause the resultant differences in bonding to superimpose upon the effect of surface charge density although the latter effect does appear to be dominant for the metal centres reported herein.

Table 5.1 Data concerning the $\Delta H^{\neq}/\Delta S^{\neq}$ correlation for ligand exchange on metal ions.

Metal Ion	$\Delta G^{\neq}$ kJ mol^{-1}	$\hat{T}$[a] K	95% C.I. of $\hat{T}$ K		m[b]	T_{hm} K	r nm	m^{+}/r^{2} nm^{-2}	Ref.
Mg^{2+}[c]	42.0	252.8	262.4	243.2	21	223	0.072	$3.85 \times 10^{+2}$	6
Al^{3+}[c]	69.5	410.0				-	0.053	$10.68 \times 10^{+2}$	5
Sc^{3+}[c]	73.3	385.3	394.7	375.9	17	-	0.0745	$5.41 \times 10^{+2}$	6
Be^{2+}	74.4	440.7	499	382.6	44	-	0.027	$27.4 \times 10^{+2}$	-
Be^{2+}	71.9	282.8	289.0	276.6	25	326.7	0.027	$27.4 \times 10^{+2}$	-

[a] $\hat{T}$ = Estimate of the isokinetic temperature from linear regression.

[b] m = Number of $\Delta H^{\neq}/\Delta S^{\neq}$ pairs.

[c] For six coordinate unidentate oxygen donor complexes.

On the basis of the data shown in figure 5.1 and reported elsewhere[5,6,11] both $\Delta G^{\neq}$ and $\hat{T}$ tend to increase as the surface charge density of the metal centre becomes greater with the consequence that as $\Delta H^{\neq}$ decreases $\Delta S^{\neq}$ becomes increasingly negative and the lability of the different metal centres become similar.

Contributions to $\Delta H^{\neq}$ and $\Delta S^{\neq}$ from within the first coordination sphere are likely to reflect the surface charge density of the metal centre more markedly than those arising from outside the first coordination sphere. Any deviation of the observed $\Delta H^{\neq}/\Delta S^{\neq}$ parameters from the line of best fit may indicate that interactions from outside the first coordination sphere contribute towards the activation parameters. The problem which then arises, is how to determine whether or not the line of best fit does describe the contributions to $\Delta H^{\neq}/\Delta S^{\neq}$ from within the first coordination sphere.

The effect of the surface charge density of the metal ion at the surface of the first coordination sphere and beyond should attenuate with distance or with the ability of the ligand to transmit it. Thus if the labilities toward ligand exchange of metal centres of dissimilar surface charge densities are similar this may indicate that interactions from outside the first coordination sphere are making substantial contributions to $\Delta H^{\neq}$ and $\Delta S^{\neq}$. Similarly if for a particular system a change of diluent results in a change in the activation parameters with no change in the ligand exchange mechanism then these differences may be due to interactions outside the first coordination sphere making contributions to $\Delta H^{\neq}$ and $\Delta S^{\neq}$.

At present the available data does not permit separate quantification of the effects of interactions arising from within and exterior to the first coordination sphere on the dynamics of ligand exchange but their combined effect is illustrated by the almost seven orders of magnitude variation in lability (298.2 K) exhibited by

beryllium(II) (the inertness of the $[Be(tppo)_4]^{2+}$ system indicates the range of lability may be greater than seven orders of magnitude) and the wide variations in $\Delta H^{\neq}$ and $\Delta S^{\neq}$ seen in Figure 5.1.

5.3 Summary

The dynamics of the ligand exchange process on beryllium(II) species in non-aqueous solution is controlled by three factors. Firstly the nature of the metal ion itself, i.e. the surface charge density of the beryllium(II) ion. Secondly the nature of the ligand, namely electronic and steric effects of the ligand are important. Thirdly the diluent used affects the ligand exchange mechanism particularly when steric crowding by the ligand is intermediate in nature. The interplay of the above factors will determine the rates and mechanisms of ligand exchange on the beryllium(II) species.

Figure 5.1

Isokinetic plot for ligand exchange on beryllium(II). Individual systems are identified by: identifying number; exchanging ligand; solvent; reference. The following abbreviations are used for the solvent: CD_3CN, an; CD_3NO_2 or CH_3NO_2, nm; CD_2Cl_2 or CH_2Cl_2, dm; $(CD_3)_2CO$, ac; $O\overline{COCH(Me)CH_2O}$, md. Circles denote systems which undergo ligand exchange through a D or I_d mechanism alone. 1): hmpa: md:[12]; 2): dmadmp: nm:[12]; 2): tmdamp: md: [12]; (datum point 2 denotes two coincident data sets); 3): tmu: nm:[17]; (these five smaller circles denote the data for five different solutions over a 44 fold variation in $[tmu]_{free}$); 4): tmu: an;[17]; data for solutions over a 20 fold variation in $[tmu]_{free}$ are encompassed by this circle); 5): dmmp: dm:[17]; (data for all solutions are encompassed by this circle); 6): dmadmp: md:[12]; 7): dmmp: dmmp:[17]; 8): tmp: tmp:[18]; 11): mmpp: an:[17]; (data for all solutions in are encompassed by this circle); 12): tmp: dm;[18]; (the four smaller circles denote data for four different solutions); 15): mmpp: dm:[17]; 18): water: water:[13]; 19): water: ac:[14]; 20): dmso: dmso:[19]. Squares denote systems which undergo ligand exchange through an A mechanism alone. 10): mmpp: nm:[17]; 13): dmmp: nm:[12]; 14): tmp (^9Be study): nm:[12]; 16): tmp (^1H study): nm: [12]; 17): dmso: nm:[17]. The upper and lower triangular points 9) represent the data pertaining to the first and second order terms of the two term rate law for dmmp exchange in CD_3CN [17]. The solid line represents the linear regression line obtained for the weighed data for all of those systems undergoing exchange through a D or an I_d mechanism. The broken line represents the analogous regression line for the six coordinate magnesium(II) systems. The diamond points represent data for ligand exchange on four coordinate zinc(II) where for a), b) and c) the ligands are $S=C(NMe_2)_2$, tppo, hmpa; the solvents are:- dm, dm, dm, the mechanisms are:- D, D, A[16]. In general the datum point symbols are either of a size which encompasses one standard deviation in $\Delta H^{\neq}$ and $\Delta S^{\neq}$ or these errors are shown extending outside the symbol. Strictly the magnitude of such errors in an isokinetic plot should be shown as an elipsoid (J. Mandel and F.J. Linning, *Analyt. Chem.*, 29, 743 (1957).) but the presentation of the data adopted in the Figure is more convenient for illustrative purposes.

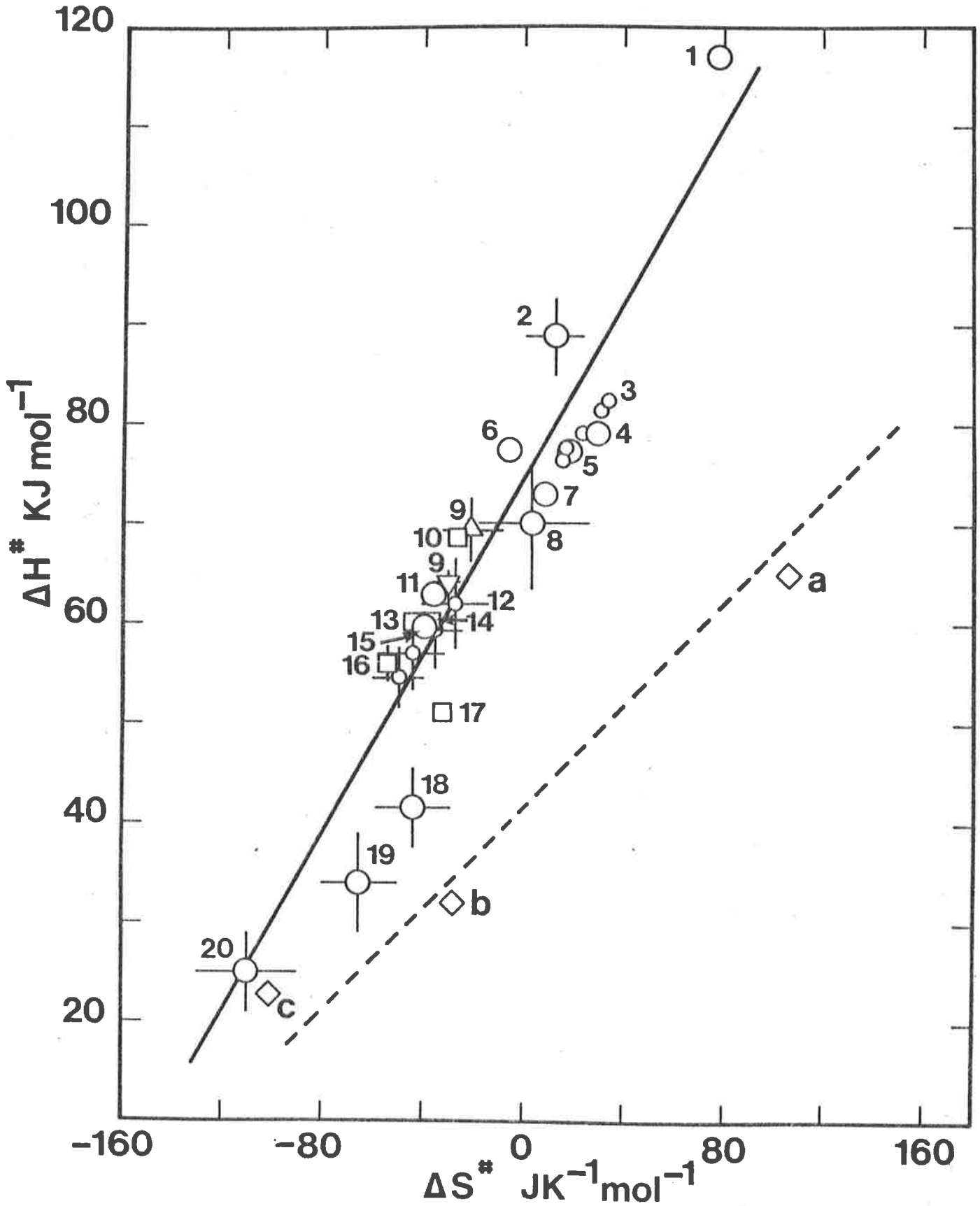
120
100
80
60
40
20
$\Delta H^{\#}$ KJ mol^{-1}
-160
-80
0
80
160
$\Delta S^{\#}$ JK^{-1}mol^{-1}
1
2
3
4
5
6
7
8
9
10
9
11
12
13
14
15
16
17
18
19
20
a
b
c

REFERENCES: CHAPTER 5

1. S.F. Lincoln, *Pure Appl. Chem.*, 51, 2059 (1979).
2. K. Kustin and J. Swinehart, *Prog. Inorg. Chem.*, 13, 116 (1970).
3. H. Hoffman, *Pure Appl. Chem.*, 41, 327 (1975).
4. P. Fischer, H. Hoffman and G. Platz, *Ber. Bunsenges Phys. Chem.*, 76, 1060 (1972).
5. G.J. Honan, *Ph.D. Dissertation*, The University of Adelaide, 1979.
6. D.L. Pisaniello, *Ph.D. Dissertation*, The University of Adelaide, 1980.
7. R.R. Krug, W.G. Hunter and R.A. Greiger, *J. Phys. Chem.*, 80, 2335, 2341 (1976).
8. H.P. Bennetto and E.F. Caldin, *J. Chem. Soc. (A)*, 2198 (1971).
9. E.F. Caldin and H.P. Bennetto, *J. Soln. Chem.*, 2, 217 (1973).
10. C.H. Langford, J.P.K. Tong and A.E. Merbach, *Can. J. Chem.*, 53, 702 (1975).
11. D.L. Pisaniello and S.F. Lincoln, *Inorg. Chem.*, (in press).
12. J.-J. Delpuech, A. Peguy, P. Rubini and J. Steinmetz, *Nouv. J. Chim.*, 1, 133 (1977).
13. J. Frahm and H.-H. Fuldner, *Ber. Bunsenges. Phys. Chem.*, 84, 173 (1980).
14. J. Frahm, *Ber. Bunsenges. Phys. Chem.*, 84, 754 (1980).
15. J. Crea and S.F. Lincoln, *J. Chem. Soc. (Dalton)*, 2075 (1973).
16. See chapter 3.
17. See chapter 4.
18. J. Crea and S.F. Lincoln, *J. Chem. Soc. (Dalton)*, 2075 (1973).
19. D.H. Devia and H. Strehlow, *Ber. Bunsenges. Phys. Chem.*, 83, 627 (1979).

CHAPTER 6: EXPERIMENTAL

6.1 Origin and Purification of chemicals

6.1.1 *Perchlorates*

Hydrated zinc perchlorate (B.D.H.) was used without further purification. Hydrated beryllium perchlorate was prepared by the reaction of stoichiometric amounts of $BeCO_3$ (B.D.H.) and concentrated perchloric acid (Merck) and the resultant solution dried *in vacuo* over P_2O_5. The perchlorates were analysed for metal ion content by an ion exchange method described by Vogel[1].

6.1.2 *Dehydrating agents*

Triethyl orthoformate (Koch-Light) was used without further purification. Linde 4A molecular sieves were successively washed with distilled water and ethanol to remove impurities and then activated by heating at 650 K in a furnace for eight hours.

6.1.3 *Ligands*

The liquids dmf (B.D.H.), nmf (B.D.H.), nma (B.D.H.), dea (Fluka), def (Fluka), dma (B.D.H.), dmso (Fluka), hmpa (Koch-Light), dmmp (Aldrich), tmp (B.D.H.), tmu (Fluka) and mmpp (Strem) were distilled under reduced pressure onto Linde 4A molecular sieves and stored under a dry nitrogen atmosphere. The solids npa (L. Light), dmu (Fluka), tmtu (Fluka) and tppo(Fluka) were dried *in vacuo* over P_2O_5 for several days before use.

6.1.4 *Diluents*

The deuterated solvents CD_2Cl_2 (C.E.A., France and Aldrich), CD_3CN (C.E.A., France and M.S. & D.) and CD_3NO_2 (C.E.A., France and M.S. and D.) were distilled and dried over Linde 4A molecular sieves.

6.2 Preparation of metal complexes

hexakis (N,N-dimethylformamide) zinc(II) diperchlorate

hexakis (N,N-dimethylacetamide) zinc(II) diperchlorate

tetrakis (dimethylmethylphosphonate) beryllium(II) diperchlorate

pentakis (dimethylmethylphosphonate) zinc(II) diperchlorate

tetrakis (dimethylsulphoxide) beryllium(II) diperchlorate

tetrakis (methylmethylphenylphosphinate) beryllium(II) diperchlorate

tetrakis (N-methylacetamide) beryllium(II) diperchlorate

tetrakis (N-methylacetamide) zinc(II) diperchlorate

tetrakis (N-phenylacetamide) beryllium(II) diperchlorate

pentakis (trimethylphosphate) zinc(II) diperchlorate

tetrakis (1,1,3,3-tetramethyl-2-thiourea) zinc(II) diperchlorate

The above complexes were prepared using a procedure similar to that of van Leeuwen and Groeneveld[2] and Karayannis[3] *et al*. The hydrated metal perchlorate was dissolved in a five fold excess of triethylorthoformate per mole of water and the solution heated at 325 K for 1 hour. A slight excess over the stoichiometric amount of ligand was added and the solution heated for a further hour. The solution was then placed in a dry nitrogen flushed glove box, and on the addition of anhydrous diethyl ether the complex precipitated. After which the precipitate was filtered, washed with anhydrous diethyl ether and dried with dry nitrogen prior to vacuum drying for several hours, to remove any traces of solvent. The product yields for these preparations were in the range 75 - 90%.

tetrakis (N,N-dimethylacetamide) beryllium(II) diperchlorate

pentakis (dimethylsulphoxide) zinc(II) diperchlorate

tetrakis (hexamethylphosphoramide) zinc(II) diperchlorate

tetrakis (1,1,3,3-tetramethylurea) zinc(II) diperchlorate

The preparation of these complexes was similar to that of the previous complexes except that a precipitate was formed immediately upon the addition of the ligand to the triethylorthoformate solution.

tetrakis (triphenylphosphine oxide) beryllium(II) diperchlorate

tetrakis (triphenylphosphine oxide) zinc(II) diperchlorate

The preparation of these complexes differed from the method described in Section 6.2 in that the solid ligand was dissolved in dry ethanol prior to its addition to the triethylorthoformate solution.

tetrakis (N,N-diethylacetamide) beryllium(II) diperchlorate

tetrakis (N,N-dimethylformamide) beryllium(II) diperchlorate

tetrakis (1,1,3,3-tetramethylurea) beryllium(II) diperchlorate

The above preparative method failed to yield any solid even after several washings with anhydrous diethyl ether. However, when the ether was decanted from the resultant oil and a solution of teof and ligand added and allowed to stand for 24 hours, a solid was formed. As these metal solvato complexes are potentially explosive only small quantities were used (and these handled with care). Due to the toxic nature[13] of beryllium compounds, extreme care was exercised in their handling to avoid contamination.

No method for the preparation of crystalline complexes from several ligand/metal perchlorate combinations was found. These combinations plus relevant observations are listed below.

Metal perchlorate/ligand Combination	Observations
$Zn(ClO_4)_2$/tpp	Solid which was unstable and formed an oil (once) out of solution.
$Be(ClO_4)_2$/dmu	
$Be(ClO_4)_2$/def	Oil which failed to crystallise.
$Zn(ClO_4)_2$/nmu	

Metal perchlorate/ligand Combination	Observations
$Zn(ClO_4)_2$/nmtu	Oil was formed plus decomposition of the ligand.
$Zn(ClO_4)_2$/tu	

6.3 Elemental Analysis

Microanalyses were performed by the Australian Microanalytical Service, Melbourne. Metal ion content and stoichiometry of the complexes were quantitatively determined by the method of Vogel[1].

A known weight of complex was dissolved in water and eluted through a (Dowex 50 W mesh) cation exchange column (in the H^+ form). The acidic effluent was titrated against standardised sodium hydroxide (See Table 6.1). For those complexes (marked with an asterisk) which had a low water solubility a water/ethanol mixture ($\sim$ 50% v/v) was used. (It has been shown that pH measurements in aqueous ethanol solutions accurately reflect aqueous pH values[4].)

6.4 Preparation of nmr samples

The nmr solutions were prepared by the successive addition of weighed quantities of complex, ligand and inert diluent into a 1 cm^3 or 2 cm^3 volumetric flask, giving both molality and molarity of the solutions. Dilutions were then made by the addition of the appropriate inert diluent to weighed amounts of a concentrated solution. After which portions ($\sim$ 0.5 cm^3) of each solution were degassed and sealed under vacuum in 5 mm o.d. nmr tubes. To ensure anhydrous conditions all transfers etc. were carried out in a dry nitrogen atmosphere and all glassware was dried in an oven at > 400 K for at least 24 hours prior to use.

Table 6.1 Analytical Results

		% Metal	% C	% H	% N, P or S
$[Zn(tmtu)_4](ClO_4)_2$	calcd.	8.2	30.3	6.0	14.1
	found	8.1	30.0	6.0	14.0
$[Zn(tmu)_4](ClO_4)_2$	Calcd.	9.0	33.0	6.6	15.4
	found	8.9	33.0	6.6	15.4
$[Zn(dmf)_6](NlO_4)_2$	calcd.	9.3	30.8	6.0	12.0
	found	9.3	30.6	6.1	11.9
$[Zn(dma)_6](ClO_4)_2$	calcd.	8.3	36.6	6.9	10.7
	found	8.3	36.7	6.9	10.7
$[Zn(nma)_4](ClO_4)_2$	calcd.	11.7	25.9	5.1	10.1
	found	11.7	25.8	5.1	9.8
$[Zn(hmpa)_4](ClO_4)_2$	calcd.	6.6	29.4	7.3	17.1
	found	6.5	29.3	7.3	N. 17.0
$[Zn(tmp)_5](ClO_4)_2$	calcd.	4.6	18.6	4.6	16.0
	found	4.6	18.3	4.6	16.1
$[Zn(dmmp)_5](ClO_4)_2$	calcd.	7.5	20.3	5.1	17.5
	found	7.4	19.5	5.2	16.0
*$[Zn(tppo)_4](ClO_4)_2$	calcd.	4.7	62.7	4.4	9.0
	found	4.6	61.1	4.3	8.9
$[Zn(dmso)_5](ClO_4)_2$	calcd.	9.98	-	-	-
	found	9.79	-	-	-
$[Be(dmso)_4](ClO_4)_2$	calcd.	1.73	18.46	4.64	-
	found	1.71	20.0	5.1	-
$[Be(tmu)_4](ClO_4)_2$	calcd.	1.34	35.7	7.19	16.6
	found	1.43	34.5	6.95	16.1
$[Be(mmpp)_4](ClO_4)_2$	calcd.	1.01	43.1	4.98	13.9
	found	1.10	41.8	4.97	13.6

Table 6.1 (Continued)

		% Metal	% C	% H	% N, P or S
$[Be(dmmp)_4](ClO_4)_2$	calcd.	1.28	20.5	5.15	17.6
	found	1.28	20.3	5.2	17.10
*$[Be(tppo)_4](ClO_4)_2$	calcd.	0.682	65.4	4.6	9.4
	found	0.689	65.2	4.6	9.9
$[Be(nma)_4](ClO_4)_2$	calcd.	1.80	28.8	5.6	11.2
	found	1.79	28.0	5.7	10.5
$[Be(dma)_4](ClO_4)_2$	calcd.	1.62	34.5	6.5	10.1
	found	1.62	33.8	6.4	9.5
$[Be(dmf)_4](ClO_4)_2$	calcd.	1.80	28.8	5.6	11.2
	found	1.79	28.6	5.4	10.9
$[Be(dea)_4](ClO_4)_2$	calcd.	1.35	43.1	7.83	8.38
	found	1.34	43.0	7.69	8.41
$[Be(npa)_4](ClO_4)_2$	calcd.	1.20	51.3	4.85	7.48
	found	1.25	51.0	4.91	7.30

6.5 Instrumentation

For the $[Zn(tmtu)_4]^{2+}/tmtu/CD_2Cl_2$ system[5] the proton nmr spectra were recorded at 90 MHz on a Bruker HX-90E nmr spectrometer operating in the pulsed free precession mode. For the other systems ^1H nmr and broad band ^1H decoupled ^{31}P nmr spectra were recorded at 90 MHz and 36.43 MHz respectively on a modified Bruker HX-90E spectrometer (quadrature detection) in a pulsed fourier transform mode. An internal ^2H lock was used (with deuterated diluents) in both cases. The temperature was controlled to within ± 0.3 K by a copper constantan thermocouple using a Bruker (B-VT 1000) variable temperature unit which was periodically checked using standard methanol and ethylene glycol samples[6]. The spectra (containing kinetic data) were stored as 1 K (1024 datum points) blocks on disk (Diablo Disk System) and were later simulated (using the Nicolet BNC-12 mini computer of the spectrometer) utilising a lineshape generating program adapted[9] from published methods[7,8].

6.6 Infrared Analysis

All infrared samples were prepared under anhydrous conditions and were immediately recorded on a Perkin Elmer 457 grating infrared spectrophotometer using either NaCl plates or cells. The infrared spectra obtained were used to help characterise the complexes prepared. As expected no absorption bands typical of O-H stretching modes (in the region 3200 - 3600 cm^{-1}) were observed indicating the absence of either free or bound H_2O. All spectra were consistent with the presence of non-coordinated perchlorate ion (ClO_4^-). The change from ionic perchlorate to unidentate and bidentate perchlorato groups lowers the symmetry from T_d to C_{3v} to C_{2v} respectively which results in significant changes to the infrared spectrum[10,11]. Furthermore, the reduction in P=O, S=O, C=O and C=S stretching frequencies for the

complexes (c.f. those found for the free ligand) are indicative of oxygen to metal and sulphur to metal[12] bonding respectively.

REFERENCES: CHAPTER 6

1. A.I. Vogel, in "*Quantitative Inorganic Analysis*", 3rd. ed., Longmans Green and Co., London, 1961, p. 702.
2. P.W.N.M. van Leeuwen and W.L. Groeneveld, *Inorg. Nucl. Chem. Lett.*, 3, 145 (1967).
3. M.N. Karayannis, C. Owens, L.L. Pytlewski and M.M. Labes, *J. Inorg. Nucl. Chem.*, 31, 2059 (1969).
4. R.G. Bates, M. Paabo and R.A. Robinson, *J. Phys. Chem.*, 67, 1833 (1963).
5. Section 3.2.
6. A.L. Van Geet, *Anal. Chem.*, 40, 2227 (1968).
7. T. Nakagawa, *Bull. Chem. Soc. Jap.*, 39, 1006 (1966).
8. T.H. Sidall III, W.E. Stewart and F.D. Knight, *J. Phys. Chem.*, 74, 3580 (1970).
9. E.H. Williams, *Ph.D. Dissertation*, The University of Adelaide, 1980.
10. B.J. Hathaway and A.E. Underhill, *J. Chem. Soc.*, 3091 (1961).
11. M.R. Rosenthal, *J. Chem. Ed.*, 50, 331 (1973).
12. M. Schafer and C. Curran, *Inorg. Chem.*, 5, 265 (1966).
13. J. Schubert, *Scientific American*, 199, 27 (1958).

LIST OF PUBLICATIONS

1. "A Proton Magnetic Resonance Study of Ligand Exchange on Tetrakis(tetramethylthiourea) Zinc(II) Ion."
   M.N. TKACZUK and S.F. LINCOLN
   Aust. J. Chem., 32, 1915 (1979).

2. "A Phosphorus-31 Nuclear Magnetic Resonance Study of Ligand Exchange on Tetrakis(hexamethylphosphoramide) Zinc(II) Ion."
   M.N. TKACZUK and S.F. LINCOLN
   Aust. J. Chem., 33, 2621 (1980).

3. "A Phosphorus-31 Nuclear Magnetic Resonance Study of Triphenylphosphine Oxide Exchange on Magnesium(II) and Zinc(II)."
   S.F. LINCOLN, D.L. PISANIELLO, T.M. SPOTSWOOD and M.N. TKACZUK
   Aust. J. Chem., 34, 283 (1981).

4. "A Proton NMR Study of the Dynamics of Ligand Exchange on Tetrakis(1,1,3,3-Tetramethylurea) Beryllium(II) and its Dimethyl Sulphoxide Analogue."
   S.F. LINCOLN and M.N. TKACZUK
   Ber. Bunsenges. Phys. Chem., 85, 433 (1981).

5. "Proton Magnetic Resonance Study of Ligand Exchange on Tetrakis(methylmethylphenylphosphinate) Beryllium(II) and Tetrakis(dimethylmethylphosphonate) Beryllium(II) in Non-Aqueous Solvents."
   M.N. TKACZUK and S.F. LINCOLN
   Ber. Bunsenges. Phys. Chem., (in press).